CATCHMENT SCALE RUNOFF FROM EARTHEN LANDFILL FINAL COVERS

By

Tryambak Kaushik

A DISSERTATION

Submitted to
Michigan State University
in partial fulfillment of the requirements
for the degree of

Civil Engineering – Doctor of Philosophy

2014

ABSTRACT

CATCHMENT SCALE RUNOFF FROM EARTHEN LANDFILL FINAL COVERS

By

Tryambak Kaushik

Earthen landfill final covers (EFCs) offer cheap alternative to the conventional covers for isolating municipal solid waste underlain with a liner system, from precipitation and render minimum deep percolation. Earthen covers or alternative covers as they are often referred to in the literature, do not function as a hydraulic barrier similar to conventional covers. EFCs store precipitation water in storage layers during winter season and release it back to atmosphere in summer season. Although surface runoff had been long identified as one of the most important design variable of EFCs which controls predicted percolation, yet minimum literature is available on the catchment scale measurement and modeling of surface runoff from EFCs. The primary aim of this dissertation was to identify 1) critical factors governing the measured surface runoff from catchment scale EFCs, 2) accuracy of water balance and unsaturated flow models in predicting catchment scale hydrology of instrumented EFCs and 3) change in surface runoff from EFCs of different soil types and soil thicknesses at a regional scale in different climates of Texas. Two catchment scale EFCs were instrumented at Austin Community Landfill (ACL) in semiarid climate of Austin, Texas. Surface runoff from each catchment was collected with a custom designed storm water collection system consisting of high capacity tanks fitted with automated actuator valves. Soil water contents were monitored at several locations of both catchments for twenty three months. Upper catchment with smaller runoff length generated higher runoff than lower catchment. Seasonal variation in total precipitation, average precipitation intensity, precipitation return period, antecedent soil water content, PET/P and vegetation cover resulted in relatively high runoff in Winter 2012 and Fall

2013 than intermediate seasons. UNSAT-H was able to predict annual runoff from both catchments relatively accurately than RZWQM. UNSAT-H was not able to accurately predict daily runoff at ACL. Validated UNSAT-H model was subsequently used to predict surface runoff in different climatic regions of Texas. Annual and daily surface runoff-precipitation correlated better for wet regions than dry regions.

Keywords: Landfill covers, catchment scale runoff instrumentation and measurement, water balance modeling, unsaturated flow, UNSAT-H, RZWQM

I dedicate this dissertation to my parents

ACKNOWLEDGMENTS

I am grateful to Prof. Milind V. Khire for his continuous support and guidance. I had an unprecedented opportunity to work with him on several field-scale, laboratory scale and numerical modeling projects. His critical inputs and continuous motivation to achieve high research standards greatly helped me in this research.

I am equally thankful to my PhD guidance committee members consisting of Prof. Mantha S. Phanikumar, Prof. Muhammed Emin Kutay and Prof. Brad Rowe for their insightful reviews and comments to improve my dissertation.

I will also like to express my gratitude to Waste Management Inc. and Texas Solid Waste Association of North America for providing financial support and site access for this work. Department of Civil and Environmental Engineering at Michigan State University provided access to laboratory facilities to conduct experiments and helped financially with several fellowships during this research work. Jason Ritter of Campbell Scientific Inc. provided help for remote data acquisition systems. Terry Johnson and Michael Caldwell of Waste Management Inc. helped with site access to Austin Community Landfill.

I am thankful to civil engineering faculty, my family, relatives and friends, without whose unending support, I would not have been able to complete this work.

TABLE OF CONTENTS

LIST OF TABLES

LIST OF FIGURES

KEY TO SYMBOLS AND ABBREVIATIONS

a	=	curve fitting parameter for modified Brooks Corey function (Ahuja et al. 2000)
a_c	=	area of cross-section of drainage valve
A	=	area of cross-section of above ground storage tank
ACAP	=	Alternative Cover Assessment Project
ACL	=	Austin Community Landfill
ACL-D	=	UNSAT-H simulations with constant hourly precipitation intensity (1 cm/hr) at ACL
ACL-H	=	UNSAT-H simulations with as measured hourly precipitation intensity at ACL
AFC	=	alternative final cover
APY	=	average precipitation year
AST	=	above ground storage tank
ASTM	=	American Society for Testing and Materials
B	=	curve fitting parameter for modified Brooks Corey function (Ahuja et al. 2000)
BGS	=	below ground surface
C_2	=	curve fitting parameter for modified Brooks Corey function (Ahuja et al. 2000)
Cc	=	coefficient of gradation
Cu	=	uniformity coefficient
C_v	=	constriction coefficient of valve
CFR	=	Code of Federal Regulations
CH	=	high plasticity clay

D	=	deep drainage or percolation
D_{10}	=	diameter in the particle-size distribution curve corresponding to 10% finer
D_{50}	=	diameter in the particle-size distribution curve corresponding to 50% finer
D_{60}	=	diameter in the particle-size distribution curve corresponding to 60% finer
EFC	=	earthen final cover
ET	=	evapotranspiration
ETC	=	evapotranspirative cover
g	=	acceleration due to gravity (9.81 m/s^2)
G_s	=	specific gravity of soil solids
GCLs	=	geo-synthetic clay liners
GI	=	green infrastructure
h	=	suction head
h_{bk}	=	curve fitting parameter for modified Brooks Corey function (Ahuja et al. 2000)
h_{dry}	=	maximum suction to which top soil node can dry in UNSAT-H
h_l	=	water level in tank
HDPE	=	high-density polyethylene
k	=	average water flux rate into the tank with the drainage valve closed
K(h)	=	unsaturated hydraulic conductivity at a given suction value of h
K_{sat}	=	saturated hydraulic conductivity
K_{TS}	=	saturated hydraulic conductivity of top soil
$K(\theta)$	=	unsaturated hydraulic conductivity at a given volumetric water content value of θ
l	=	pore-interaction term for van Genuchten (1980) function

L	=	lower catchment percent runoff
LID	=	low impact development
LL	=	liquid limit
m	=	curve fitting parameter for van Genuchten (1980) function
MSW	=	municipal solid waste
n	=	curve fitting parameter for van Genuchten (1980) function
N_1	=	curve fitting parameter for modified Brooks Corey function (Ahuja et al. 2000)
N_2	=	curve fitting parameter for modified Brooks Corey function (Ahuja et al. 2000)
NCDC	=	National Climate Data Centre
NOAA	=	National Oceanic and Atmospheric Administration
NSRDB	=	National Solar Radiation Database
NTU	=	Nephelometric Turbidity Unit
p	=	curve fitting parameter for relating predicted runoff to precipitation
P	=	precipitation
PET/P	=	potential evapotranspiration to precipitation ratio
PI	=	plasticity index
Precip.	=	precipitation
PVC	=	polyvinyl chloride
q	=	curve fitting parameter for relating predicted runoff to precipitation
r	=	curve fitting parameter for relating predicted runoff to precipitation
R^2	=	correlation coefficient
R_O	=	surface runoff
RCRA	=	Resource Conservation and Recovery Act
S_t	=	source or sink term for water

SM	=	silty sand
SM-ML	=	non-plastic sandy silt
SP	=	uniformly graded medium sand
SWCC	=	soil water characteristic curve
t	=	time
U	=	Upper catchment percent runoff
U-ACL	=	UNSAT-H simulations for ACL site with in-situ measured climate data
U-AUS	=	UNSAT-H simulations for Austin site with climate data from NOAA
UHCF	=	Unsaturated hydraulic conductivity function
USCS	=	Unified Soil Classification System
USEPA	=	United States Environmental Protection Agency
WPY	=	wet precipitation year
z	=	vertical coordinate
α	=	curve fitting parameter for van Genuchten (1980) function
β	=	curve fitting parameter for relating WPY annual water balance variable to APY annual water balance variable
γ	=	curve fitting parameter for relating WPY annual water balance variable to APY annual water balance variable
γ_d	=	dry unit weight
Δ	=	change
ΔS	=	change in soil water storage
θ	=	volumetric water content
θ_r	=	residual water content
θ_s	=	saturated water content

λ	=	curve fitting parameter for modified Brooks Corey function (Ahuja et al. 2000)
ω	=	gravimetric water content

INTRODUCTION

BACKGROUND ON LANDFILL COVERS

Municipal solid waste (MSW) generally consists of packaging products, food waste, newspapers, plastic waste, glass waste, etc. It may sometimes also consist of construction and demolition waste and non-hazardous industrial waste. Landfills are common mode of disposing such community waste. Landfills are usually isolated spots outside city or community establishments where the waste is permanently sequestered to prevent environmental pollution.

There were 1908 MSW landfills reported in the year 2011 by United States Environment Protection Agency (USEPA 2013). The closure of these solid waste containment facilities is regulated by Resource Conservation and Recovery Act (RCRA) or superseding state regulations in United States. The regulations typically require to cap these waste containment facilities with a final cover depending on the liner system below MSW. The primary function of the final covers is to limit the infiltration escaping into MSW, limit fugitive landfill gas emissions and odors, and provide sustainable foundation for future infrastructure development such as recreational sites, golf course or parking lot.

The constructed final cover usually consists of several layers of soil to meet USEPA requirements. USEPA (1992) regulations mandate inclusion of a hydraulic barrier layer in the final cover having a low hydraulic conductivity ($<10^{-5}$ to 10^{-7} cm/s). Such covers are usually called conventional covers and may either consist of low conductivity natural soils or "composite barrier" of a geo-membrane underlain by a low conductivity soil depending on the landfill liner. Sometimes, geo-synthetic clay liners (GCLs) are used to serve as the hydraulic barrier in final covers.

The hydraulic barrier layer for conventional covers is regulated to have a minimum thickness of 45 cm (1.5 feet). A soil erosion layer to sustain native plant growth and prevent erosion of barrier layer must also be overlain the hydraulic barrier layer. This soil erosion layer usually has a minimum thickness of 15 cm (6 inch).

EARTHEN LANDFILL FINAL COVERS

RCRA regulations guidelines allow the use of alternative designs in lieu of conventional covers subject to the same performance criterion. The alternative designs of landfill covers or alternative final covers (AFCs) or earthen final covers (EFCs) must perform "equivalent" to conventional covers, for limiting maximum percolation to a value smaller than or equal to the conventional cover [CFR 258.60(b) (1), United States Government 2002]. The alternative designs are also expected to meet other criteria of conventional covers, e.g., erosion protection, etc.

Nyhan et al. (1990) presented one of the earliest studies on the performance of EFCs located in arid regions of New Mexico. Subsequently over the last two decades, several field-scale studies had been conducted in several parts of United States to identify design variables controlling the performance of EFCs (Benson and Khire 1995; Nyhan et al. 1997; Khire et al. 1997; Ward and Gee 1997; Albright et al. 2004; Mijares et al. 2012). EFCs store infiltration water in wet season and release it to atmosphere as evapotranspiration (ET). EFCs depend on land-surface interaction processes and hence are often also called water balance covers or evapotranspirative covers (ETCs).

EFCs offer lucrative advantages over the conventional covers for MSW landfills due to the absence of geo-membrane layer. The construction cost of EFCs usually amounts to 35% to 72% of construction cost of conventional covers. The total cost of EFCs can range from approximately $176,000 to $ 275,000 per hectare depending on soil type, soil thickness, climate and other design

variables (Hauser et al. 2001). High cost of conventional covers had also been attributed to geo-membrane layer which alone accounted for 23% to 31% of the total construction cost (Hauser et al. 2001). EFCs also offer long term advantage as a sustainable design system which is self-renewing with lower post closure maintenance costs. The repair of EFCs is also cheaper wherein a depression or hole can be easily back filled without compromising overall performance of the cover unlike a hole in geo-membrane of conventional cover which can be relatively expensive to repair. EFCs are also subject to bio-technical reinforcement from deep plant roots and less susceptible to slope failures and top soil erosion.

EFCs can be monolithic covers consisting of a single storage layer to store precipitation and release it as ET. Capillary barriers are EFCs generally similar in design to monolithic covers but underlain with an additional layer of coarse grained soil. The coarse grained soil offers a capillary break increasing the storage capacity of storage layer and consequently reducing deep percolation. Capillary barriers function only in arid or semiarid climates (Khire et al. 2000).

NUMERICAL MODELING

Permitting of EFCs often requires field-scale demonstration of the final cover to evaluate its equivalency with the conventional cover. However, because the construction of field-scale test section to demonstrate equivalency is often expensive and requires a few years of data collection numerical models are routinely used to model and design EFCs. Numerical models represent the physical processes of soil atmosphere interactions in the form of mathematical equations which can be numerically solved to simulate water flow in soil layers over several years. The physical processes implemented in numerical models are broadly categorized under water balance process and unsaturated flow process. These models vary in complexity depending on the method of

solution. Some models are simple box models of source or sink terms while others implement algorithms to solve partial differential equations.

Several field studies have been conducted that demonstrate Richards' equation (Richards 1931) based water balance models such as UNSAT-H provide relatively accurate predictions of MSW landfill cover hydrology (Khire et al. 1997; Khire et al. 1999; Bohnhoff et al. 2009; Mijares and Khire 2012). HYDRUS, Vadose/W, HELP and LEACHM are other commercial and public domain models which have been extensively used for modeling landfill covers (Khire et al. 1997; Ogorzalek et al. 2008; Bohnhoff et al. 2009). Water balance of landfill cover system is usually expressed as

$$D = P - ET - R_O - \Delta S \tag{I-1}$$

where, D is deep drainage or percolation, P is precipitation, ET is evapotranspiration, R_O is runoff and ΔS is change in water storage of soil layers. Precipitation is input parameter while evapotranspiration, surface runoff, change in soil water storage and deep drainage are predicted parameters based on meteorological data, soil properties, and soil geometry using Richards' equation. Richards' equation in its 1-D form is expressed as

$$\frac{\partial \theta}{\partial t} = \frac{\partial}{\partial z}\left[K(h)\frac{\partial \psi}{\partial z} + K(h) \right] - S_t(z,t) \tag{I-2}$$

where, θ is volumetric water content, h is matric suction head, K(h) is unsaturated hydraulic conductivity at matric suction h, S_t is source or sink term, t and z are time and space co-ordinates. UNSAT-H utilizes finite-difference scheme to solve Richards' equation while Vadose/W and HYDRUS use finite-element schemes. Precipitation, evapotranspiration and surface runoff are physical processes modeled at the surface of the top soil layer resulting in change of deep drainage over a specified time period.

Runoff is usually one of the second largest components of predicted water balance while percolation is usually the smallest. However percolation, in-spite of usually being the smallest component of water balance, is also the single most important parameter for evaluating performance of EFCs. A small error in the prediction of surface runoff can result in either an over or under prediction of percolation. Hence, accurate measurement of runoff is necessary to calibrate the numerical models.

Scanlon et al. (2002) simulated water balance of engineered covers located in Texas (0.14 acre) and Idaho (0.002 acre) with HELP, HYDRUS, SHAW, SoilCover, SWIM, UNSAT-H and VS2DTI and concluded that overestimation of runoff affected all water balance parameters including percolation. Bohnhoff et al. (2009) modeled a 200 m^2 (0.05 acre) monolithic cover underlain by a lysimeter at Altamont, California using UNSAT-H, VADOSE/W, HYDRUS and LEACHM and identified over prediction of surface runoff as the key reason for underestimation of soil water storage and percolation. Khire et al. (1999) monitored the performance of a capillary barrier located in the semiarid region of western United States using an instrumented lysimeter having areal extent of 0.05 acre. They indicated that UNSAT-H (Fayer 2000) estimated zero runoff resulting in over prediction of percolation. Although surface runoff has been repeatedly cited as a critical parameter for improving accuracy of water balance predictions, field validation of runoff has been carried out at a scale that is much smaller than the catchment scale (Khire et al. 1997; Albright et al. 2004; Bohnhoff et al. 2009).

Surface runoff measured from majority of field studies on landfill covers has been carried out on test sections with less than or equal to 20 m (65 ft) length and 200 m^2 (0.05 acres) areal extent (Albright et al. 2004). However, the storm water collection system for landfill final covers usually consists of contour drains with catchment area of each drain much larger than 200 m^2.

Runoff travels several hundred meters in a swale before it is shed off from the cover. Hence in order to validate the numerical models, catchment scale measurement of runoff is more appropriate.

OBJECTIVES

The key objectives of this dissertation are to: (1) measure surface runoff from an earthen final cover (EFC) which has been in service for approximately six years; (2) validate numerical models used for design of EFCs against field measured hydrology data set; and (3) use validated models to predict regional scale variation in annual and daily runoff for Texas.

METHODOLOGY

A catchment scale EFC was instrumented in semiarid climate of Austin, Texas to measure surface runoff and soil water contents. Austin Community Landfill (ACL) located in Travis County, Texas was capped with a final cover approximately ten years ago in 2004-2005. Hence, the surface and soil conditions at ACL were deemed to represent long term conditions.

The monitoring system was divided in two parts: 1) runoff measurement system; and 2) soil water measurement system. Two adjacent catchments were instrumented to measure surface runoff and soil water contents. The upper catchment had areal extents of 30 m × 122 m (0.9 acres) while the lower catchment had areal extents of 53 m × 122 m (1.6 acres). A berm of approximately 30 cm in height, prevented surface water runoff from the upper catchment flowing into the lower catchment. Storm water monitoring system was installed in mid-December 2011 when the vegetation on the cover was relatively scant due to antecedent drought year (6 percentile annual precipitation). The soil water monitoring system was divided in three nests of embedded sensors for the two catchments. Upper catchment had top nest and lower catchment had middle and bottom

nests with co-located suction and water content sensors at several depths below the ground surface. The data collected over twenty three months was used to evaluate the key variables governing measured surface runoff from EFC at a catchment scale. UNSAT-H and RZWQM were subsequently used to model measured runoff and identify their limitations in accurately representing the hydrological processes of EFCs. The validated UNSAT-H model was used to predict surface runoff from EFC with different soil types and different thicknesses for several stations in Texas.

DISSERTATION ORGANIZATION

This dissertation has been organized into three sections. The three sections are three standalone technical papers.

The first paper elaborates on the intricacies involved in the design of dedicated surface runoff collection system for two catchment scale landfill cover test sections. The instrumentation helped to identify factors affecting surface runoff from landfill covers over cyclic dry and wet seasons at a catchment scale. The paper uses several field evidences and natural hill slope runoff hydrology principles to explain engineered hill slope EFC runoff hydrology.

The second paper presents a comparison of the measured surface runoff with the predicted surface runoff from UNSAT-H and RZWQM. The comparison of measured and predicted data set helped to identify the strengths and limitations in the implementation of hydrological processes in numerical models.

Third paper uses UNSAT-H model to predict regional scale water balance for Texas. Surface runoff predictions for EFCs as a function of soil type and thickness in different climates of Texas are compared. A best fit polynomial correlation was established between precipitation and predicted surface runoff for different climatic regions in Texas. Peak daily surface runoff map

and daily runoff-precipitation correlations were developed as an aid for the design of storm water collection system of EFCs in Texas. Correlation of predicted water balance variables for a wet year with average year were also developed at a regional scale of Texas which can serve as guidance for preliminary EFC designs.

PAPER 1: SURFACE RUNOFF AT AN INSTRUMENTED CATCHMENT SCALE EARTHEN FINAL COVER

ABSTRACT

Water balance models are routinely used to design earthen final covers (EFCs) for landfills. Percolation is usually the smallest and most important component of these water balance models. Accurate prediction of other large water balance parameters such as runoff and evapotranspiration is thus necessary for accurate percolation prediction. However, limited literature is available to calibrate models with catchment scale runoff. With the objective to measure runoff from engineered clay layers, two catchment scale EFCs were instrumented in semiarid climate of Austin, Texas. Upper and lower catchments had an areal extent of 3716 m^2 (0.9 acre) and 6503 m^2 (1.6 acre), respectively. Co-located water content and suction sensors were used to measure temporal soil-water variations at several depths in different locations of both catchments. Customized high capacity tanks (11.3 m^3 and 19 m^3) fitted with actuator valves were used to measure runoff. Upper catchment with lower runoff length recorded more total runoff (12%) than lower catchment (8%) over the twenty three months of monitoring period. A seasonal variation in cumulative monthly percentage runoff was observed for both catchments, which peaked to 22.5% and 17% for upper and lower catchments respectively in early spring 2012. It continuously declined thereafter to a minimum value of 7.6% and 5.5% by September 2013 and again increased to 12% and 8% in November 2013. Percentage runoff increased with daily precipitation intensity for Winter 2012 and Fall 2013, but no correlation could be established in other intermediate seasons. Thus daily precipitation intensity could not be used as an independent variable to predict runoff for all seasons at Austin. Seasonal variation in total precipitation, average precipitation intensity, precipitation return period, antecedent soil water content, PET/P and vegetation cover

were the several reasons responsible for the observed seasonal runoff variation. Runoff recorded for EFC was primarily governed by 'fill and spill' mechanism with saturated and connected plots contributing to the total runoff. No subsurface runoff was recorded at ACL due to hydraulically disconnected plots at catchment scale. Vegetation affected overland flow connectivity, surface roughness and infiltration to reduce runoff.

INTRODUCTION

Earthen final covers (EFCs) are used in lieu of conventional final covers to restrict infiltration into MSW depending on the underlain bottom liner system (Albright et al. 2004). Monolithic covers and capillary barriers are the two primary designs used as EFCs. These designs utilize natural hydrological processes to limit deep percolation and usually offer economic benefits over conventional covers (Hauser et al. 2001). EFCs contain compacted fine grained soil layer of high storativity which stores infiltration and releases it back as evapotranspiration (ET). EFCs are permitted by regulators as long as it is demonstrated that the EFC is hydraulically equivalent to the conventional cover [CFR 258.60(b) (1), United States Government 2002]. EFCs are routinely permitted in arid climate of United States but only on case-by-case basis in sub-humid or humid climates. The primary reason for limited acceptance of EFCs in sub-humid or wetter climates is lack of long term field data on hydrologic performance of these covers, which served as the primary motivation for this study.

Equivalency demonstration of EFCs usually involves construction of field-scale test section and monitoring it for a few years which is expensive. Hence water balance and unsaturated flow numerical models such as HELP, UNSAT-H, VADOSE/W, LEACHM, HYDRUS have been used for the last two decades for design of EFCs. Several small scale lysimeter studies on existing landfill covers of areal extent less than 0.1 acre have been conducted to validate the numerical

solution of Richards' equation (Richards 1931) from these models. Khire et al. (1999) simulated a lysimeter in dry climate of western United States with UNSAT-H, and observed over prediction of percolation due to under-estimation of measured runoff water. Scanlon et al. (2002) simulated lysimeters located in Texas (0.14 acre) and Idaho (0.002 acre) with HELP, HYDRUS, SHAW, SoilCover, SWIM, UNSAT-H and VS2DTI. Overestimation of runoff by all the codes was identified to affect percolation and other water balance variables. To achieve reasonable landfill water balance predictions, Scanlon et al. (2005) had to calibrate saturated hydraulic conductivity of 50 mm surface crust to accurately predict runoff. Ogorzalek et al. (2008) cautioned against runoff predictions by LEACHM, HYDRUS, and UNSAT-H for accurate water balance modeling of a capillary barrier cover in Polson, Montana. Recently, Bohnhoff et al. (2009) also reported over prediction of runoff as the key reason for error in soil water storage and percolation predictions by UNSAT-H, VADOSE/W, HYDRUS and LEACHM for a 200 m^2 (0.05 acre) lysimeter of monolithic cover at Altamont, California. Further, runoff travel distance for test sections of the majority of field studies were less than 20 m (Khire et al. 1999; Albright et al. 2004). But runoff travels several hundred meters in a swale before being shed off from the cover. Hence in order to validate numerical models, catchment scale measurement of runoff is more appropriate.

OBJECTIVE

An existing EFC located in semiarid climate (Austin, Texas) was instrumented with the primary objective of measuring catchment scale runoff. Data was collected for almost two years to identify the parameters which control runoff. The study also aimed at validating water balance numerical models. The numerical modeling is presented in paper 2.

Austin Community Landfill (ACL) located at Austin, Texas was instrumented in mid-December 2011. Austin has a semiarid climate, with a 50 year mean annual precipitation of about

84 cm (33 inch). EFC and surface water management system at ACL were installed about six years ago before the site instrumentation. The hydraulic properties of the cover soils and the natural vegetation were thus deemed to represent typical long-term conditions.

FIELD SETUP

A typical cross-section of the instrumented landfill cover is shown in Fig. 1-1. The cover consisted of 90 cm thick (3 ft) compacted native clay overlain with 15 cm (0.5 ft) thick top soil to support vegetation. The landfill cover is sloped at 1V to 4H. The clay soil is a high plasticity clay (CH) as per USCS and served as the soil water storage layer. As per the compaction specifications, the clay was compacted in lifts to achieve greater than or equal to 95% of standard proctor effort and 0% to 5% of the optimum moisture content. Table 1-1 presents the geotechnical soil properties for the clay soil.

Shelby tube samples of 7 cm (2.8 inch) diameter were collected from upper 20 to 30 cm (8 to 12 inch) of the cover. The samples had an average saturated hydraulic conductivity of 10^{-6} cm/sec measured using flexible wall permeameter (ASTM D5084). Storage layer was constructed to an average saturated hydraulic conductivity of 5×10^{-8} cm/sec (Golder Associates Inc. 2005). However, after long-term exposure to several cycles of drying and wetting the saturated hydraulic conductivity of the storage layer had increased to 10^{-6} cm/sec (Fig. 1-2). Although in-situ hydraulic conductivity of the vegetative layer was not measured, it was expected to lie in the range of 10^{-3} to 10^{-2} cm/s due to coarse gradation of the soil and macro-pores formed due to root penetration. Two storm water catchments of the cover were instrumented to measure runoff (Fig. 1-1). The upper catchment had an areal extent of 30 m × 122 m (0.9 acres) while the lower catchment had an areal extent of 53 m × 122 m (1.6 acres). A berm, approximately 30 cm in height, prevented runoff from the upper catchment flowing into the lower catchment. The storm water measurement

system was installed in mid-December 2011 when the vegetation on the cover was relatively scant. The key reason for scant vegetation at the time of installation was relatively low precipitation during the preceding year. In the year 2011, the site received a total precipitation of about 50 cm which is 6 percentile based on 50 year historical precipitation record.

INSTRUMENTATION

Upper catchment was instrumented with one nest (top nest) while the lower catchment had two nests of co-located suction and water content sensors at different depths (Fig. 1-1). Storage layer water content sensors in middle and bottom nests were connected in mid-February 2012. The middle nest and bottom nest vegetative layer sensors located at 15 cm (6 inch) depth were added in early November 2012. The top nest water content sensor at 30 cm (12 inch) depth went bad in June 2012 and the middle nest water content sensor at 90 cm (36 inch) depth went bad in January 2013.

Water content sensors were calibrated for vegetative layer and storage layer soils. Suction sensors used in the current study can measure matric suction accurately within the range of 10 kPa to 2,500 kPa (Campbell Scientific Inc. 2009). Precipitation was measured with a tipping bucket. Sensors to measure solar radiation, relative humidity and air temperature were also installed at the site.

Runoff Measurement

Instrumentation to measure runoff consisted of these three components: 1) runoff collection system; 2) runoff transportation system; and 3) runoff storage system. Runoff from each catchment was collected with a collector pad located at lowest elevation of the catchment. The collector pad consisted 7.5 m wide by 7.5 m long and 15 cm thick pea gravel underlain by 1.5 mm thick HDPE

Table 1-1. Geotechnical properties of storage layer soil

Geotechnical Property	**Storage Layer**
USCS Classification	CH
D_{10} (mm)	0.000026
D_{50} (mm)	0.00048
D_{60} (mm)	0.00098
C_u	38
C_c	0.47
Liquid Limit (LL)	75
Plasticity Index (PI)	49
Optimum Water Content (%) for Standard Proctor	26.8
Maximum Dry Density (kN/m^3) for Standard Proctor	14.61
Saturated Hydraulic Conductivity (7 cm diameter Shelby Tube Samples)	10^{-6}
In-situ Dry Density (kN/m^3) of Shelby Tube Sample	15.2 to 16.5

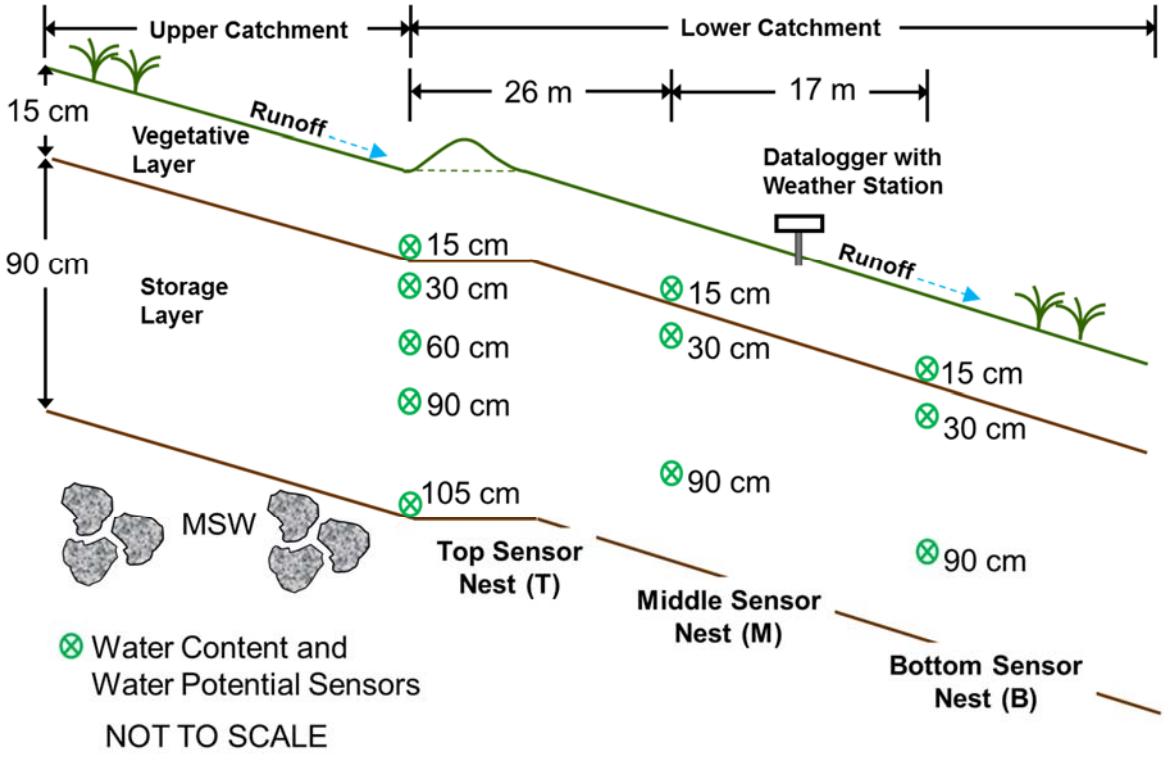

Figure 1-1. Cross section of instrumented final cover at Austin Community Landfill

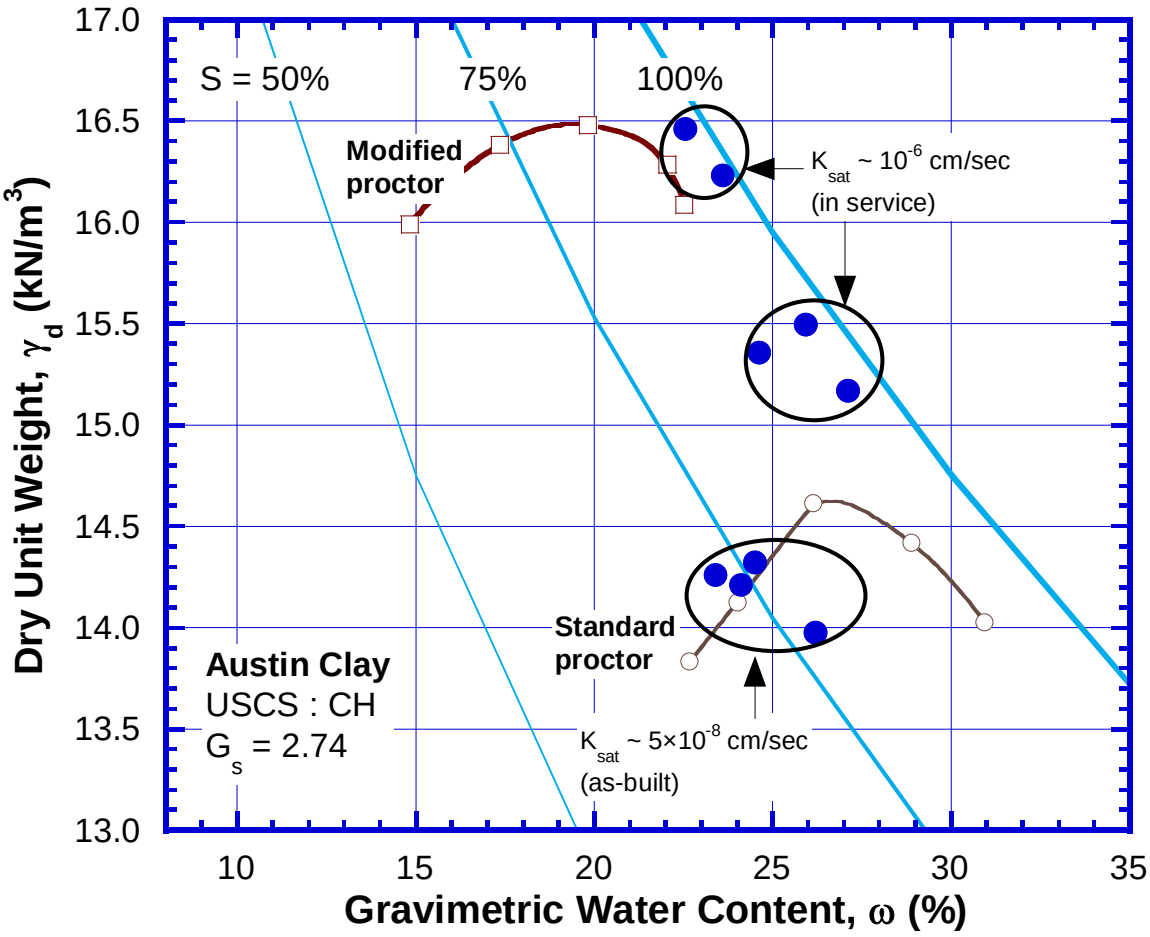

Figure 1-2. Proctor compaction curve and saturated hydraulic conductivity of storage layer

geomembrane (Fig. 1-3). A customized hydraulic network of 15 cm diameter (6 inch) PVC pipes was installed to transport runoff water from the collector pads to an above ground storage tank (AST) under gravity gradient. The pipe diameter and sloping layout were designed for free water flow from a maximum runoff intensity of 2.5 cm/hr. The runoff intensity was never exceeded during the monitoring period. Pea gravel on the collector pad acted as a hydraulic filter preventing pipe clogging due to debris flow usually accompanying runoff water from a landfill cover. The upper catchment drained into a 2.3 m tall and 11.3 m^3 (3,000 gallon) AST. A larger 19 m^3 (5,000 gallon) capacity and 3.6 m tall AST was used to collect runoff from the lower catchment. Water level in each tank was recorded in real time with two piezometers. Actuator valve fitted to each tank was used to automatically drain the tanks whenever water level surpassed a pre-defined threshold (Fig. 1-4). A datalogger smartly activated the actuator valves depending on the piezometer water levels and thus prevented the tank overflow.

Filling while Draining - Runoff Measurement

During the course of a typical runoff collection event, a condition frequently arose wherein the actuator valve would be draining the tank while the runoff was concurrently flowing into the tank. This event was abbreviated as "filling while draining." During filling while draining events, change in piezometer level cannot be used directly to calculate runoff. Hence, equation 1-1 was used to estimate volume of water entering the tank during filling while draining.

$$\frac{dh_l}{dt} = \frac{a_c}{A} C_v \sqrt{2gh_l} - k \qquad (1\text{-}1)$$

where, a_c is cross-sectional area of the drainage valve, A is cross-sectional area of the tank, g is acceleration due to gravity, h_l is water level measured by piezometer at time t and k is average rate of water flow into the tank when the drainage valve is close. Constriction coefficients (C_v) were

Figure 1-3. Runoff collector pad for lower catchment

Figure 1-4. Actuator controlled valve draining upper catchment AST

independently estimated for each tank by draining the tanks when there was no inflow. Table 1-2 presents a summary of constant parameters used to solve equation 1-1. Equation 1-1 was solved in MATLAB with ODE45 and CFTOOLBOX to estimate net inflow (k) and consequently net runoff for filling while draining period.

A typical storm event on 18 February 2012 resulted in 3.3 cm precipitation. During the 9 hours of precipitation event, the upper catchment tank auto-drained 5 times (Fig. 1-5a) and consequently recorded 1.1 cm (33%) runoff (Fig. 1-5b).

Turbidity Measurement

Turbidity sensors were installed in both upper and lower tanks on 7 November 2013 (Campbell Scientific Inc. 2013; Bringhurst and Adams 2011) to quantify the mass of eroded sediments in surface runoff from each catchment. Turbidity sensors use near infra-red light and two photo diodes to measure optical scatter due to the suspended particles. The sensor response reported in Nephelometric Turbidity Units (NTU), depends on the size, composition and shape of suspended particles. Turbidity sensors were calibrated using top soil from the test sections. Soil passing through No. 100 sieve (0.15 mm) was used for calibration. Higher concentration of suspended top soil resulted in more light scattering and consequently higher NTU (Fig. 1-6). A polynomial curve fit related suspended soil concentration with the measured NTU for ACL

$$y = -204.4 + 896.1x - 233x^2 + 31x^3 \qquad y \leq 8000 \text{ NTU} \tag{1-2}$$

where, y is Nephelometric Turbidity Unit (NTU) and x is top soil concentration in (gm/L). In order to minimize the bias in sensor readings due to residual tank sediments from old runoff events, the tanks were flushed with the standing water after each runoff storm. Upper catchment turbidity sensor went bad on 17 July 2013 and no turbidity values were available there afterwards for the upper catchment.

Table 1-2. Constant parameters used in filling while draining equation

Parameter	Value
a_c	182 cm^2
A (upper AST)	45250 cm^2
A (lower AST)	52718 cm^2
C_v (upper AST)	0.65
C_v (lower AST)	0.75
g	981 cm/s^2

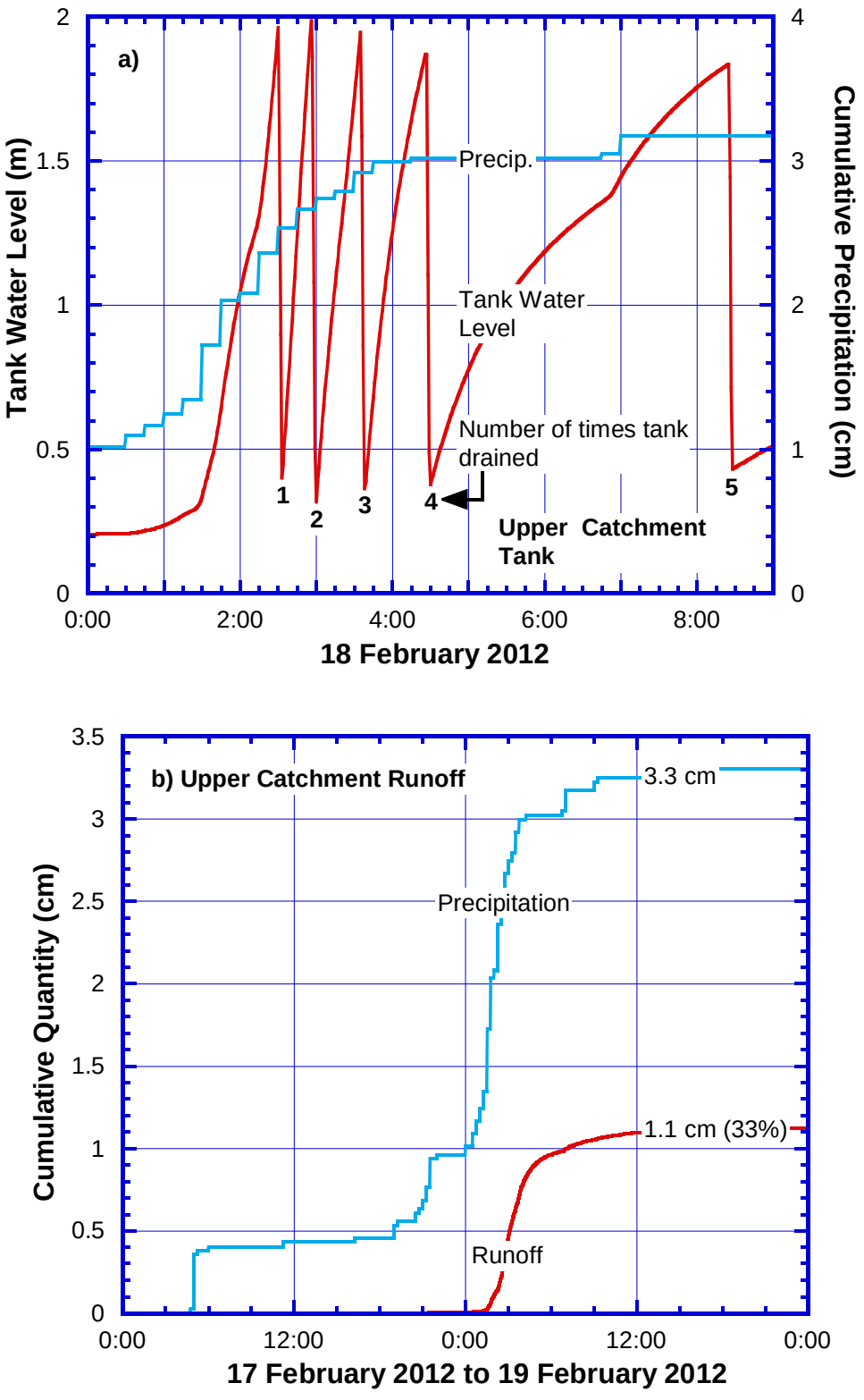

Figure 1-5. Tank drain cycles (a) and cumulative runoff (b) on 18 February 2012 from upper catchment

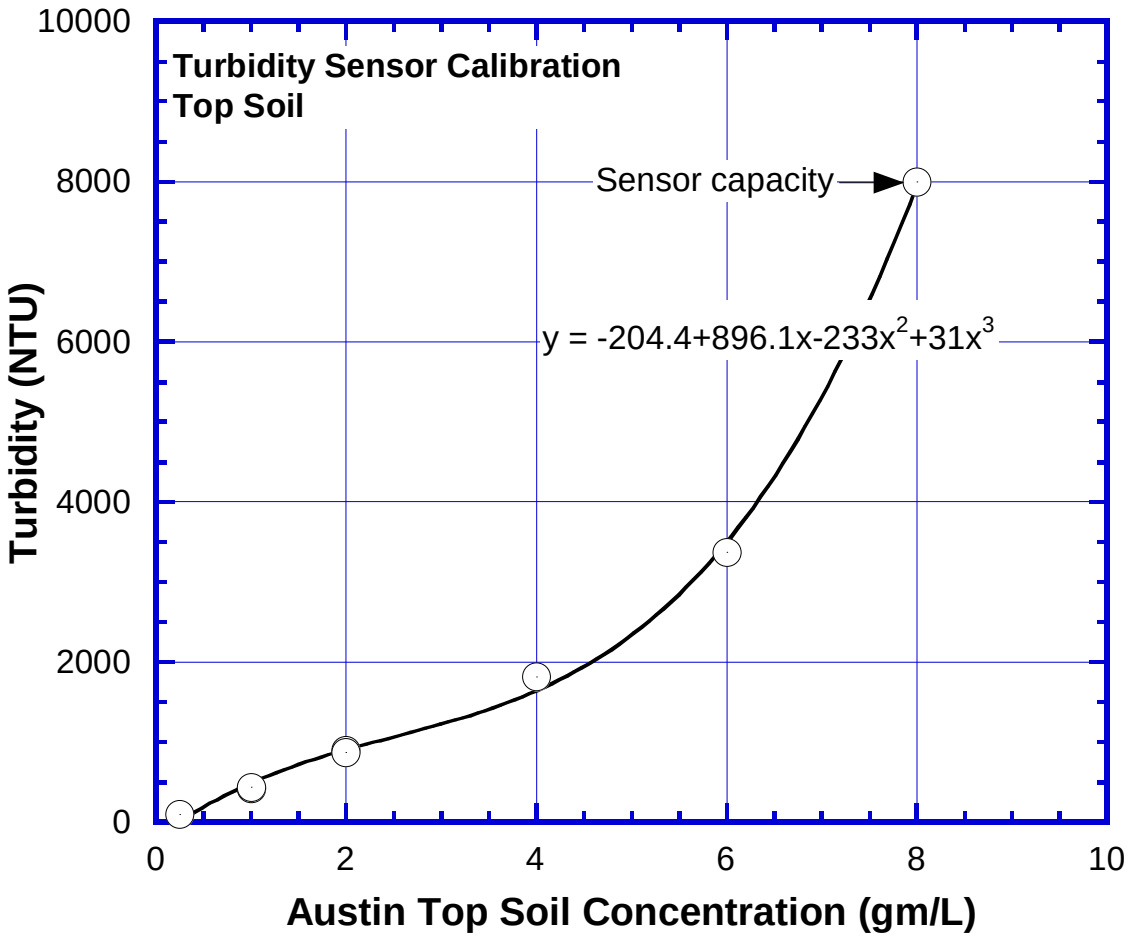

Figure 1-6. Turbidity sensor calibration plot for top soil

RESULTS AND DISCUSSION

Daily precipitation intensity was defined as the total precipitation within twenty four hour period. The total precipitation was proportionally scaled to twenty four hour period for runoff storm events lasting more than twenty four hours. For the ease of discussion in this paper, the monitoring period was divided in three seasons. Season 1 (three months) was assumed to last from 15 December 2011 to 20 March 2012 with 39 cm precipitation (PET/P=0.8), followed by Season 2 (eighteen months) which started on 21 March 2012 and ended on 20 September 2013 with 109 cm precipitation (PET/P=3.0). Season 3 (two months) was the last season and extended from 21 September 2013 to 15 November 2013 with 29 cm precipitation (PET/P=0.8). Return period was defined as the time period between successive precipitation events of the same magnitude. Hence, a precipitation with relatively low return period is more likely to occur on a typical day than a precipitation with high return period. Soil moisture content was normalized to degree of saturation, which is frequently used in lieu of soil moisture for the ease of discussion.

A total precipitation of 177 cm was recorded for twenty three months of the monitoring period starting 15 December 2011. 81 cm precipitation occurred in the first twelve months and 96 cm precipitation occurred over the remaining eleven months. Penman equation was used to calculate a total potential evapotranspiration (PET) of 377 cm (PET/P = 2.1) for twenty three months with UNSAT-H (Fayer 2000). Out of total 132 storms recorded in twenty three months, only 29 storms produced runoff. ACL received an average precipitation of 0.26 cm/hr over the monitoring period. The maximum and minimum precipitation for the same period were 6.1 cm/hr and 0.02 cm/hr, respectively. Upper catchment recorded a maximum event runoff of 4.7 cm (from 6.6 cm precipitation), a minimum event runoff of 0.007 cm (from 1.4 cm precipitation), and average event runoff of 0.7 cm. Lower catchment recorded a maximum event runoff of 3.6 cm

(from 6.6 cm precipitation), a minimum event runoff of 0.002 cm (from 1.4 cm precipitation), and average event runoff of 0.5 cm in the monitoring period.

Measured Runoff at Annual Time Scale

Upper catchment recorded a total of 21 cm (12% of precipitation) runoff and lower catchment recorded a total of 14 cm (8% of precipitation) runoff for the monitoring period (Fig. 1-7).

Albright et al. (2004) measured the water balance over multiple years for several instrumented landfill covers. The field instrumentation and monitoring was part of a nation-wide Alternative Cover Assessment Project (ACAP) spread across seven states of United States consisting of 10 m × 20 m (0.05 acre) lysimeter test sections. The sites with PET/P ratio between 2 to 5 were classified as semiarid by Albright et al. (2004). Hence in the current study, ACL at Austin (PET/P=2.1) was designated as a semiarid region. As a part of ACAP, monolithic covers were constructed in Altamont (California), Boardman (Oregon) and Sacramento (California). Altamont, California (PET/P = 3) in semiarid region, with average annual precipitation of 36 cm recorded highest total runoff value at 9.3% of precipitation. EFC at Altamont consisted of a 45 cm (1.5 feet) thick vegetative layer and 60 cm (2.0 feet) thick storage layer. Both layers were constructed with compacted clay (USCS classification-CL) of mean saturated hydraulic conductivity of 1.7×10^{-7} cm/sec. Although, ACL site received almost double the annual precipitation than Altamont, yet runoff at both locations was in the same range for similar PET/P. Intuitively, higher precipitation at ACL was expected to generate higher runoff. It may however, be noted that the catchment size and runoff lengths at ACL site were at least an order greater than Altamont lysimeter which resulted in longer residence time for re-infiltration and consequently decrease in net runoff.

Boardman, Oregon received an average annual precipitation of 22.5 cm (PET/P≈4) but did not record any runoff. Sacramento, California received an average precipitation of 44 cm/yr (PET/P≈3) and recorded 7.6% and 4.8% runoff from 108 cm and 245 cm thick soil covers, respectively (Albright et al. 2004). Lower runoff at these sites than ACL can be attributed to lower precipitation and higher PET relative to ACL.

Upper and lower catchments had same horizontal travel distance along the swale of 122 m but different runoff lengths of 30 m and 53 m, respectively before runoff entered runoff collection pads. Longer runoff travel distance resulted in greater infiltration due to higher detention time and greater surface roughness (Duley and Ackerman 1934; Mutchler and Greer 1980). Consequently, smaller total runoff was recorded for the lower catchment.

Wilcox et al. (1997) measured runoff for two catchments at Pajarito Plateau of north central part of New Mexico. The larger catchment with area of 485 m^2 recorded 0.6% runoff while the smaller catchment with area of 355 m^2 recorded 2.0% runoff. Merz and Plate (1997) observed lower runoff from larger contributing area for loess soil in Menzingen, Germany. Moreno-de las Heras et al. (2010) recognized greater overland flow residence time as the critical variable governing re-infiltration which resulted in less runoff for larger catchments. Similar observation was made by Mayor et al. (2011) wherein they identified inverse power law relationship between total runoff and contributing area for semiarid Mediterranean climate. Gomi et al. (2008) measured 2 to 10 times higher runoff from small plots of 1 m^2 area compared to large plots (approximately area of 200 m^2), for the same monitoring period. Hence, findings of this study on engineered hill slopes are similar to several field-scale runoff studies on natural hill slopes reported in literature.

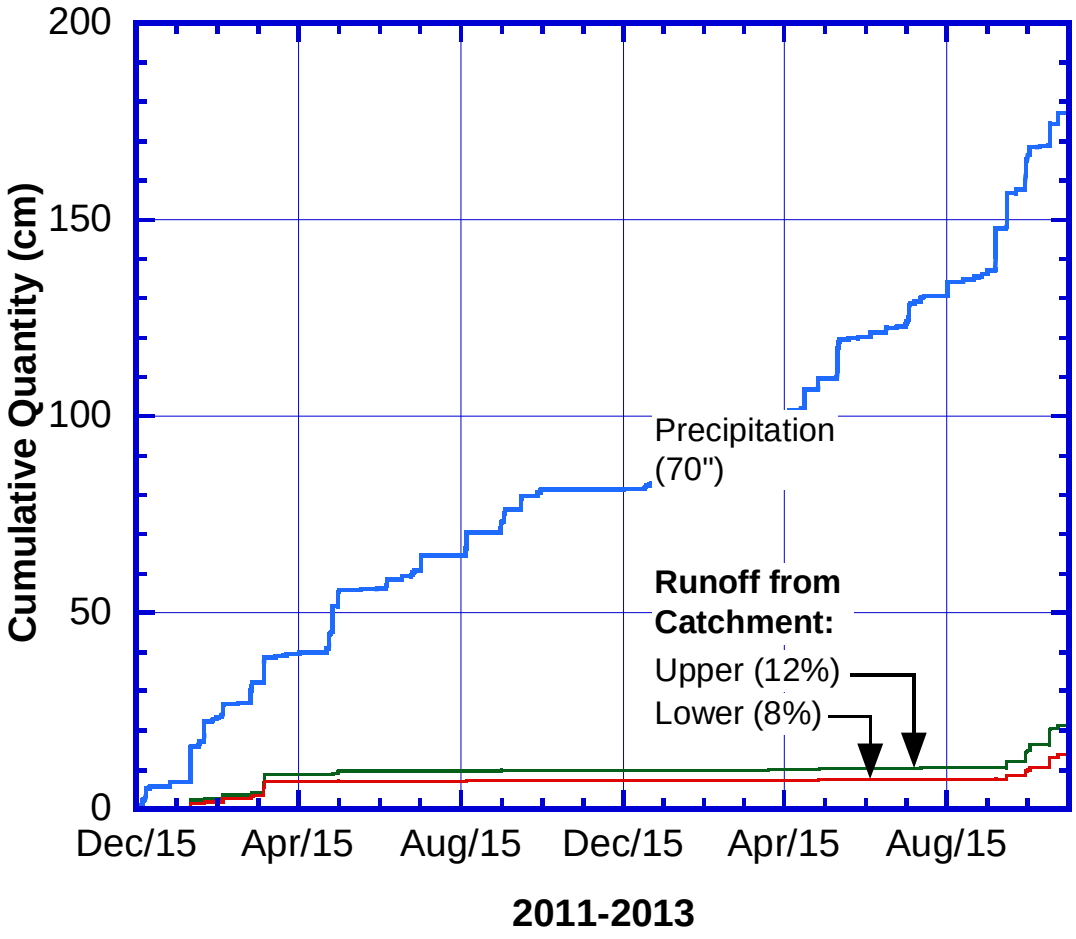

Figure 1-7. Measured runoff at Austin Community Landfill

Measured Runoff at Monthly and Seasonal Time Scale

Upper catchment consistently generated greater cumulative runoff than lower catchment for all seasons (Fig. 1-7). Further, the measured cumulative runoff varied non-linearly with respect to cumulative precipitation over successive seasons in the twenty three months of monitoring period. A steep rise in cumulative runoff during Season 1 immediately after instrumentation was observed which was followed by a minimal increase in cumulative runoff for Season 2. A steep rise in cumulative runoff with cumulative precipitation was again measured in Season 3. Cumulative percentage monthly runoff for the upper and lower catchment peaked at 22.5% and 17% by April 2012 but decreased to minimal values of 7.6% and 5.5% in September 2013, respectively (Fig. 1-8). However, cumulative percentage monthly runoff again recorded an increase in the following months and finally ended at 12% and 8% for upper and lower catchment respectively, by November 2013. A similar variation in percentage runoff was observed by Palleiro et al. (2014) for humid climate of Mero catchment in north-west Spain. Minimal runoff was observed at Mero catchment in early autumn, which quickly peaked to a maximum value in late autumn and gradually recessed to a minimal value through winter, spring and summer, in that order. Uneven seasonal precipitation distribution with maximum precipitation events in autumn and winter seasons, amounting to 70% of total precipitation, were attributed as the reasons responsible for non-uniform seasonal runoff at Mero catchment.

Measured Runoff at Event Time Scale

Similar to monthly and annual time scale, upper catchment with smaller runoff travel distance produced more runoff than lower catchment for all individual storm events except for the storm on 9 March 2012 (Fig. 1-9). The storm on 9 March 2012 recorded smaller 8.2% runoff for

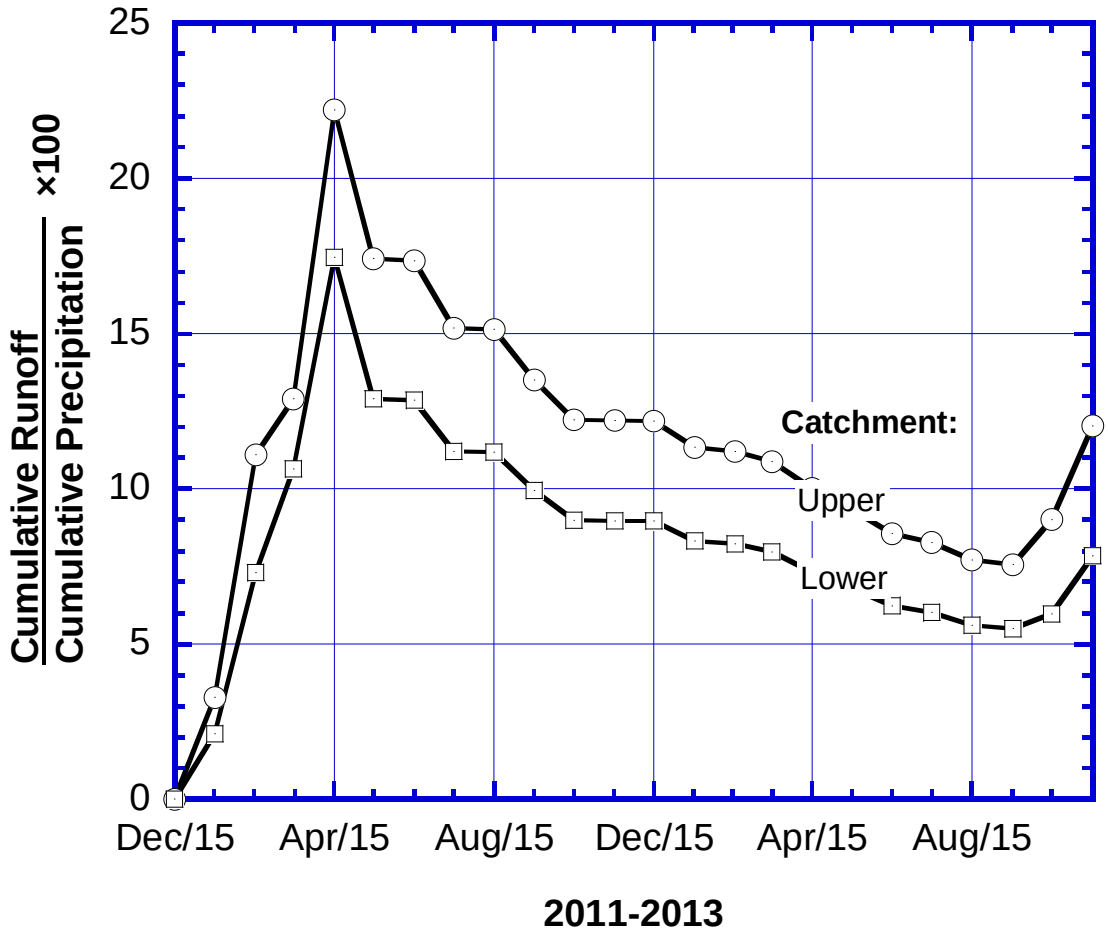

Figure 1-8. Measured cumulative monthly runoff to precipitation ratio for ACL

upper catchment than lower catchment runoff (14%). This anomaly was presumed to be interplay of several spatially varying factors such as precipitation, soil hydraulic properties, antecedent soil moisture, and localized surface depressions. These factors affect infiltration and runoff connectivity at a catchment scale hill slope and consequently affect total recorded runoff (Wood et al. 1986; Dunne et al. 1991; Imeson et al. 1992; van de Giesen et al. 2000; Vigiak et al. 2006). Local discontinuities in catchment overland flow paths also rendered detention time and runoff volume independent of slope length and resulted in smaller recorded runoff volume from longer slope length (Gomi et al. 2008). However, detailed spatial and temporal instrumentation necessary to quantify these variables was not done at ACL.

The two geometrically similar rectangular catchments also had similar vegetation cover for the monitoring period. An attempt was thus made to relate runoff response of the two catchments at event time scale. Surprisingly, the percentage runoff for individual events from upper catchment and lower catchment were found to be related by a power law irrespective of spatial-temporal variation of soil hydraulic properties, antecedent volumetric water content and surface depressions (Fig. 1-9). The governing correlation equation was found to be

$$L = 0.48(U^{1.06}) \quad (1\text{-}3)$$

where, L is lower catchment percent runoff and U is upper catchment percent runoff. Coefficient of fit (R^2) for the above equation was 0.97, reflecting a high degree of correlation between runoff generated by upper and lower catchments. Such high correlation also reinforced the hypothesis that at the catchment scale intra-catchment runoff hydrology of two hill slopes was similar and net runoff volume from each EFC hill slope was primarily controlled by runoff travel distance.

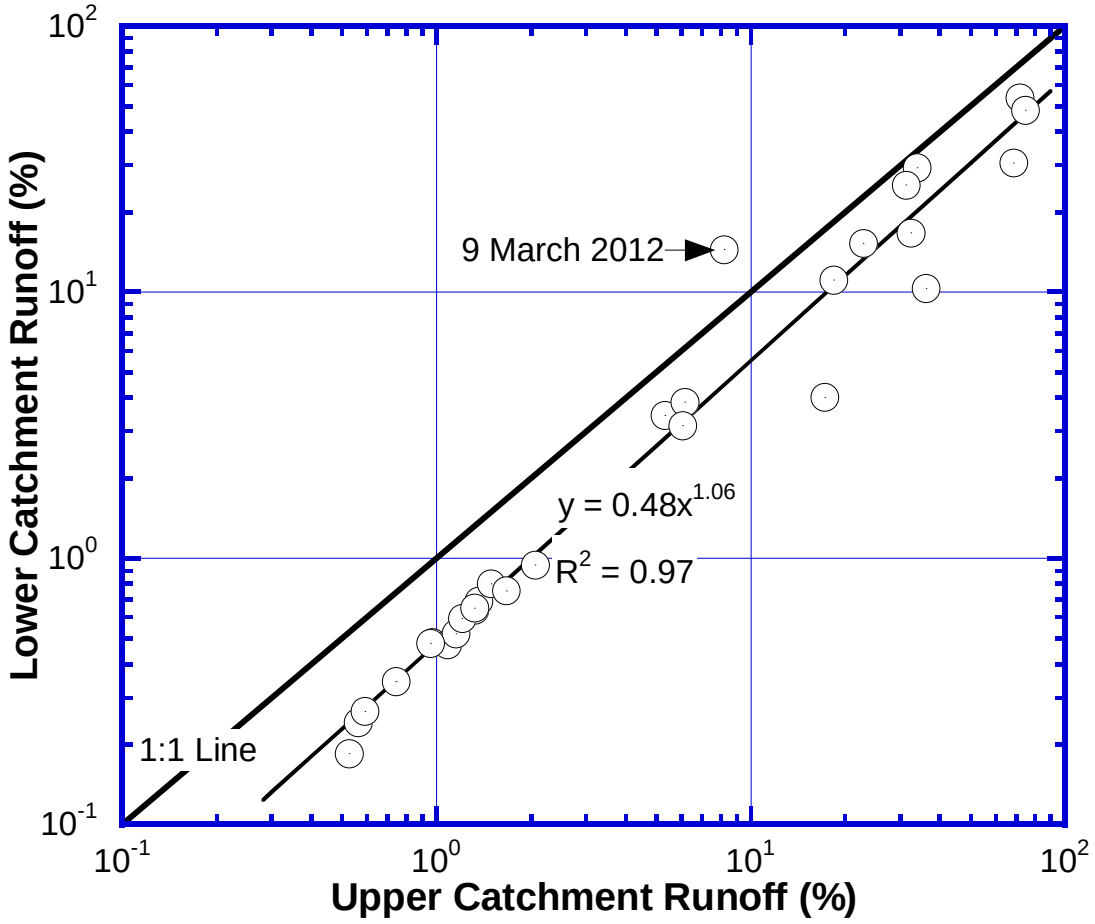

Figure 1-9. Comparison of measured runoff from lower catchment and upper catchment

Scale Dependent Runoff - Cause and Effect

Non-uniform behavior of runoff-precipitation relationship at different temporal scales were ascribed to several factors: (1) total precipitation, (2) average precipitation intensity, (3) precipitation return period, (4) antecedent soil water content, (5) PET/P and (6) vegetation cover. A summary of the relative effects of these factors in different seasons is presented in Table 1-3.

Austin site experienced 32 cm precipitation during Winter 2012, but only 11 cm in the same months of the following year (Winter 2013). Less precipitation consequently recorded lower total runoff in Winter 2013 (1% runoff) than Winter 2012 (13% runoff) for the upper catchment. Average precipitation intensity was the second factor. Higher average precipitation intensity generates more runoff because more water in excess of soil water capacity was available for runoff. Season 1 and Season 3 received average precipitation of 14 cm/month which was more than double the average precipitation intensity of 6 cm/month recorded in Season 2 resulting in relatively less runoff in Season 2. Precipitation return period was the third factor governing seasonal runoff volume. Season 1 and Season 3 had relatively smaller return period of daily precipitation intensity than Season 2 resulting in more daily precipitation and consequently more runoff (Fig. 1-10). Antecedent soil water content was the fourth factor governing change in measured runoff volume. Lower antecedent soil water content resulted in more infiltration and less runoff in Season 2 than in Season 1 and Season 3. The change in vegetative layer soil water contents of the upper catchment generally varied from 0.01 cm^3/cm^3 to 0.1 cm^3/cm^3 in Season 1 and Season 3 due to different precipitation intensities (Fig. 1-11). However, 70% precipitation events in Season 2 recorded greater than 0.1 cm^3/cm^3 change in volumetric water content for similar daily precipitation intensities implying relatively more infiltration and less runoff in Season 2. Similar observation was also made for middle and bottom nests of lower catchment. Lower antecedent soil

water content also resulted in relatively poor hydraulic connectivity of individual runoff source plots ("hot spots") within the catchment resulting in lower runoff length and less net catchment runoff (Gomi et al. 2008). The concept of runoff connectivity is discussed later in the paper. Fifth, potential evapotranspiration varied with season resulting in non-uniform evaporation loss. Season 1 and Season 3 with PET/P value of 0.8 experienced less evaporation loss than Season 2 (PET/P = 3.0) suggesting that more precipitation was available for runoff in Season 1 and Season 3. Finally, vegetation density almost doubled from Season 1 to Season 2 (Fig. 1-12). Increase in vegetation density increased canopy abstraction, opportunistic infiltration due to denser roots, surface roughness for runoff transport, and soil water loss as transpiration which resulted in lower catchment runoff.

Lower runoff generated in Season 2 at ACL was in line with observations of Hewlitt and Hibbert (1967) at Appalachian Mountains of western North Carolina, where runoff was produced from saturated plots and the runoff contributing area decreased with decreasing soil water contents. Hence, high antecedent in-situ soil water contents resulted in relatively small infiltration and greater runoff for Season 1 and Season 3 (Dunne and Black 1970a, b; Weyman 1973; Johnson and Gordon 1988; Francis and Thornes 1990; Bochet et al. 2006). Further, Austin experienced a draught prior to the instrumentation in 2011, with only 6 percentile precipitation (50 cm) in 2011. This resulted in scant vegetation canopy and consequently very little plant abstraction losses which resulted in greater runoff in Season 1 (Fig. 1-12). Denser plant foliage in Season 2 increased opportunistic infiltration due to denser root penetration thereby decreasing net runoff. Denser vegetation also increased surface roughness for runoff transport. Hence, opportunistic infiltration and surface roughness incrementally lowered the net recorded runoff at the catchment scale EFC (Leys et al. 2010; Abrahams et al. 1994; Dunne et al. 1991). van de Giesen et al. (2000, 2005)

Table 1-3. Relative effect of parameters governing catchment surface runoff

Season	**1**	**2**	**3**
Date	15 December 2011 to 20 March 2012	21 March 2012 to 20 September 2013	21 September 2013 to 15 November 2013
Measured runoff	High	Low	High
Total precipitation	High	Low	High
Average precipitation intensity	High	Low	High
Precipitation return period	Low	High	Low
Antecedent soil water content	High	Low	High
PET/P	Low	High	Low
Vegetation cover	Low	High	High

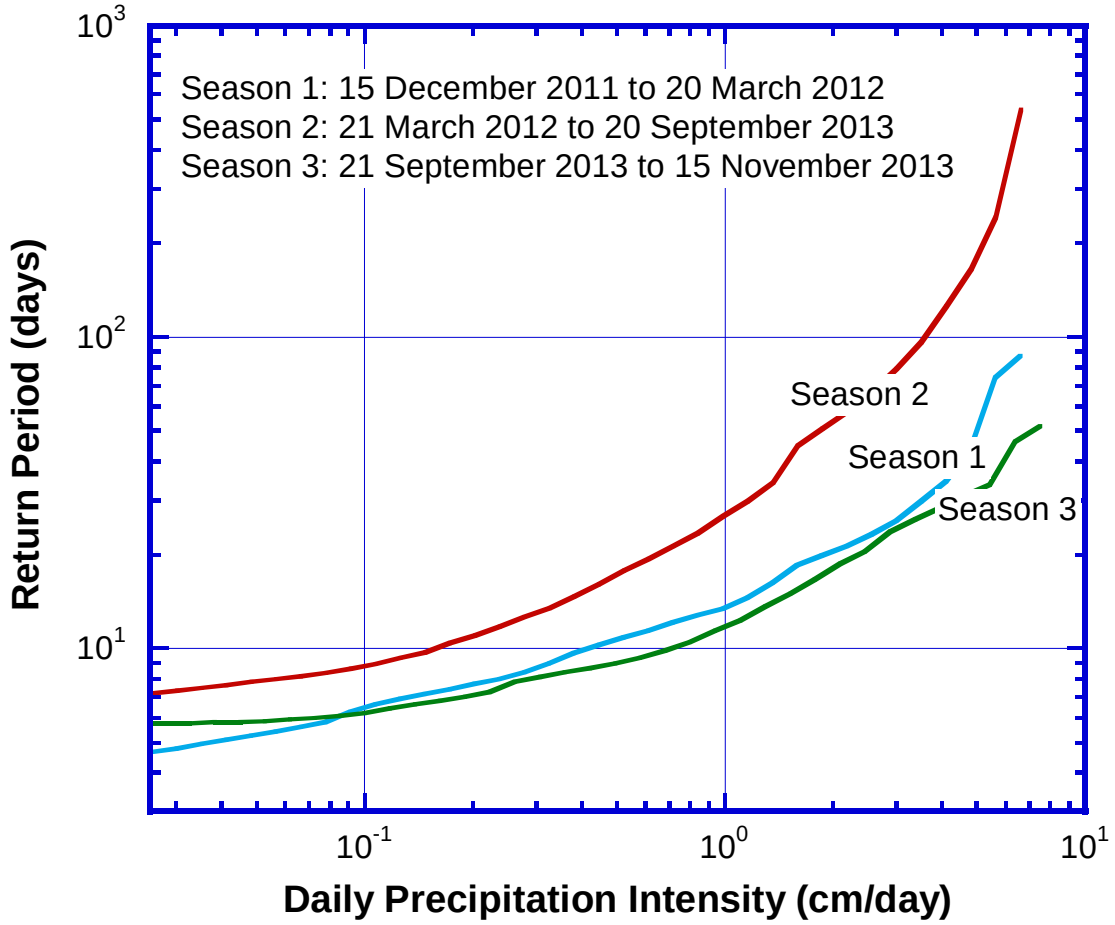

Figure 1-10. Seasonal variation of daily precipitation intensity return period at ACL

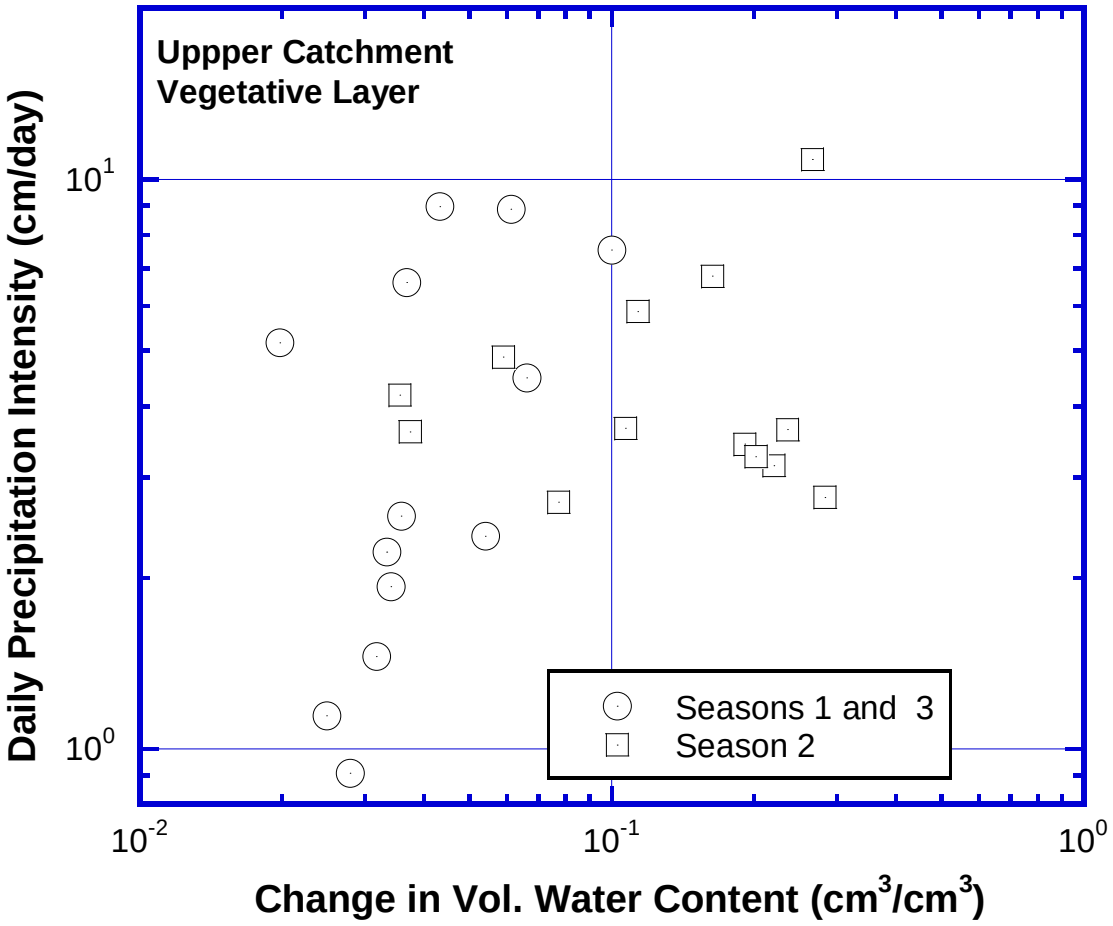

Figure 1-11. Change in volumetric water content of vegetative layer in upper catchment with daily precipitation intensity for Seasons 1 and 3 versus Season 2

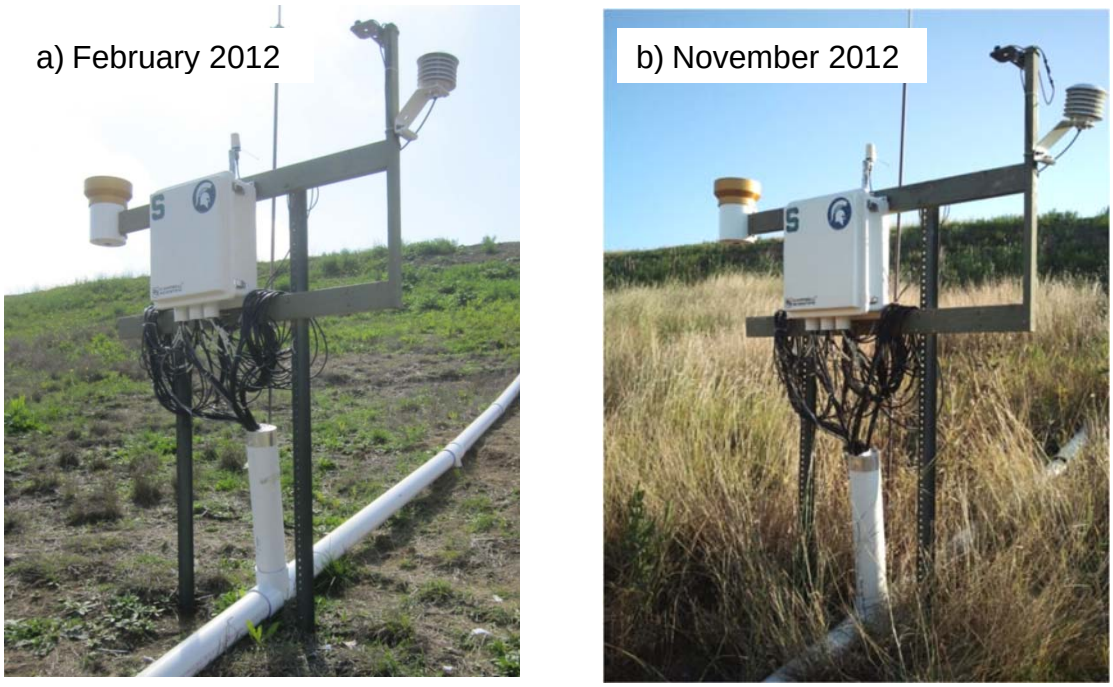

Figure 1-12. Increased vegetation cover from February 2012 to November 2012

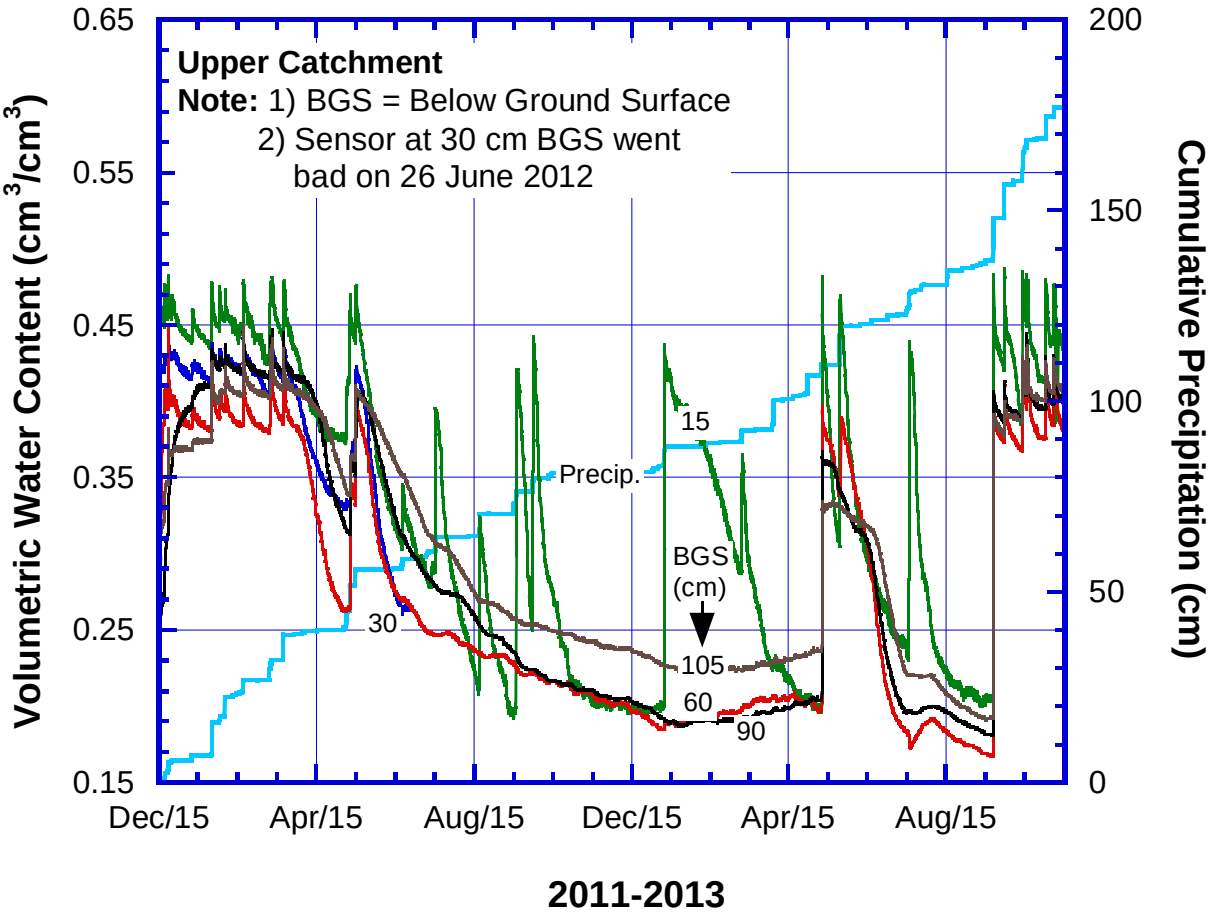

Figure 1-13. Measured volumetric water contents in upper catchment

highlighted the importance of increased residence time and consequently reduced unit area runoff due to more vegetation cover in West Africa. Similar effect of vegetation was also observed by Moreno-de las Heras et al. (2010) on a comprehensive study of twenty plots in Utrillas, Spain. Slopes with 60% vegetation cover generated 10% average runoff compared to 25% average runoff from 1% vegetative slope for the identical precipitation events in Utrillas. Hence, similar factors were found to govern engineered hill slope runoff processes at EFCs as reported in literature for the natural hill slopes.

Runoff recorded at ACL was found to be a complex interplay of the several factors described above. Relatively high antecedent soil water contents were recorded in Season 1 and Season 3 as presented in Fig. 1-13 (only top nest data is presented for the brevity of presentation). More water was available in Season 1 and Season 3 to fill unsaturated plots and generate runoff, due to combined effect of relatively more precipitation, average precipitation intensity, small precipitation return period and lower PET/P. Similarly, lower antecedent soil water contents in Season 2 was also the combined result of relatively large evaporation losses due to high PET/P and relatively large transpiration loss due to large vegetation density. Even until September 2013, 17 months after the observed high runoff in April 2012, the soil water contents had not risen to the levels they were in Winter 2012 (Fig. 1-13). Thus, analysis of any single factor in isolation from the other factors governing hill slope runoff hydrology easily lead to counter-intuitive erroneous conclusions. Two examples are presented here to highlight such complex interplay. In the first example, higher average precipitation intensity of 3.4 cm/day on 28 September 2012 in Season 2 was recorded than 2.2 cm/day precipitation on 18 February 2012 in Season 1, irrespective of similar total precipitation (Fig. 1-14). But an order higher runoff of 1.12 cm was recorded on 18 February 2012 (34% of 3.3 cm precipitation) compared to 0.03 cm runoff on 28 September 2012

(0.7% of 3.43 cm precipitation) for the upper catchment. Higher runoff was expected from higher daily precipitation intensity and an observation of higher daily precipitation intensity generating lower runoff is counter-intuitive. However, the interplay of greater vegetation cover and lower antecedent soil water content resulted in high intra-catchment losses and lower net recorded runoff on 28 September 2012 in Season 2 than 18 February 2012 in Season 1. In the second example, higher recorded runoff in Season 3 than Season 2 with similar vegetation cover was also counter intuitive. However, such observation can be explained with higher antecedent soil water contents and lower daily precipitation intensity return period of Season 3 than Season 2 (Fig. 1-10 and Fig. 1-13).

Daily precipitation intensity correlated positively with generated percent runoff (which is runoff expressed as fraction of daily precipitation), i.e., higher runoff was generated for higher daily precipitation intensity during Season 1 and Season 3 for both catchments. But no such correlation could be established for percent runoff generated in Season 2 (Fig. 1-15). An interplay of several factors governing runoff was responsible for such non-linear relationship as discussed earlier. Palleiro et al. (2014) identified non-linear relationship between runoff and precipitation with maximum correlation in winter (R^2=0.63) and no-correlation in summer season (R^2=0.01) due to seasonal variation of water table in Mero catchment of Spain. Precipitation and soil water dynamics were attributed as the reason for such observation. La Torre Torres et al. (2011) found seasonal variation in runoff-rainfall ratios with higher correlation in wet season than in dry season for Turkey Creek watershed of South Carolina, due to interplay of seasonal variation of precipitation amount, precipitation intensity and soil water storage. Hence as runoff-precipitation intensity correlation was season dependent and complex interplay of several factors, daily precipitation intensity could not be used as a standalone variable to predict runoff at ACL.

Soil Water Contents and Soil Suctions

Figures 1-13 presents the water contents at different depths for top nest of upper catchment. It was observed that the sensor in vegetative layer at 15 cm (6 inch) below ground surface, being near to the ground surface responded to precipitation events relatively quickly than the sensors at deeper depths. Further, in the top nest after the end of Season 1, soil started to dry out and sensors at deeper depths (60 cm and 90 cm) located in the clay storage layer recorded continual decrease in water contents until relatively high precipitation occurred in May 2013 in Season 2. The water content at deeper depths monotonically decreased from May 2013 to September 2013 due to relatively lower precipitation in Summer 2013. Only the top sensor (15 cm below ground surface) responded frequently to the precipitation events during Season 2. Higher daily precipitation intensity in Season 3 resulted in higher water content at all depths.

For brevity, measured matric suction values of only top nest are presented for brevity (Fig. 1-16). Suction sensors behaved in opposite fashion than water content sensors. During Season 1, the suction was relatively low (80 cm) corresponding to relatively high soil saturation recorded by the water content sensors. With the onset of Season 2 in late March 2012, the soil started drying and the suction sensors recorded an increase in values. It was further noticed that similar to the water content sensor located at 15 cm (6 inch) depth, the suction sensor in vegetative layer being nearest to the ground surface responded relatively frequently to the onset of precipitation and subsequent drying events, than the deeper suction sensors.

Subsurface Flow, Overland Flow and Runoff Connectivity

In order to understand subsurface runoff hydrology of EFCs, the subsurface flow at ACL was divided in high conductivity vegetative layer and low conductivity storage layer. The water depth in excess of observed precipitation on downhill locations, due to surface overland flow from

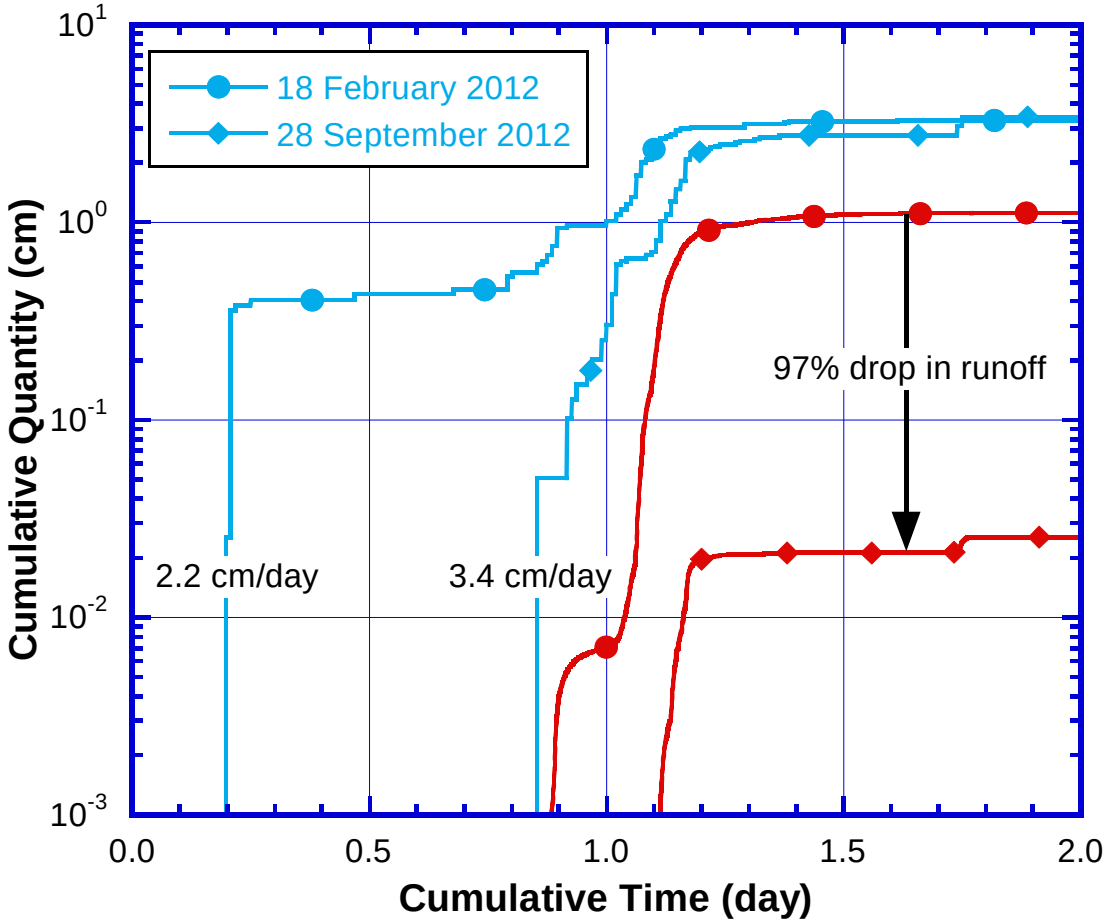

Figure 1-14. Change in cumulative runoff from February 2012 to September 2012 for similar cumulative precipitation

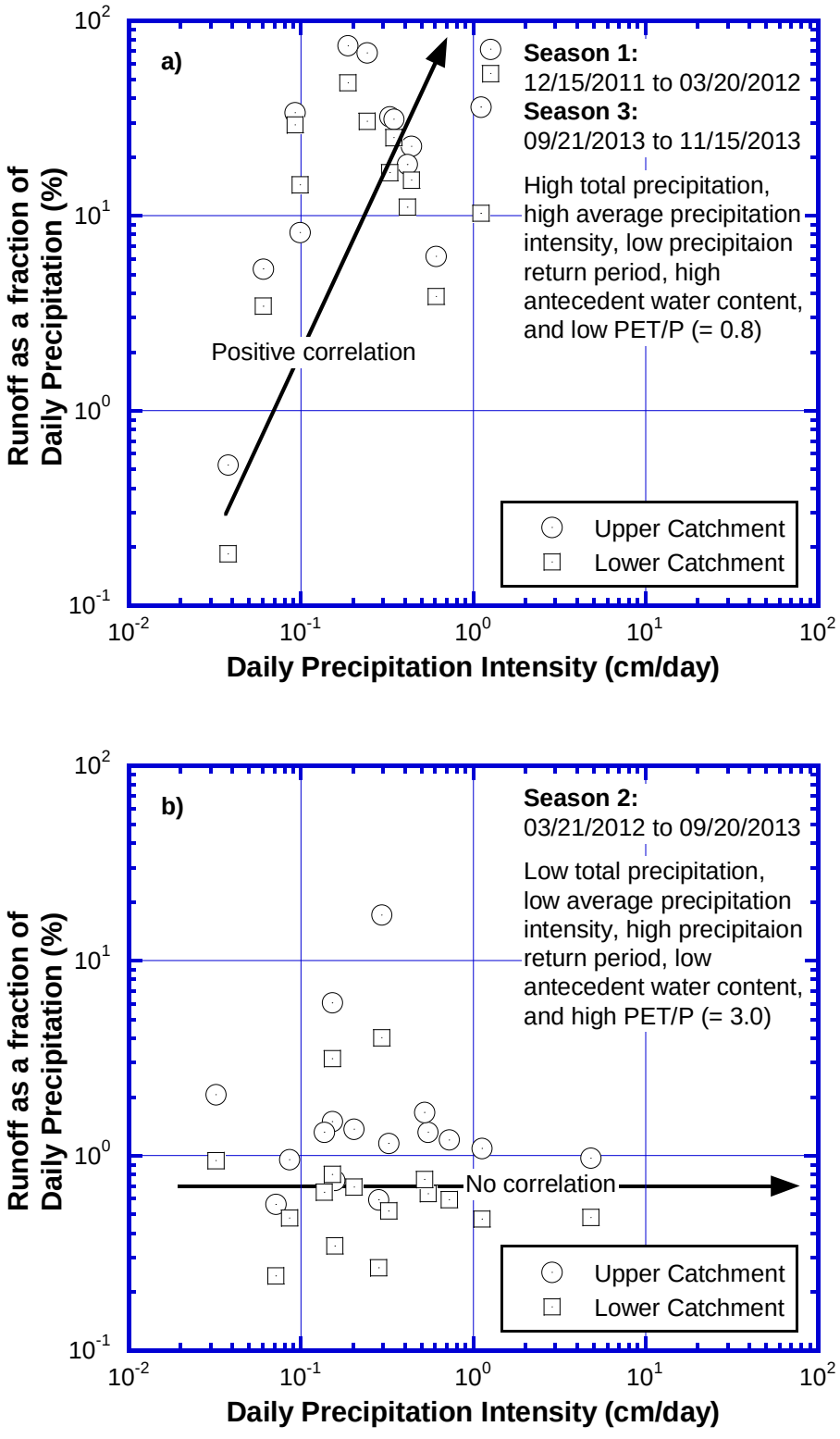

Figure 1-15. Correlation between measured percent runoff and daily precipitation intensity in different seasons

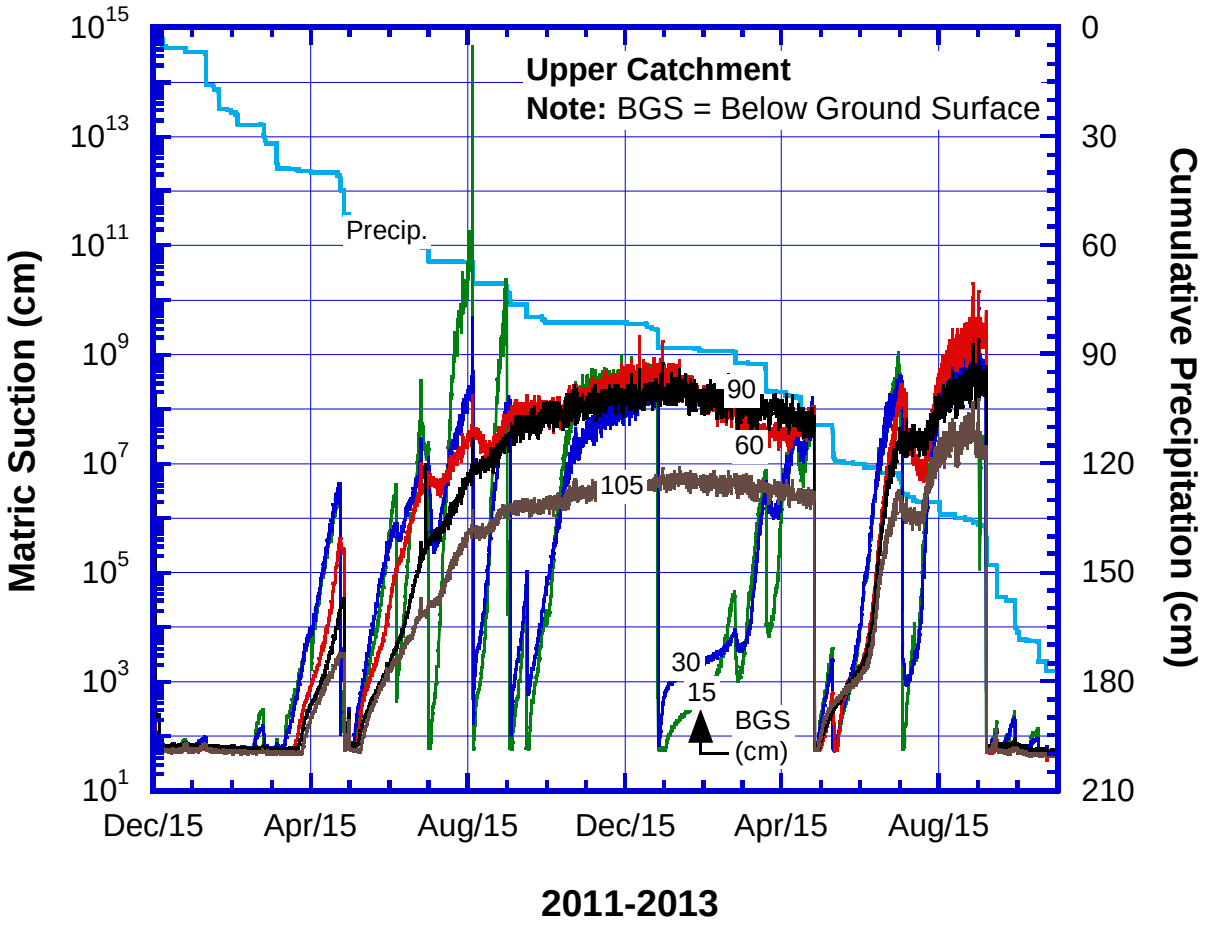

Figure 1-16. Measured soil matric suctions in upper catchment

uphill, for the same precipitation event was defined as precipitation overloading. Hence, middle nest of lower catchment at relatively higher elevation was subjected to less precipitation overloading, than bottom nest located at a lower elevation along the same vertical transect of the same catchment. Consequently more water was expected to infiltrate the bottom nest than the middle nest (Dunne et al. 1991). But higher soil water contents for middle nest than bottom nest were observed for all seasons (Fig. 1-17). This observation was also in contrast to findings of Hewlett and Hibbert (1967). According to Hewlett and Hibbert (1967), subsurface flow on hill slopes increases water content at downhill locations thereby saturating them. This saturated zone generates majority of runoff. The saturated zone expands uphill as more subsurface water from uphill becomes available for saturation creating a variable source area which generates runoff from hill slopes. Thus, according to variable source area concept, a runoff generating saturated wedge moves 'bottom-upwards' (Dunne and Black 1970a; Weyman 1973). This concept of lateral subsurface water flow from uphill to downhill formed the basis hill slope hydrology for several decades (Weyman 1973; Buttle and Turcotte 1999). Recently, an alternative 'top-down' approach underlined with 'fill and spill' mechanism has been proposed to explain hill slope hydrology (Spence and Woo 2003; Tromp-van Meerveld and McDonnell 2006a, b). According to fill and spill mechanism, isolated plots within a catchment must fill their soil water storage to saturation and then spill the excess water thereof for achieving connectivity and generate hill slope runoff. For low precipitation events in Panola Mountain Research Watershed of Georgia, isolated saturation plots uphill were disconnected from downhill saturation plots by intermediate unsaturated zones (Tromp-van Meerveld and McDonnell 2006b). As the precipitation exceeded a threshold value, the previously unsaturated plots were filled with water and created a dense network of connected saturated plots, which consequently recorded 75 times more subsurface

runoff than low precipitation events below the threshold precipitation. Consequently, Tromp-van Meerveld and McDonnell (2006b) argued that runoff generation and transport is a 3-D spatial process where lower elevation plots on a hill slope are not necessarily hydraulically connected to high elevation plots along the same vertical transect of the hill slope and consequently a two-dimensional transect analysis of hill slope runoff can be misleading in identifying runoff generation and runoff transport processes on natural hill slopes. The foregoing discussion makes an attempt to apply these subsurface runoff concepts from natural hill slopes to engineered landfill slopes of EFC at ACL.

As water content sensors were not installed in vegetative layer in Season 1, no definite conclusion can be made on subsurface lateral flow in vegetative layer of lower catchment during high runoff events of Season 1. However after November 2012, when the water content sensors in vegetative layer were installed, water content values in middle nest were always higher than bottom nest indicating minimal subsurface lateral recharge of vegetative layer from middle nest to bottom nest of lower catchment (Fig. 1-17a). Similar runoff dis-connectivity was also observed for storage layer of middle and bottom nests for Season 2 and Season 3 (Fig. 1-17b). A complex interplay of the lower hydraulic conductivity, relatively less precipitation and short storm durations allowed minimal lateral subsurface flow for Season 2 and Season 3 (Hewlett and Hibbert 1967). This finding was consistent with the findings of Albright et al. (2004) who measured lateral drainage as only a small fraction (0%-5%) of total water balance for plot scale lysimeters and concluded that barrier layer does not impact hydrology of conventional covers. Mijares and Khire (2012) measured negligible lateral flow (~0.5 cm) in one year of monitoring period from earthen cover lysimeter located in sub-humid climate of Detroit. Further, Freeze (1972) conducted sensitivity analysis in upstream-area modeling and evaluated a threshold conductivity of 0.001

cm/sec for subsurface flow to occur. Hence, in the absence of subsurface lateral flow in EFC, runoff recorded at ACL after Winter 2012 was primarily overland flow generated by fill and spill mechanism. Spence and Woo (2003) also observed the fill and spill mechanism in sub-arctic Canadian Shield where surface runoff was recorded only after filling the valley storage.

It may however be noted that the plot saturation due to fill and spill must be followed by spatial runoff connectivity to generate net runoff from the hill slopes (Tromp-van Meerveld and McDonnell 2006b; Gomi et al. 2008). Spatial variability in hydraulic conductivity, micro-topography, rainfall intensity, vegetation cover and runoff depth relative to surface roughness can constrain overland runoff flow connectivity on a hill slope (Dunne et al. 1991; El-Hassanin et al. 1993; Darboux et al. 2002; Mueller et al. 2007). Large surface roughness and more infiltration in vertical macro-pores of deciduous forest slopes resulted in high overland runoff dis-connectivity creating less runoff transfer and lower total recorded runoff volume as compared to sparse slopes of Japan (Gomi et al. 2008). Thus, local surface flow discontinuities presumably due to high vegetation cover hydraulically isolated middle nest from bottom nest and overland flow from middle nest did not feed the bottom nest. Consequently, middle nest and bottom nest were not connected hydraulically for the monitoring period after Winter 2012. Unfortunately, the soil water instrumentation at ACL was limited only to a single vertical transect and consequently sufficient data was unavailable to quantify the complex runoff processes at intra-catchment scale.

Runoff connectivity was also closely linked to non-uniform runoff-precipitation behavior at different temporal scale. Lower antecedent soil water contents in Season 2 resulted in relatively more water being used to fill the unsaturated plots (i.e., higher infiltration in Fig. 1-11) leaving insufficient water to connect isolated saturated plots to generate net hill slope runoff. Hence, lower

antecedent soil water content and poor runoff connectivity resulted in poor runoff-precipitation correlation in Season 2 (Fig. 1-15).

Runoff Generation Threshold

Runoff-precipitation relationship at ACL showed a threshold behavior at 0.8 cm/day precipitation intensity. No runoff was recorded at ACL site for precipitation less than 0.8 cm/day while 69% storm events greater than 0.8 cm/day recorded runoff irrespective of seasonal variation in total precipitation, average precipitation intensity, precipitation return period, antecedent soil water content, PET/P and vegetation cover (Fig. 1-18). A minimum precipitation was necessary for abstraction loss by plant canopy. In addition, a minimum precipitation was also required to fill local depressions for creating continuous overland flow paths and generate net runoff. Similar observation was reported at Japanese cypress natural slopes, where threshold precipitation of 1 mm to 1.5 mm in 20 minutes was necessary to fill local depressions and achieve a minimum infiltration before overland flow paths could hydraulically connect to create overland flow network (Gomi et al. 2008).

Fig. 1-19 presents antecedent degree of saturation of upper 30 cm cover soil in upper catchment versus daily precipitation intensity. It was observed that threshold daily precipitation intensity (0.8 cm/day) necessary to generate runoff was not affected by antecedent degree of saturation as runoff was recorded from upper catchment for several antecedent saturation values ranging from 40% to 90%. Generally 90% antecedent moisture saturation was necessary to generate runoff from precipitation intensity less than 2.0 cm/day, while antecedent degree of saturation did not significantly affect runoff generation for storm events with precipitation intensity greater than 2.0 cm/day. Precipitation intensity of 0.8 cm/day to 2.0 cm/day was generally sufficient to fill isolated plots with only 90% antecedent soil saturation and spill the remaining

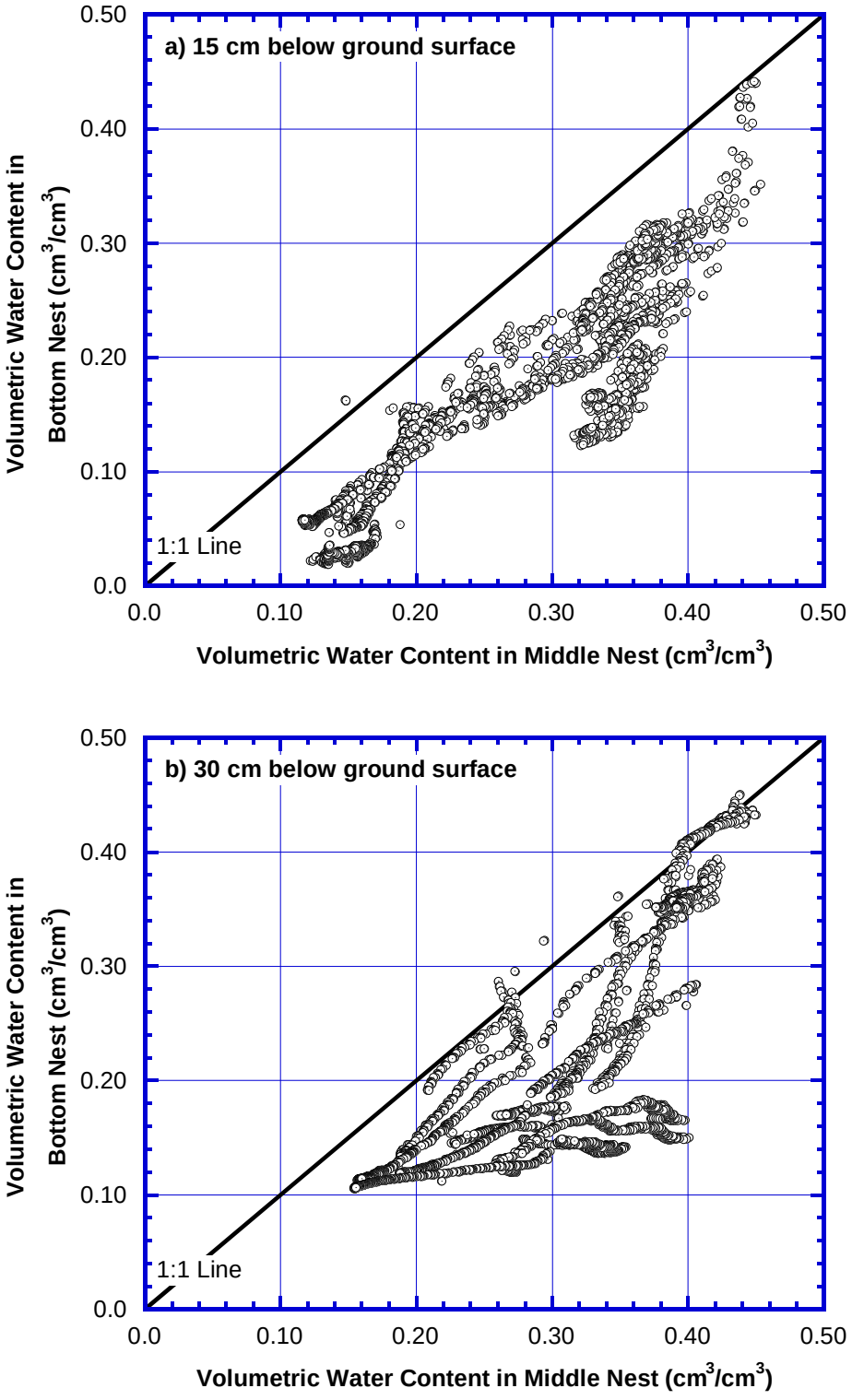

Figure 1-17. Measured volumetric soil water content at 15 cm below ground surface (a); and 30 cm below ground surface (b) of middle nest and bottom nest

precipitation to create connected flow paths for net runoff collection. However, precipitation intensities greater than 2.0 cm/day were able to fill, spill and hydraulically connect intra-catchment isolated plots with a wider range (40% to 90%) of antecedent saturation. Although no significant effect of antecedent saturation on threshold precipitation necessary to generate runoff was evident, yet antecedent saturation significantly affected the runoff volume generated and consequently runoff-precipitation relationship as discussed earlier and presented in Fig. 1-15.

Runoff Water Quality - Sediment Yield

Runoff from EFC was assumed to erode only top soil layer of 15 cm thickness of both catchments. Higher runoff in upper catchment generated higher sediment yield for upper catchment than lower catchment for same precipitation event (Fig. 1-20). Sediment yield decreased with plot length of vegetative slopes due to down slope re-infiltration of runoff which diminished travel distance of eroded soil sediments (Moreno-de las Heras et al. 2010). Higher sediment yield was observed for larger runoff events, as more overland runoff eroded more top soil (Fig. 1-21). Similar results were reported for vegetative slopes in Spain, where sediment yield decreased with runoff volume (Moreno-de las Heras et al. 2010). Measured runoff correlated to measured sediment yield with a power law for both upper and lower catchments (Fig. 1-21). More erosion was measured for lower catchment than upper catchment for total runoff below 0.055 cm but upper catchment recorded more erosion for runoff larger than the threshold value of 0.055 cm.

FUTURE RESEARCH

Although the data presented in this article is first-ever catchment scale runoff analysis for engineered hill slopes of EFCs, yet the current study was limited in soil water instrumentation along single vertical transect only. Hence the author acknowledges the limitation of discussion to

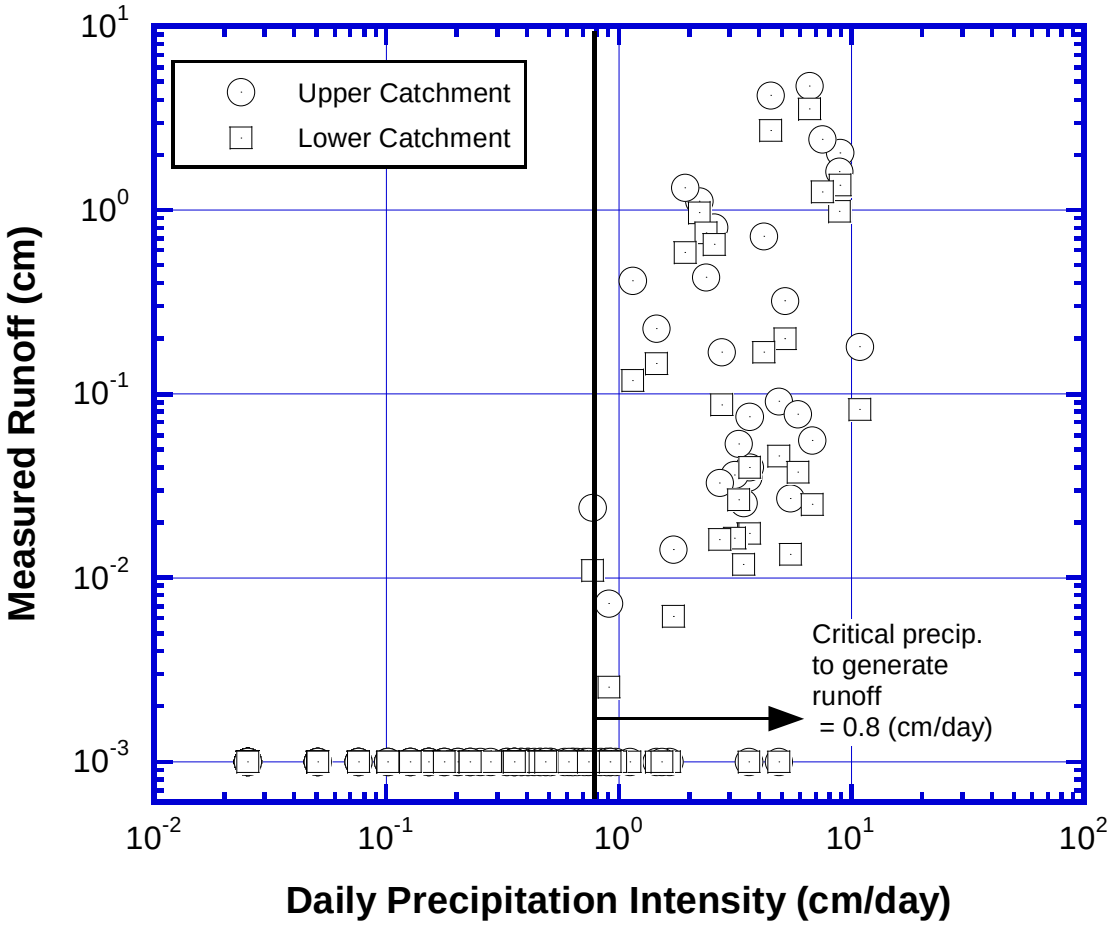

Figure 1-18. Measured runoff versus daily precipitation intensity at ACL

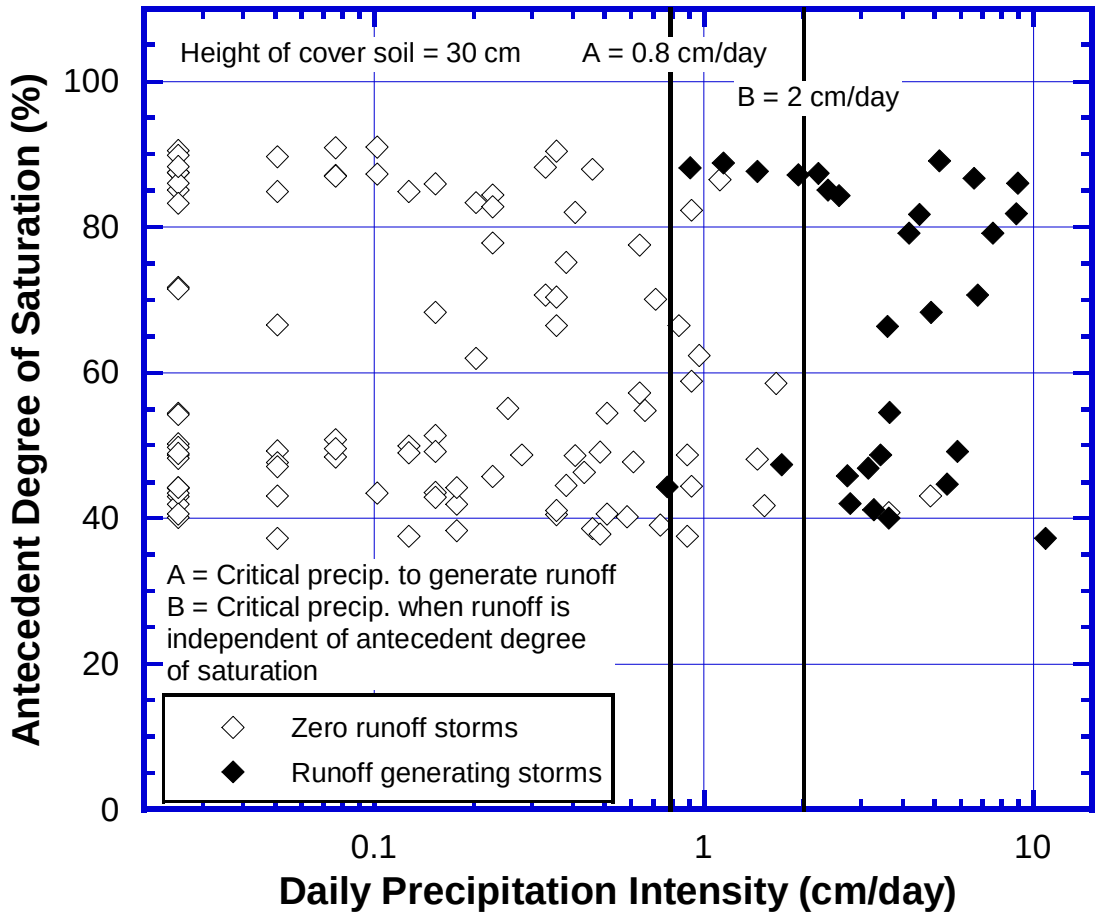

Figure 1-19. Variation of antecedent degree of saturation with daily precipitation intensity for 30 cm deep soil

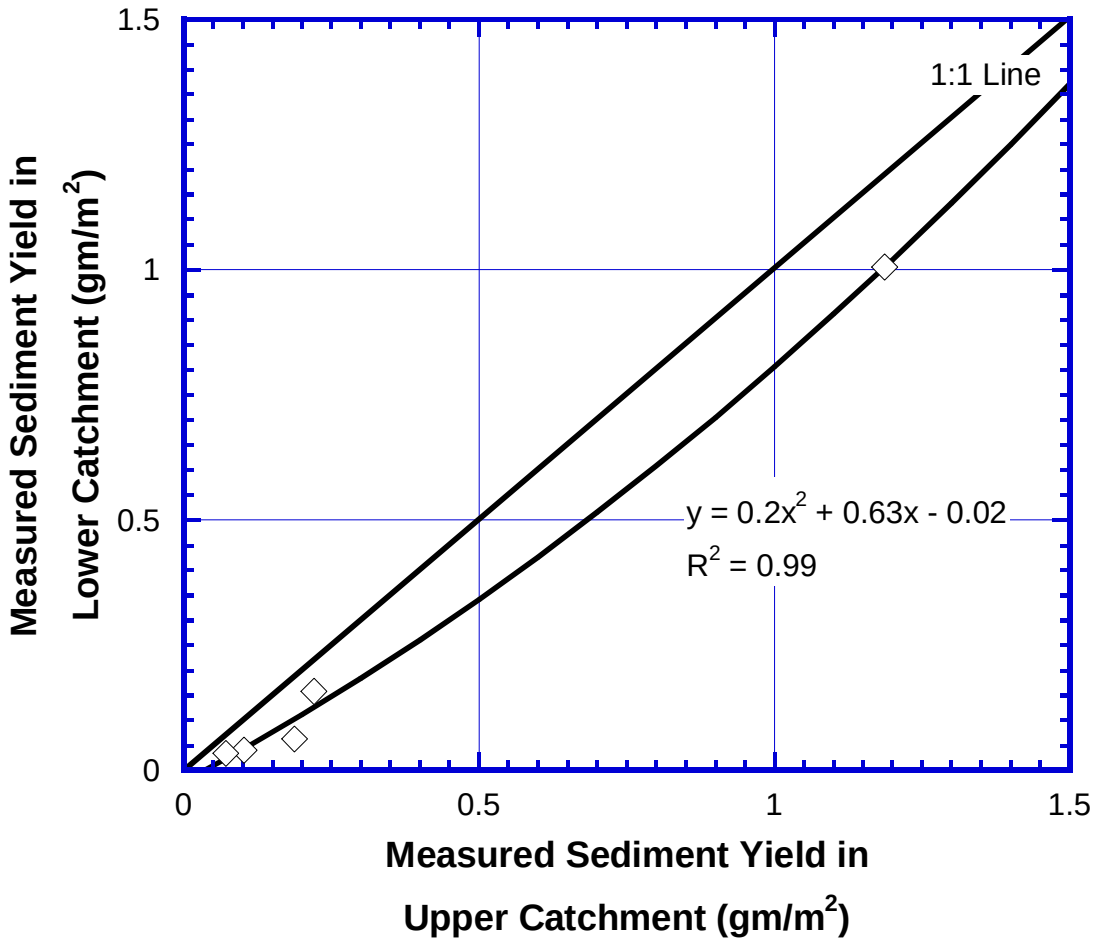

Figure 1-20. Event scale comparison of sediment yield from lower and upper catchments

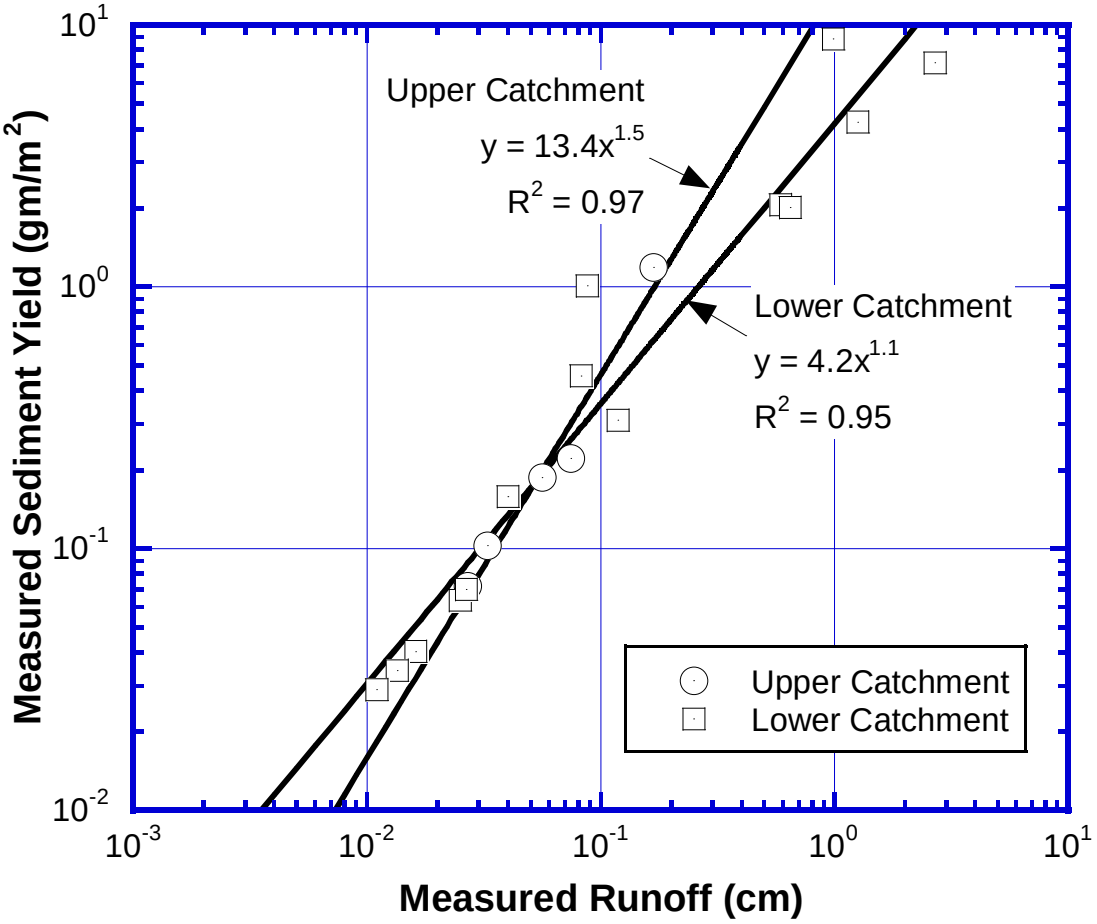

Figure 1-21. Measured runoff versus measured sediment yield for lower and upper catchments

explain more realistic three-dimensional physical processes governing a hill slope EFC hydrology. As an example, the instrumentation was unable to identify runoff "hot-spot" distribution within the catchment. A more distributed set of water content and suction sensors across the catchment is needed to accurately characterize not only soil water retention and hydraulic conductivity properties but also the effect of local landscape and topography of the catchment on runoff generation (Western et al. 1999). Although, construction of a catchment scale lysimeter to measure percolation can be economically and logistically prohibitive, yet a small lysimeter within the landfill catchment can be useful to precisely quantify scale effects on runoff and other water balance parameters from EFCs. The spatial and temporal measurement of plant canopy (leaf area index, etc.) and soil water repellency can provide more insight in hill slope runoff generation processes (Miyata et al. 2007; Gomi et al. 2008). Hydro-chemical studies on runoff water can help to quantify overland runoff connectivity networks, sediment concentrations and chemical leaching across landfill covers (Godsey et al. 2012). Lastly, effect of hysteresis in soil water storage and runoff response must be evaluated to accurately model and predict deep percolation from hill slopes (Graham et al. 2010).

SUMMARY AND CONCLUSIONS

EFC located in a semiarid climate of Austin, Texas was instrumented to measure catchment scale runoff and soil water storage. Two instrumented landfill catchments designated as upper catchment and lower catchment had the areal extent of 3,716 m^2 (0.9 acre) and 6,503 m^2 (1.6 acre), respectively, and runoff lengths of 30 m and 53 m, respectively. EFC consisted of 15 cm thick vegetative layer underlain by a 90 cm thick compacted storage layer. The data collected over twenty three months is presented in this paper. Following key observations were made:

1) Total runoff of 12% and 8% was recorded for upper catchment and lower catchment, respectively. Upper catchment with smaller runoff length and smaller areal extent had less re-infiltration than lower catchment. Hence, more runoff was collected from upper catchment.
2) Winter 2012 (Season 1) and Fall 2013 (Season 3) recorded more runoff than intermediate seasons. Percent runoff and daily precipitation intensity correlated positively during Season 1 and Season 3, but no correlation could be established for the intermediate season. Seasonal variation of runoff was attributed to complex interplay of total precipitation, average precipitation intensity, precipitation return period, antecedent soil water content, PET/P and vegetation cover. Daily precipitation intensity could not be used as a standalone variable to predict runoff from EFC at ACL.
3) Runoff generated by the upper catchment correlated by a power law to the runoff generated by the lower catchment for the same precipitation events. The power law relationship was not significantly affected by spatial and temporal variation of precipitation, soil hydraulic properties, antecedent soil water content and surface depressions implying that the two catchments had similar intra-catchment runoff hydrology.
4) Runoff hydrology of EFC was generally governed by three-dimensional 'fill and spill' mechanism and not by two-dimensional variable source area mechanism. Hence, middle nest did not feed bottom nest making them hydraulically disconnected for the monitoring period after Winter 2012.
5) A threshold precipitation of 0.8 cm/day was necessary for plant canopy abstraction, filling isolated unsaturated plots, spilling excess precipitation and connect them hydraulically to record net runoff from EFC catchments at ACL.

6) Higher sediment yield was recorded from the upper catchment than the lower catchment due to higher runoff produced by upper catchment.
7) Sediment yield correlated positively to measured runoff with a power law relationship for both catchments.

PAPER 2: NUMERICAL MODELING OF SURFACE RUNOFF AT AN INSTRUMENTED CATCHMENT SCALE EARTHEN FINAL COVER IN SEMIARID CLIMATE

ABSTRACT

Two catchment scale test sections of an earthen final cover (EFC), with areal extent of 3,716 m^2 (0.9 acre of upper catchment) and 6,503 m^2 (1.6 acre of lower catchment) were instrumented to measure runoff and soil water parameters at several depths. EFC is located in Austin, Texas which is classified as semiarid climate. Vertical soil water flow was monitored with co-located suction and water content sensors in top nest of upper catchment and in middle and bottom nests of lower catchment. Runoff from each catchment was measured with dedicated storm water monitoring system consisting of automated high capacity above ground storage tanks. The field data collected over fifteen months was modeled with UNSAT-H and RZWQM. The catchment scale hydrology was idealized as 1-D vertical unsaturated flow. Co-located suction and water content sensors were used to estimate the unsaturated hydraulic parameters for modeling. UNSAT-H under predicted runoff for all three nests. RZWQM was unable to model unsteady precipitation events and over predicted runoff. However, UNSAT-H predicted runoff was relatively accurate than RZWQM. Soil water contents were under predicted in wet season and over predicted in dry season by both models. UNSAT-H inaccurately predicted runoff and soil water contents at small temporal scale of daily storm-events but at seasonal and annual scale UNSAT-H predictions were relatively accurate.

INTRODUCTION

Earthen final covers (EFCs) had been used for more than two decades in lieu of conventional covers to isolate municipal solid waste (MSW) landfills depending on the hydraulic conductivity of the underlain bottom liner system and consequently prevent ground water and air pollution (Nyhan 1990; Mijares et al. 2012). Conventional covers as prescribed by United States Environment Protection Agency (USEPA 1992) usually have a geomembrane as a hydraulic barrier to impede deep percolation while EFCs store water infiltration in a storage layer and release it back to the atmosphere as evapotranspiration (ET). Although EFCs usually offer economic advantages over conventional covers, the performance of EFCs is not uniform across all regions and is influenced by local climate (Hauser et al. 2001). Hence, EFCs require field or numerical validation to prove hydraulic equivalency with respect to conventional covers [CFR 258.60(b) (1), United States Government 2002]. Several lysimeter studies had been done in last two decades to measure deep percolation and demonstrate equivalency criterion across United States in various climates. In addition to proving equivalency criterion, the lysimeter studies also helped in quantifying the underlying physical processes which govern hydraulic flow across these barriers (Khire et al. 1997; Khire et al. 1999; Khire et al. 2000; Albright et al. 2004; Scanlon et al. 2005; Mijares et al. 2012). However construction of field scale test sections is expensive and requires a few years of monitoring. With the total number of landfills in United States numbering approximately 1900 (USEPA 2013), the construction of lysimeter to measure deep percolation through EFCs at every site is both economically and logistically prohibitive. Hence, numerical models become useful in predicting the short term and long term behavior of EFCs to prevent deep percolation across in different climatic conditions. Short term simulations are usually done to simulate measured lysimeter water balance for a few years and ascertain the accuracy or calibrate

numerical codes. Long term simulations usually involve several continuous years of climate loading to predict steady state water balance parameters of EFCs.

Water flow in EFCs is governed by interplay of several physical processes broadly categorized under water balance and unsaturated flow. The physical processes of water flow across the soil-atmosphere interface are classified as water balance while the physical processes governing the subsurface water flow are classified as unsaturated flow. Numerical models differ in implementation complexity to simulate water balance and unsaturated flow in one, two or three dimensions. HELP, UNSAT-H, Vadose/W, HYDRUS, SoilCover, SHAW, SWIM, LEACHM and VS2DTI are among several public domain and commercial softwares available for predicting the hydraulic behavior of EFCs on landfill (Scanlon et al. 2002; Bohnhoff et al. 2009). Khire et al. (1997) critiqued UNSAT-H (Fayer 2000) and HELP (Schroeder et al. 1994) for several measured water balance variables from lysimeter test sections of final cover on existing MSW landfill located in semiarid climate of western United States and humid climate of eastern United States. Khire et al. (1997) found that HELP significantly over predicted percolation as compared to UNSAT-H for humid region while both models failed to capture preferential flow across clay layers in semiarid climate. UNSAT-H was further criticized to under predict deep percolation due to over prediction of overland runoff for an instrumented lysimeter section in western United States (Khire et al. 1999). Scanlon et al. (2002) compared performance of several numerical codes by modifying them to implement identical boundary conditions and hydraulic parameters. The performance of several codes was gauged against measured water balance variables of capillary barrier lysimeter test section in hot desert of western Texas and monolithic cover lysimeter in cold desert of Idaho. Runoff was under predicted by most codes and resulted in ±64% error in estimated percolation. Scanlon et al. (2005) compared short term (1-5 yr) water balance and long-term (25

year) performance of instrumented lysimeters of capillary barrier, geosynthetic clay-asphalt barrier and monolithic cover in Texas and New Mexico with UNSAT-H. The authors identified that differences in climate loading and hydraulic conductivity affected simulated water balance including runoff. Bohnhoff et al. (2009) used UNSAT-H, VADOSE, HYDRUS and LEACHM to model measured water balance variables for monolithic cover lysimeter in semiarid climate of Altamont, California. The authors observed that all models required calibration of soil properties such as hydraulic conductivity, precipitation rate, etc. to accurately predict measured runoff.

Although water balance modeling has helped to identify previously unknown variables governing performance of EFCs, yet these models are limited by inherent algorithms to accurately represent all observed physical hydrology processes of EFCs. Such inabilities are usually overcome by calibrating the model for site specific data on boundary conditions, climatic conditions or hydraulic properties. Calibration coefficients thus obtained are site-specific and cannot be applied to evaluate performance of similar covers at other sites. Such calibrated models significantly limit the scope of numerical water balance modeling for commercial applications beyond the test site, and consequently defeat the very purpose of numerical modeling. Further, calibration coefficients can fail to represent the actual scale dependent physical phenomenon and yield wrong predictions. A reverse approach is necessary to focus more efforts on measuring the physical processes accurately and adjudge the error in its simplistic implementation in a numerical code. Such approach will not limit the universal applicability of numerical of models but will help modeler to make informed decisions by quantifying error in the predictions. Unfortunately, water balance modeling for EFCs for MSW landfills has suffered a similar fate. More efforts in recent years have been concentrated on presenting a better match with measured data by calibrating input parameters and neglecting underlying physics responsible for anomaly in estimated and measured

values. Among several parameters in water balance modeling, runoff hydrology of landfill cover has received minimal attention despite its widely acknowledged effects on water balance modeling of EFCs.

Over the last two decades, lysimeter studies of EFCs have been conducted with the primary aim to measure percolation and were limited in areal extent of 0.02 acre to 0.1 acre (Khire et al. 1997, 1999; Albright et al. 2004; Mijares et al. 2012). Unfortunately, runoff from small plot scale test sections had been routinely assumed in numerical modeling to represent catchment scale runoff of the entire EFC and efforts had been focused in wrong direction to calibrate input soil properties to match measured data. Scale effects on measured runoff from natural hill slopes are known to runoff hydrologist for several decades (Eagleson 1970; Julien and Moglen 1990; van de Giesen et al. 2000; Gomi et al. 2008). But little literature is available on predicting catchment scale runoff from engineered hill slopes of EFCs. Recently, attempts have been made to measure catchment scale runoff from 4,000 m^2 (0.99 acre) landfill cover and model it with HYDRUS for humid climate of Alaska (Hopp et al. 2011). However, runoff study at Alaska site was primarily concentrated on lateral subsurface flow through a drainage layer and consequently has limited applicability in continental United States where overland runoff usually has been reported as a major water balance component of EFCs as compared to subsurface lateral flow (Albright et al. 2004).

OBJECTIVE

Catchment scale runoff was measured at an existing landfill EFC located at Austin, Texas. The test section does not have a lysimeter and consequently the soil water hydrology closely resembled actual field conditions and was not affected by artificial barrier layer (Mijares et al. 2012). No percolation measurements were made at ACL due to the absence of lysimeter. The

climate and runoff data collected over a fifteen month period was modeled with UNSAT-H (Fayer 2000) and RZWQM (Ahuja et al. 2000). The predicted results were analyzed with respect to measured data at different temporal scales.

CATCHMENT SCALE TEST SECTION

Two catchment scale test sections of a landfill cover were instrumented at Austin Community Landfill (ACL) located in Austin, Texas in mid-December 2011. The upper and lower catchments were 3,716 m^2 (0.91 acre) and 6,503 m^2 (1.61 acre) in areal extent. EFC at ACL consisted of 90 cm thick storage layer overlain by a 15 cm thick vegetative layer consisting of top soil (Fig. 2-1). Austin with total precipitation of 92 cm and potential evapotranspiration to precipitation ratio (PET/P) of about 2.5 for the fifteen month monitoring period, is classified to have semiarid climate (Albright et al. 2004). The average slope of EFC was about 1V to 4H. EFC at ACL was constructed about six years before the instrumentation. Hence, the effect of soil properties and vegetation on the measured EFC runoff and soil water content was assumed to represent long term or in-service conditions.

SOIL PROPERTIES

The storage layer of EFC at ACL is referred to as Austin clay. It was classified as a high plasticity clay (CH) as per USCS. Austin clay was compacted to greater than 98% of the maximum dry unit weight and within ±5% of optimum moisture content of standard proctor effort (ASTM D698). The compaction curve is presented in Fig. 2-2. Soil samples were collected from upper 30 cm depth using 7.5 cm diameter shelby tubes consisting of both top soil and Austin clay. Saturated hydraulic conductivity of these Shelby tube samples was measured in laboratory with a flexible wall permeameter (ASTM D5084). Fine clay soil layers governed the laboratory hydraulic

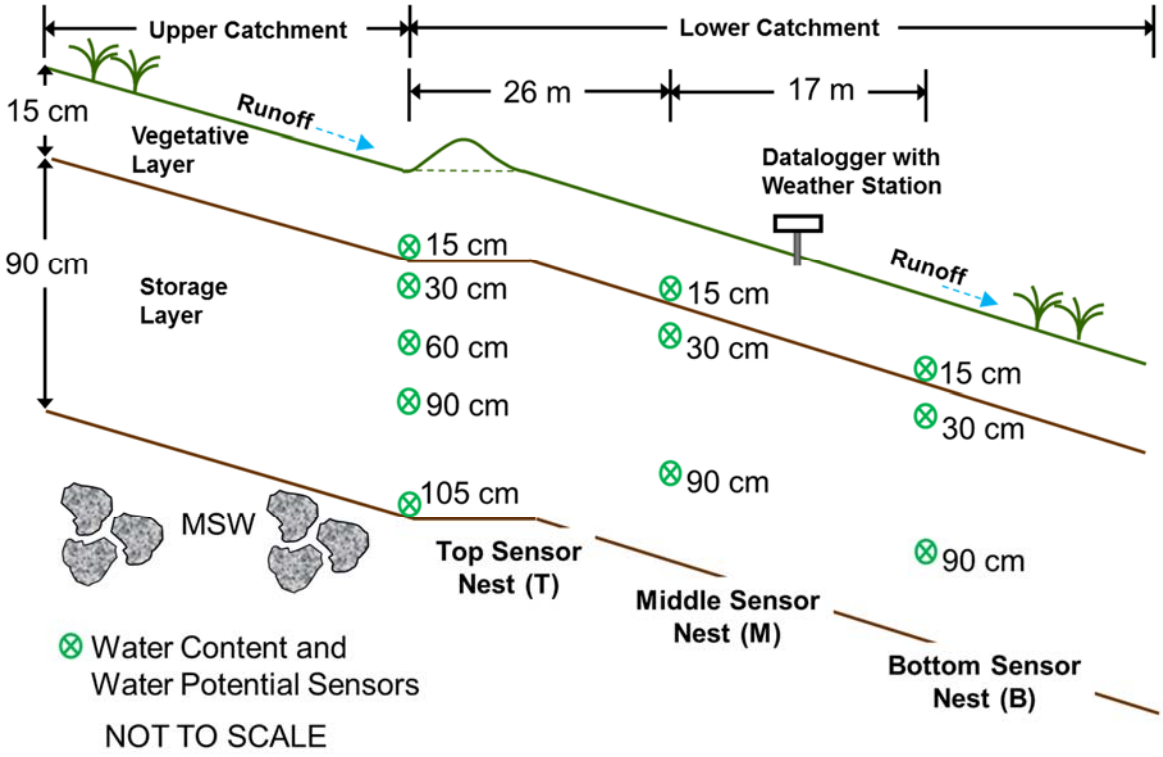

Figure 2-1. Instrumented cross-section of Austin Community Landfill (ACL)

conductivity of the core samples and reached an average value of 10^{-6} cm/sec (Fig. 2-2). As-built saturated hydraulic conductivity of the storage layer was 5×10^{-8} cm/sec (Golder Associates Inc. 2005). As-built saturated hydraulic conductivity of the storage layer increased to 10^{-6} cm/sec in about six years due to cyclic seasons of wetting and drying (Albrecht and Benson 2001). No field or laboratory tests were done to measure saturated hydraulic conductivity of top soil. EFC vegetative layer consisting of top soil was a coarse grained silt material and the hydraulic conductivity was expected to be in the range of 10^{-2} to 10^{-3} cm/sec (Scanlon et al. 2002; Scanlon et al. 2005; Mijares and Khire 2012).

INSTRUMENTATION

Runoff from the two instrumented catchments at ACL was collected in two individual high capacity tanks. The drain valves of the actuator tanks were opened and closed using an actuator that was controlled by the datalogger, to empty tanks at a pre-defined water level. The total volume of water in the tanks was used to calculate net runoff from each catchment. Approximately 30 cm high earthen berm prevented runoff from upper catchment to enter lower catchment (Fig. 2-1). The top nest in the upper catchment consisted of co-located water content and suction sensors at depths of 15 cm, 30 cm, 60 cm, and 105 cm below the ground surface. Lower catchment had middle and bottom nests of co-located water content and suction sensors at depths of 15 cm, 30 cm and 90 cm below ground surface. Top nest, middle nest and bottom nest were located in the same vertical transect. Suction sensors and water content sensors were calibrated using top soil and Austin clay. A complete set of dedicated climate sensors was also installed to measure hourly precipitation, solar radiation, and relative humidity. Average daily wind speed data from National Oceanic and Atmospheric Administration (NOAA) station at Austin executive airport located 12 km north-east of the instrumented landfill was assumed to be representative of the site. The detailed description

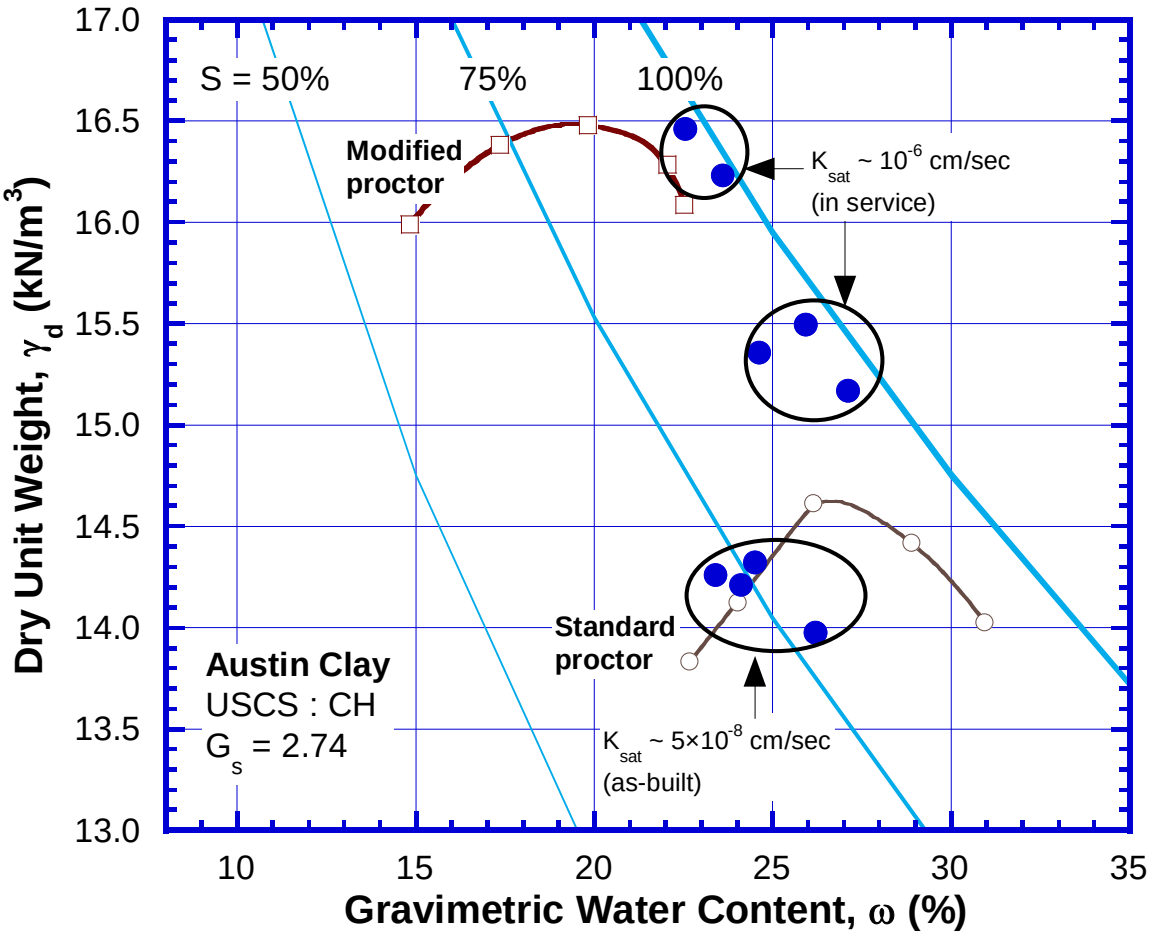

Figure 2-2. Proctor compaction curve and saturated hydraulic conductivity of Austin clay

of ACL site instrumentation and measured data is described in the paper 1.

NUMERICAL MODELING

UNSAT-H (Fayer 2000) is a public domain water balance and unsaturated flow model that has been used to simulate EFC performance in several studies (Khire et al. 1997; Scanlon et al. 2005; Mijares and Khire 2012). UNSAT-H is a finite-difference code and can simulate both heat and water flow in vertical dimension only. However, rapid infiltration events in small time intervals cannot be predicted with UNSAT-H. The primary reason for such limitation is the lack of inherent algorithms' ability to simulate multi-phase flow and account for air entrapment during rapid water infiltration.

Root Zone Water Quality Model (RZWQM version 2.42.2013) (Ahuja et al. 2000; Ma et al. 2012) is another public domain code which was developed by United States Department of Agriculture (USDA) for modeling water flow in agricultural systems. The software is a multiple domain tool as it can simultaneously simulate one-dimension vertical flow of water in soil capillaries and soil macro-pores. The software is uniquely designed to integrate biological, physical and chemical processes within several soil layers. However, no biological and chemical processes were simulated in this study and water flow was assumed to occur only through capillary pores. The software uses Green-Ampt (1911) equation to model infiltration excess runoff and Richards' equation (Richards 1931) to redistribute water within soil layers (Ma et al. 2012). The code can also simulate heat flow through soil layers but thermal analysis did not form part of the current discussion. RZWQM uses Shuttleworth and Wallace (1985) method to evaluate potential evapotranspiration unlike Penman equation (Doorenbos and Pruitt 1977) used by UNSAT-H.

INPUT PARAMETERS

Simulated vertical water movement at ACL was limited to a depth of 105 cm below ground surface as no MSW layer was simulated below EFC (Fig. 2-3). The lower boundary condition was assumed to be unit gradient which was consistent with other similar published studies (Benson 2007; Mijares and Khire 2012). Variable flux boundary was specified as the top boundary condition which forced water infiltration during precipitation event and removed water from EFC due to evapotranspiration when there was no precipitation (Fig. 2-3).

METEOROLOGICAL DATA

Climate data collected at ACL site was used as input to both models. Wind speed, solar radiation, air temperature and dew point were input as daily values in UNSAT-H but as hourly values in RZWQM. Measured hourly precipitation at ACL was used as input to both UNSAT-H and RZWQM.

SOIL MATERIAL PROPERTIES

Hydraulic properties necessary to model EFCs usually consist of soil water characteristic curves (SWCC) and unsaturated hydraulic conductivity function (UHCF). SWCC of ACL soils was assumed to follow van Genuchten fitting parameters (van Genuchten 1980) as follows

$$\theta = \theta_r + \frac{\theta_s - \theta_r}{\left(1 + \left|\alpha h\right|^n\right)^m} \tag{2-1}$$

where, θ is volumetric water content, θ_r is residual volumetric water content, θ_s is saturated volumetric water content, h is matric suction while α, n, and m are curve fitting parameters. UHCF

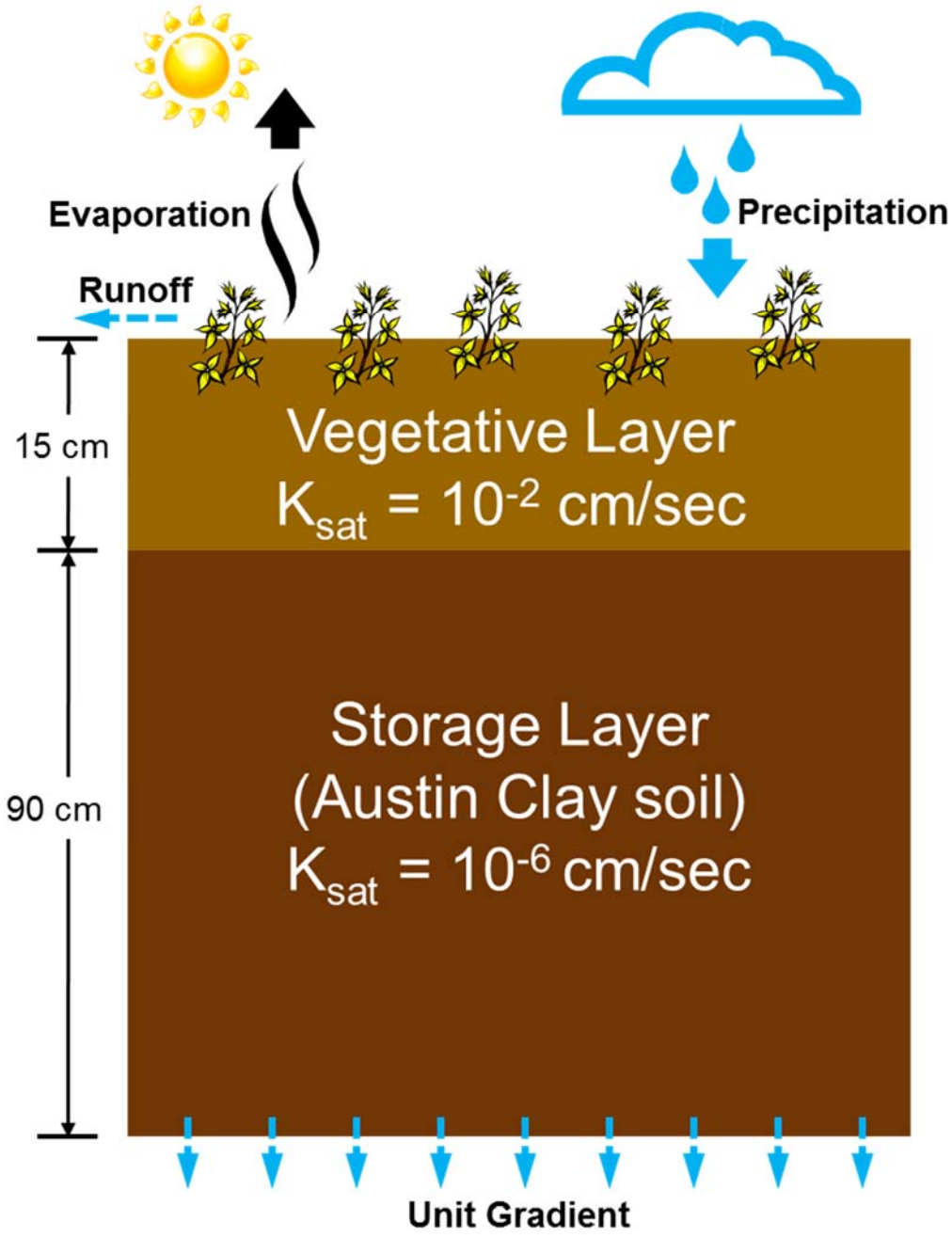

Figure 2-3. Typical 1-D cross-section of ACL simulated with UNSAT-H and RZWQM

of ACL soils was defined by van Genuchten-Maulem function (van Genuchten 1980) as follows

$$K(h) = K_{sat} \frac{\left\{1-(\alpha h)^{nm}[1+(\alpha h)^{n}]^{-m}\right\}^{2}}{[1+(\alpha h)^{n}]^{ml}} \tag{2-2}$$

where, K_{sat} is saturated hydraulic conductivity, K(h) is unsaturated hydraulic conductivity at suction h and *l* is pore-interaction term usually assumed equal to 0.5. Two modifications were implemented in the above equations to closely represent the predicted field measured unsaturated hydraulic functions. Firstly, SWCC and UHCF were not related with the same set of α and n. Secondly, pore-interaction term (*l*) in definition of UHCF was not restricted to 0.5.

Modified Brooks-Corey fitting parameters instead of van Genuchten parameters were used for RZWQM simulations (Brooks and Corey 1964; Ahuja et al. 2000) because RZWQM does not allow UHCF input with van Genuchten fitting function. Brooks Corey SWCC function defined in RZWQM is as follows

$$\theta = \theta_s + a * h \qquad \text{when, } |h| < |h_b| \tag{2-3}$$

$$\theta - \theta_r = B * \left|h\right|^{-\lambda} \qquad \text{when, } |h| \geq |h_b| \tag{2-4}$$

where, h_b is the air entry water suction, a is a constant (usually assumed zero) and λ is curve fitting parameter. UHCF was defined in RZWQM as

$$K(h) = K_{sat} * h^{-N_1} \qquad \text{when, } |h| < |h_{bk}| \tag{2-5}$$

$$K(h) = C_2 * \left|h\right|^{-N_2} \qquad \text{when, } |h| \geq |h_{bk}| \tag{2-6}$$

where, h_{bk} is the value of air entry water suction for the soil hydraulic conductivity-suction curve, and N_1, N_2 and C_2 are constants (Ma et al. 2012).

SWCC and UHCF for top soil were measured in laboratory with dewpoint potentiometer and centrifuge (Fig. 2-4). Two identical samples of top soil were prepared in relatively large PVC cylinders (15 cm diameter, 18 cm tall) for centrifuge testing. Top soil samples in PVC cylinders had an average dry density of 11 kN/m^3 (1.12 g/cm^3). The samples were spun in the centrifuge at up to 60 times the gravitational force in 1g to 3g increments (ASTM D6836). UHCF of top soil from centrifuge testing was evaluated according to the method proposed by Passioura (1977). A detailed description of estimating SWCC and UHCF with centrifuge is presented by Khire and Saravanathiiban (2012).

Laboratory experiments on large diameter core samples had been traditionally used to evaluate unsaturated soil water properties of compacted soils (Khire et al. 1997; Ogorzalek et al. 2008; Bohnhoff et al. 2009). However, such spot measurements are limited by temporal evolution of clay texture which can affect unsaturated flow properties (Benson et al. 2007). Recently Mijares and Khire (2012) conducted in-situ single-ring infiltrometer tests to measure in-situ saturated hydraulic conductivity of clay layer while SWCC of clay was evaluated based on in-situ water content and soil suction values. In this study, field data from in-situ co-located water content and suction sensors was used to evaluate representative SWCC and UHCF of Austin clay. Instantaneous profile method was used to evaluate UHCF from suction and water content data (Meerdink et al. 1996).

In evaluating SWCC from co-located suction and water content sensors data, it was observed that suction sensors had delayed response to the drying events as compared to water content sensors. A typical lag in response of co-located suction and water content sensors at 30 cm depth below ground surface in middle nest is presented in Fig. 2-5. Although water content sensor started responding to drying on 21 March 2012, it took about one more week (27 March 2012)

before suction sensor responded to the drying of the soil. Similar behavior was observed for all suction sensors. No definite spatial or temporal pattern could be established for such time lag behavior of suction sensors. Consequently each drying event of each suction sensor was analyzed separately to offset time lag of suction values with respect to corresponding water content readings while evaluating SWCC and UHCF of Austin clay (Fig. 2-6).

Hysteresis in SWCC and UHCF was ignored and only the drying curves were used to evaluate SWCC and UHCF. Hysteresis in field-scale modeling of lysimeter EFCs has been ignored by several authors for fine grained soils (Khire et al. 1997; Ogorzalek et al. 2008; Mijares and Khire 2012). Bohnhoff et al. (2009) reported that the effect of hysteresis in SWCC and UHCF, on the water balance predictions for monolithic covers was not significant as compared to sensitivity of the saturated hydraulic conductivity of the surface layer.

SWCC and UHCF for Austin clay are presented in Fig. 2-6. Table 2-1 presents a summary of the hydraulic properties of top soil and Austin clay estimated from the field and laboratory experiments.

INITIAL CONDITIONS

The initial soil water state specified in both models was consistent with the water content and suction values measured at different depths of the three sensors nests. Water content sensors in storage layer of middle and bottom nests were connected in February 2012. Hence instead of water contents, measured suction values were used as initial conditions to simulate middle and bottom nests. As vegetative layer water content sensors in middle and bottom nests were connected only in November 2012, water content values of vegetative layer in top nest were used as initial conditions for simulating vegetative layer in middle and bottom nests.

RZWQM was limited in its ability to accept initial soil water condition drier than

Table 2-1. Estimated hydraulic properties of top soil and Austin clay

Soil Water Characteristic Curve for van Genuchten		
Parameters	**Top soil**	**Austin clay**
θ_r	0.0	0.04
θ_s	0.53	0.454
α (1/cm)	0.05	0.0095
n (-)	1.22	1.08
Unsaturated Hydraulic Conductivity Function for van Genuchten-Maulem		
Parameters	**Top soil**	**Austin clay**
K_{sat} (cm/sec)	10^{-2} to 10^{-3}	10^{-6}
α (1/cm)	0.05	0.015
n (-)	1.22	2.2
l (-)	-3.0	-2.8
Soil Water Characteristic Curve for Brooks-Corey		
Parameters	**Top soil**	**Austin clay**
θ_r	0.0	0.04
θ_s	0.53	0.454
λ_1	0.0024	0.0
λ_2	0.21	0.077
h_b (cm)	38.39	80.0
Unsaturated Hydraulic Conductivity Function for Brooks-Corey		
Parameters	**Top soil**	**Austin clay**
K_{sat} (cm/sec)	10^{-2}	10^{-6}
N_1	0.0	0.0
N_2	1.8	1.02
h_{bk} (cm)	4.0	20.0

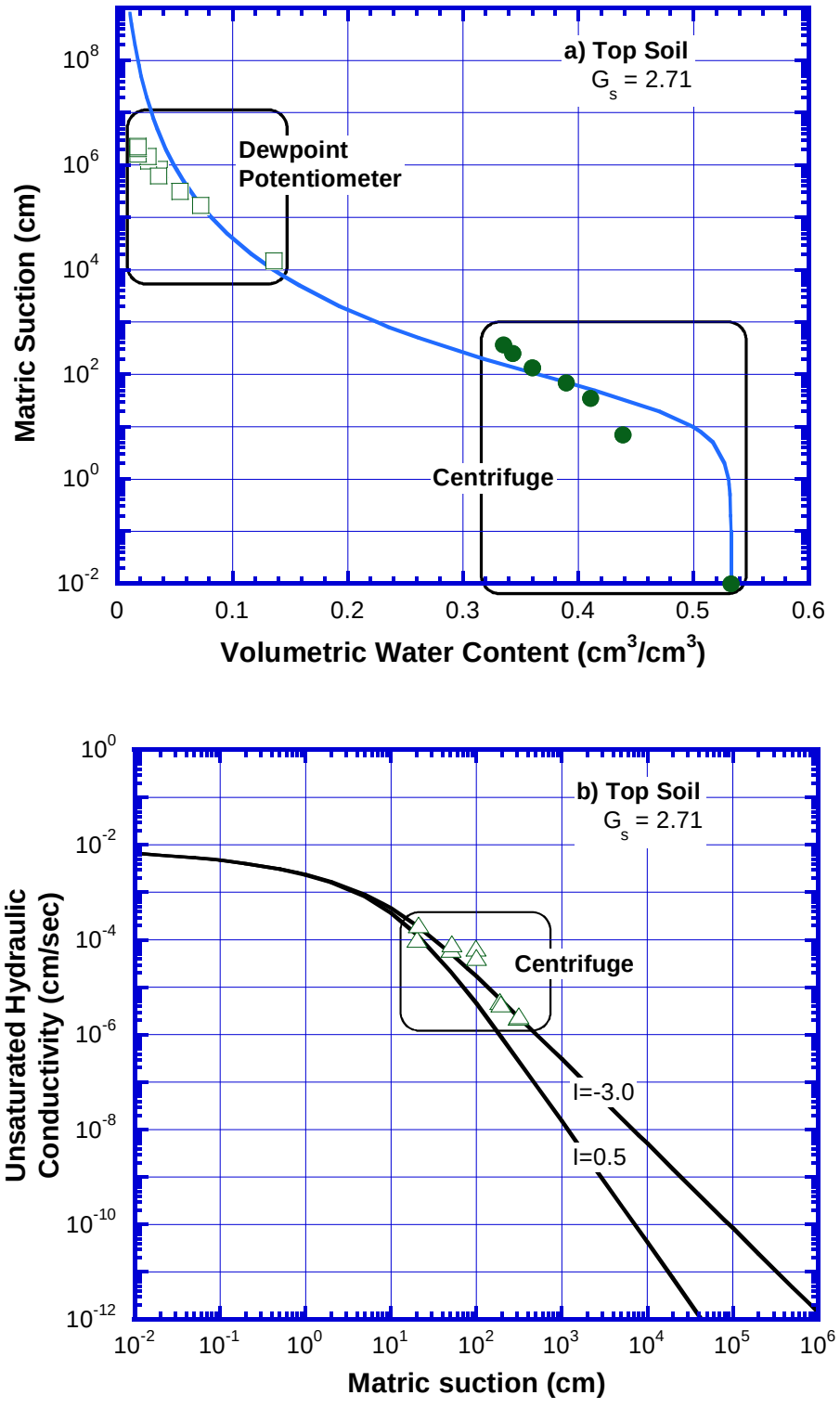

Figure 2-4. Soil water characteristic curve (a); and unsaturated hydraulic conductivity function (b) for top soil

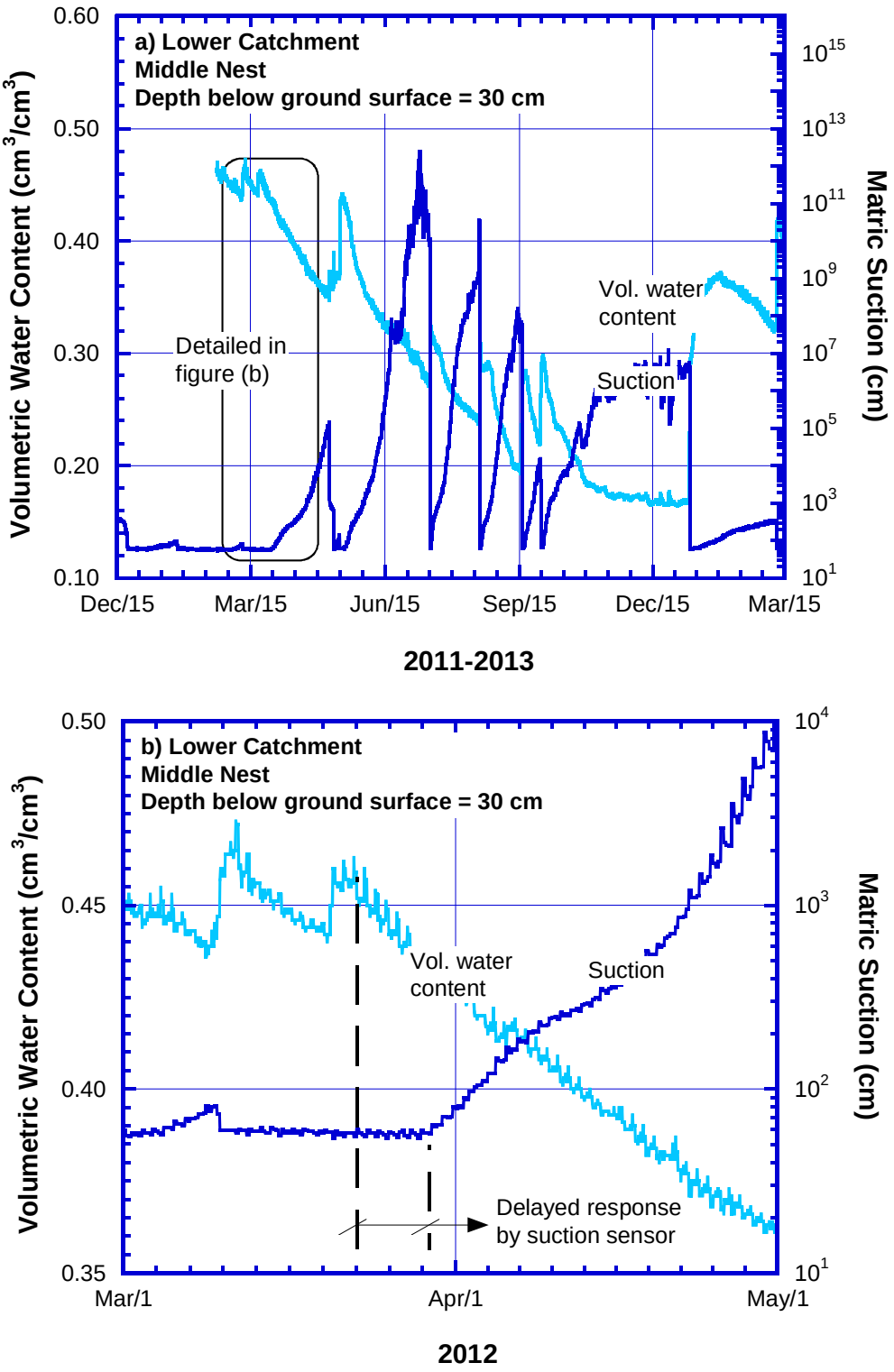

Figure 2-5. Volumetric water content and suction at 30 cm depth in middle nest (a); and delay in suction sensor response with respect to water content sensor at 30 cm depth in middle nest (b)

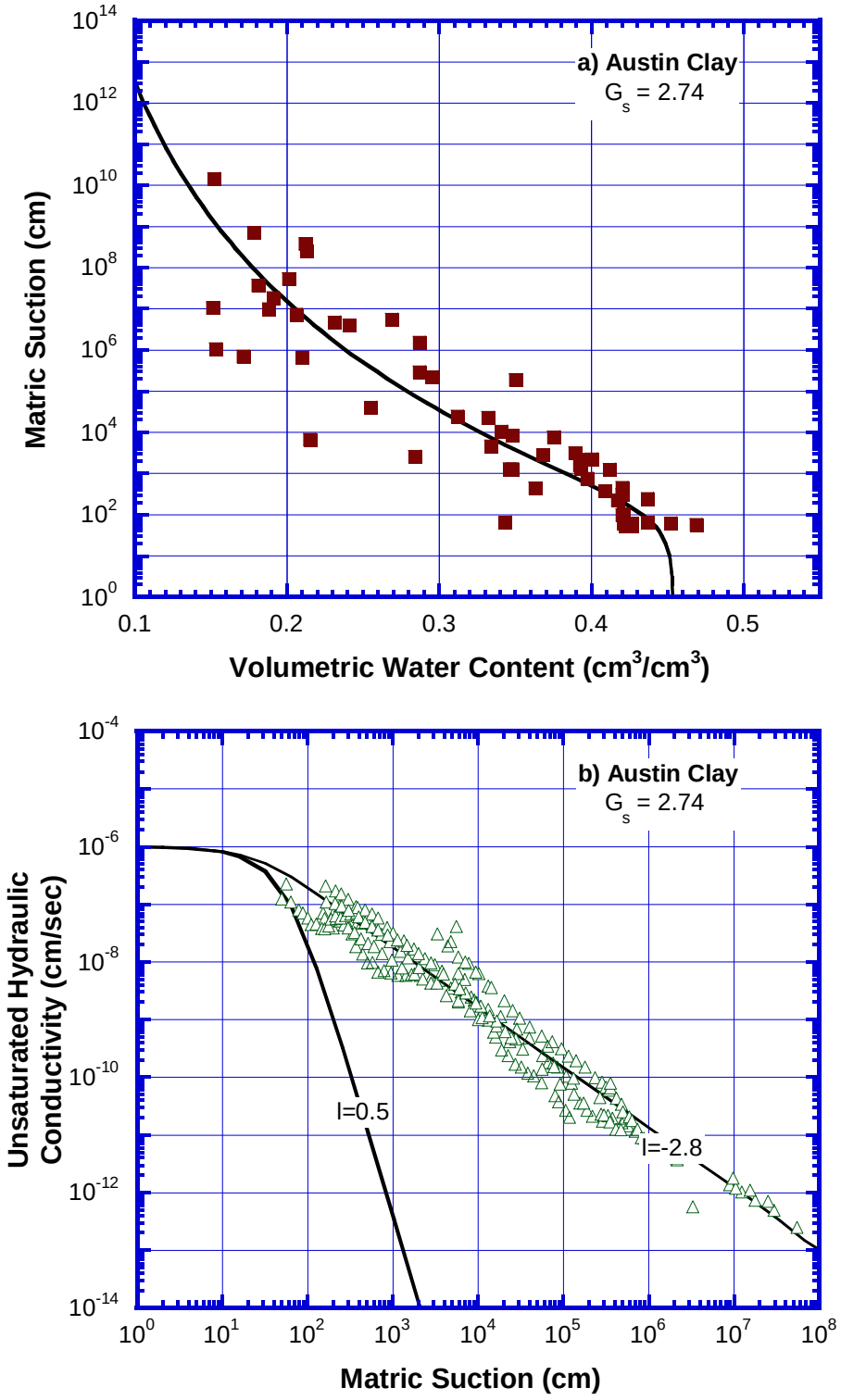

Figure 2-6. Soil water characteristic curve (a); and unsaturated hydraulic conductivity function (b) for Austin clay

2×10^5 cm (≈ 200 bars). Hence, suction values larger than 2×10^5 cm at Austin site were reduced by the program to 2×10^5 cm for all three nests.

NUMERICAL CONTROL PARAMETERS

For UNSAT-H simulations, numerical mass balance error was minimized by controlling spatial and temporal discretization. Nodal spacing near the top and bottom boundaries and vegetative layer-storage layer interface was maintained relatively small at 1 mm. Such non-uniform spatial discretization helped to reduce mass balance error for relatively large time steps and consequently reduced the total simulation time. A maximum time step of 1 hour and a minimum time step of 10^{-10} hours was used for UNSAT-H. The time step was reduced by a factor 10^{-5} with the onset of rainfall events in UNSAT-H. RZWQM internally evaluates time step intervals but utilizes user defined maximum number of iterations per time step to achieve target mass balance error before advancing to next time step. Mass balance error was less than 0.1% for all simulations.

RESULTS AND DISCUSSION

ACL site received a cumulative precipitation of 92 cm from 15 December 2011 to 15 March 2013. A total of 17 storms generated runoff during the fifteen months. Lower catchment generated 10 cm total runoff and upper catchment generated 7.5 cm total runoff (Fig. 2-7). 1-D simulations using UNSAT-H and RZWQM had same material properties and climate loading, but differed in initial water saturation conditions for different soil layers. Runoff coefficient was defined as the ratio of runoff to precipitation. No quantitative measurements of vegetation parameters such as root depth, leaf area index, etc. were done at ACL and consequently effect of transpiration was not simulated.

Table 2-2. Hydraulic properties of top soil used in different UNSAT-H simulation sets for upper catchment

Hydraulic property	**Simulation set 1**	**Simulation set 2**	**Simulation set 3**
K_{TS} (cm/sec)	10^{-2}	1.4×10^{-3}	1.4×10^{-3}
α (1/cm)	0.05	0.05	0.05
n	1.22	1.22	1.6
l	-3.0	-3.0	-2.4

Table 2-3. Summary of measured and simulated water balance variables for ACL

Source	**Catchment**	**Sensor Nest**	**Sim. set**	**K_{TS} (cm/sec)**	**Precip. (cm)**	**PET (cm)**	**Runoff (cm)**	**ET (cm)**	**Perc. (cm)**
Measured (Field)	Upper	-	-	-	92		10	-	-
	Lower	-	-	-	92		7.4	-	-
Simulated Data									
UNSAT-H	Upper	Top	1.	10^{-2}	92	227	5.2	92	0.1
			2.	1.4×10^{-3}	92	227	10	82	0.3
			3.	1.4×10^{-3}	92	227	5.6	91	0.1
	Middle	Middle	2.	6.8×10^{-3}	92	227	7.4	93	0.2
		Bottom	2.	4.3×10^{-3}	92	227	7.4	90	0.2
RZWQM	Upper	Top	1.	10^{-2}	92	204	19.7	82	0.1

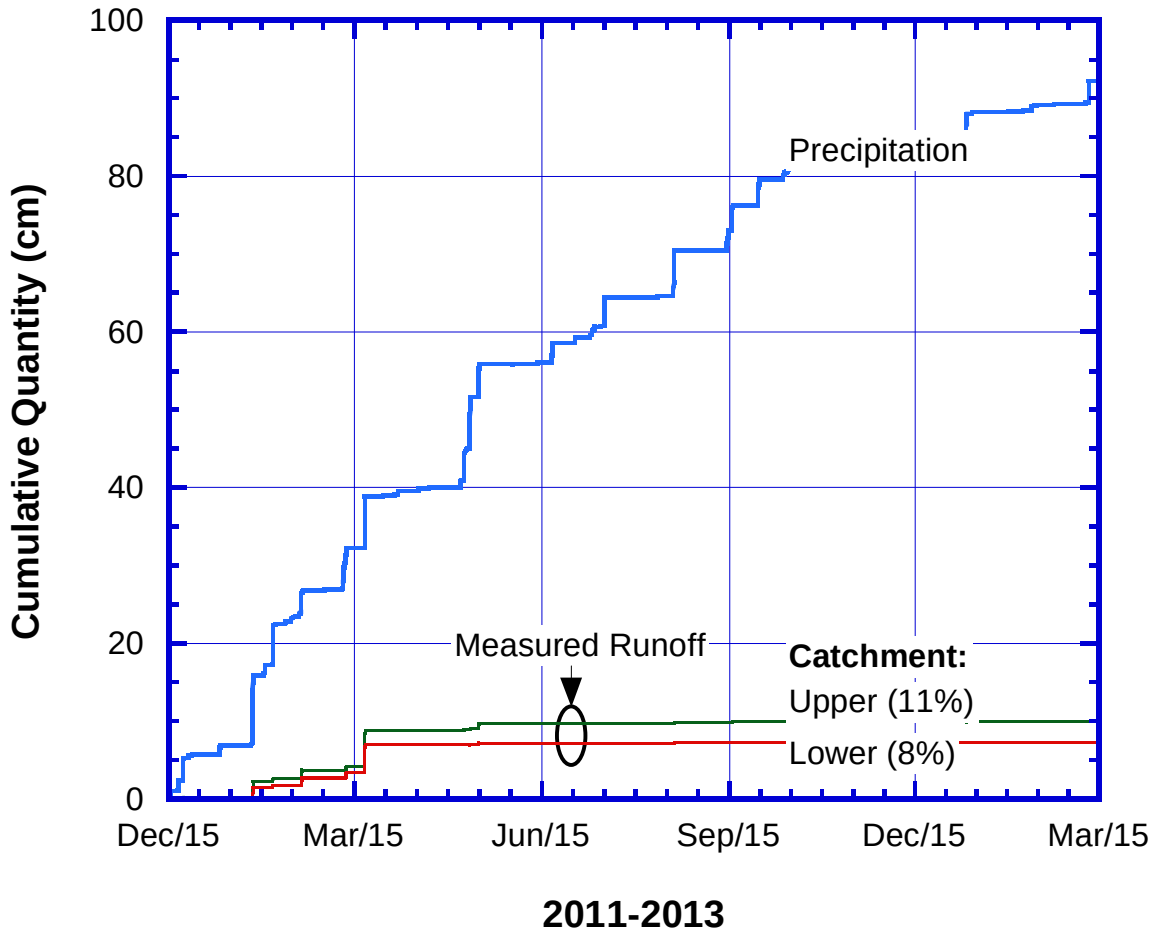

Figure 2-7. Measured runoff at Austin Community Landfill

UNSAT-H: Measured versus Predicted Runoff

EFCs are subjected to drying and wetting cycles owing to seasonal climate change, which results in evolving soil structure and subsurface flow paths (Albrecht and Benson 2001). This dynamic evolution of the subsurface flow in EFCs is further aggravated by changes in root penetration due to seasonal changes in vegetation cover. However, numerical models such as UNSAT-H and RZWQM do not model such dynamic evolution of soil structure but represent it as a static material property. Hence, field measured storage layer soil hydraulic properties were used in the model domain to closely simulate EFC runoff hydrology. UHCF of top soil was measured with laboratory experiments. However, saturated hydraulic conductivity of top soil was not measured. Consequently, hydraulic conductivity parameters of top soil were varied to conduct simulation set 1, simulation set 2 and simulation set 3 to assess the effects thereof on UNSAT-H predicted runoff hydrology of upper catchment. Table 2-2 and Fig, 2-8a present the different soil hydraulic properties used for different simulation sets and Table 2-3 presents water balance summary of all simulations.

UNSAT-H was unable to accurately predict the measured runoff with top soil saturated hydraulic conductivity (K_{TS}) of 10^{-2} cm/sec in simulation set 1. A low K_{TS} value of 1.4×10^{-3} cm/sec was used in UNSAT-H simulation set 2 which accurately predicted upper catchment measured runoff (11%). However, lowering of K_{TS} resulted in large errors with respect to measured top soil UHCF. In simulation set 3 a new set of fitting coefficients were evaluated for low K_{TS} (1.4×10^{-3} cm/sec) and measured UHCF data. UNSAT-H under predicted runoff (5.5%) for upper catchment in simulation set 3 (Fig. 2-8b). Similar behavior of UNSAT-H predictions was observed for lower catchment.

K_{TS} from simulation set 2 was varied to accurately predict measured runoff from lower catchment. K_{TS} for lower catchment increased by about 3 times (4.3×10^{-3} cm/sec for bottom nest) to 5 times (6.8×10^{-3} cm/sec for middle nest) from upper catchment K_{TS} (1.4×10^{-3} cm/sec) to accurately predict measured runoff with UNSA-H (Fig. 2-9, Fig. 2-10 and Fig. 2-11). Thus, calibrated K_{TS} for both catchments were within the same order of magnitude.

UNSAT-H predicted high cumulative monthly runoff coefficient in Winter and Spring 2012 followed lower cumulative runoff coefficient from Summer 2012 to Winter 2013 for upper catchment which was similar to the measured monthly runoff coefficient for the upper catchment (Fig. 2-12). Similar observation was made for lower catchment. However, predicted cumulative monthly runoff coefficients for the lower catchment were relatively accurate than upper catchment (Fig. 2-13).

Bohnhoff et al. (2009) had over predicted runoff for monolithic cover at Altamont, California by factor of 1.65 to 5.7 with UNSAT-H. However use of field measured UHCF and hourly precipitation intensity at ACL helped simulate the catchment scale hydrology more realistically and predict monthly and annual scale catchment runoff relatively accurately. Nonetheless, UNSAT-H predicted runoff was significantly affected by K_{TS} and UHCF fitting coefficients of top soil. Large diameter laboratory samples of top soil were not representative of the field conditions and UHCF measured thereof, failed to capture evolving top soil hydraulic properties in space and time to accurately model EFC hydrology with UNSAT-H.

RZWQM Predicted Water Balance

Unlike UNSAT-H, all three nests simulated with RZWQM predicted same water balance values because the initial saturation for all three nests was limited by a maximum allowable suction value (2×10^{5} cm). RZWQM over predicted runoff coefficient (0.21) compared to the measured

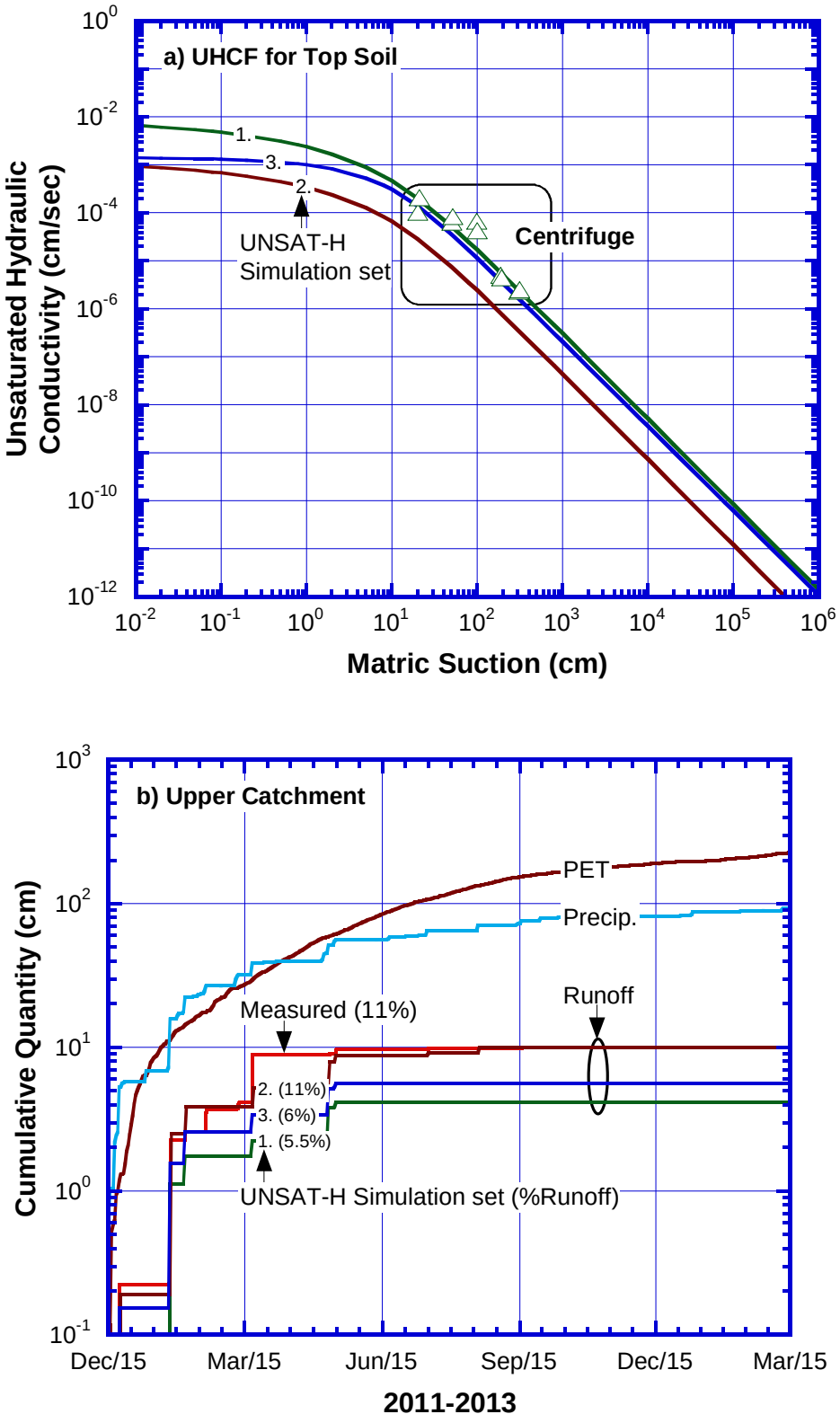

Figure 2-8. UHCF for top soil (a); and comparison of measured and UNSAT-H predicted runoff in upper catchment for different simulation sets (b)

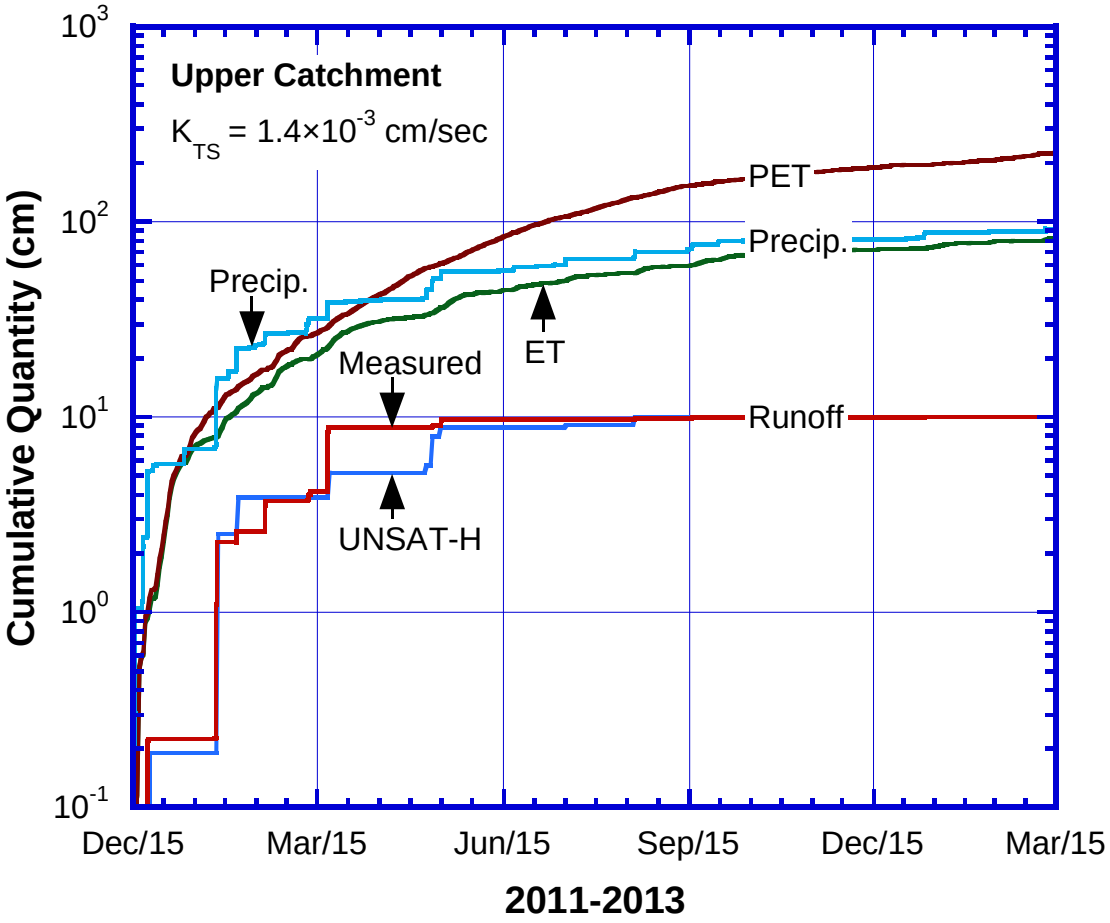

Figure 2-9. Measured and UNSAT-H predicted runoff in upper catchment

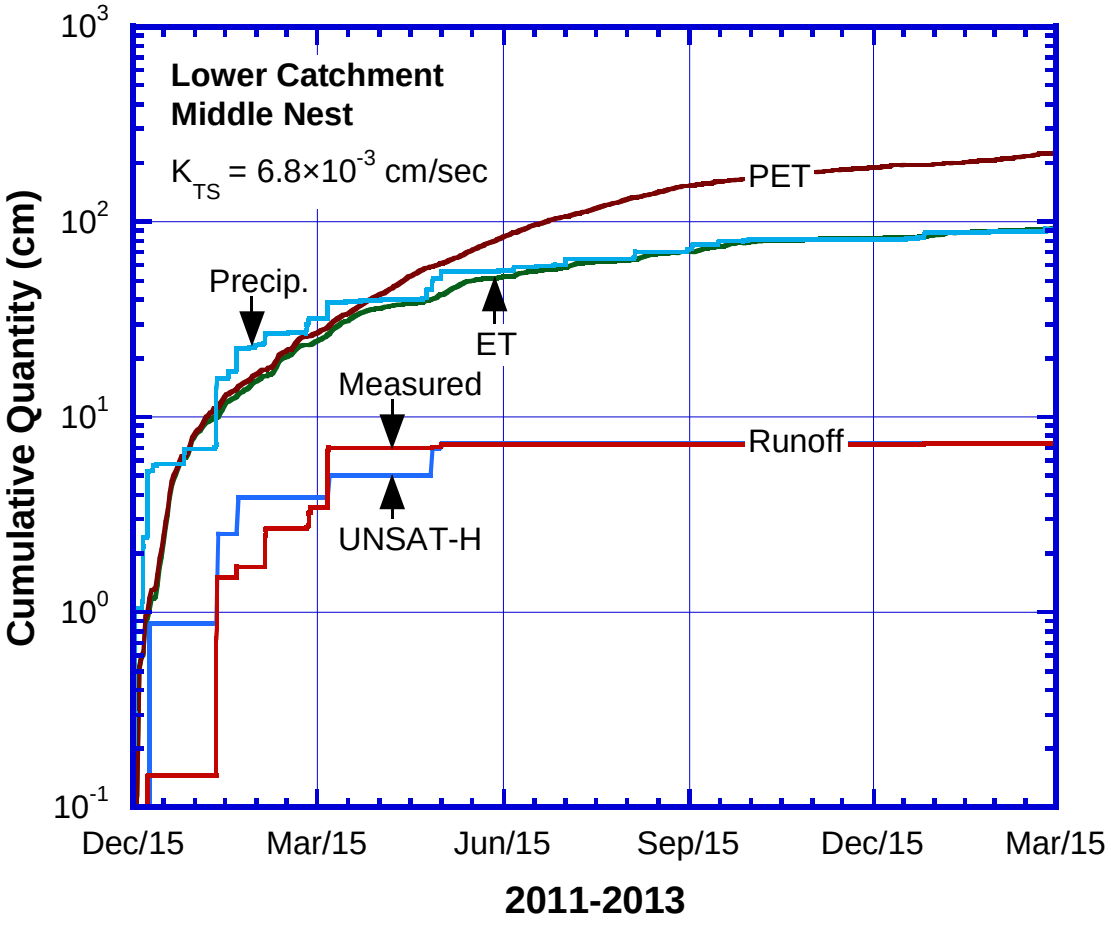

Figure 2-10. Measured and UNSAT-H predicted runoff for middle nest in lower catchment

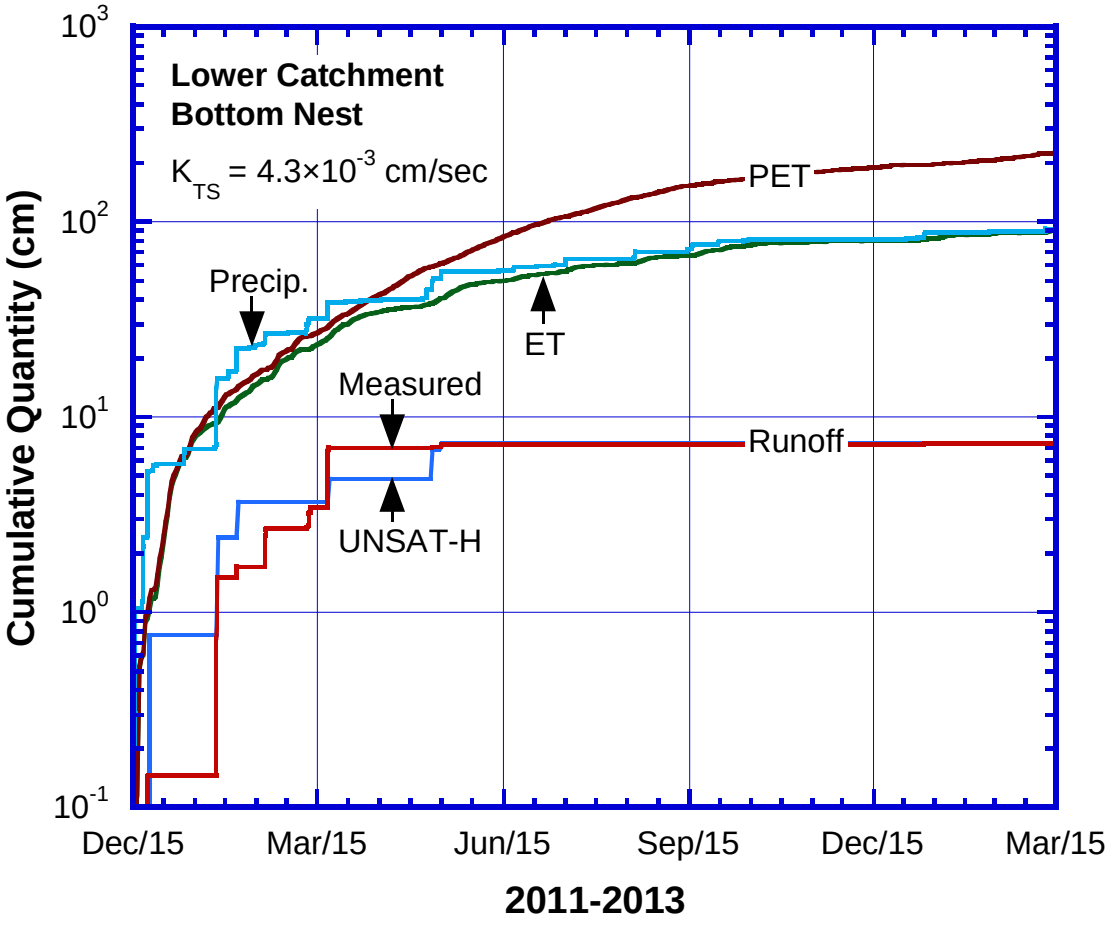

Figure 2-11. Measured and UNSAT-H predicted runoff for bottom nest in upper catchment

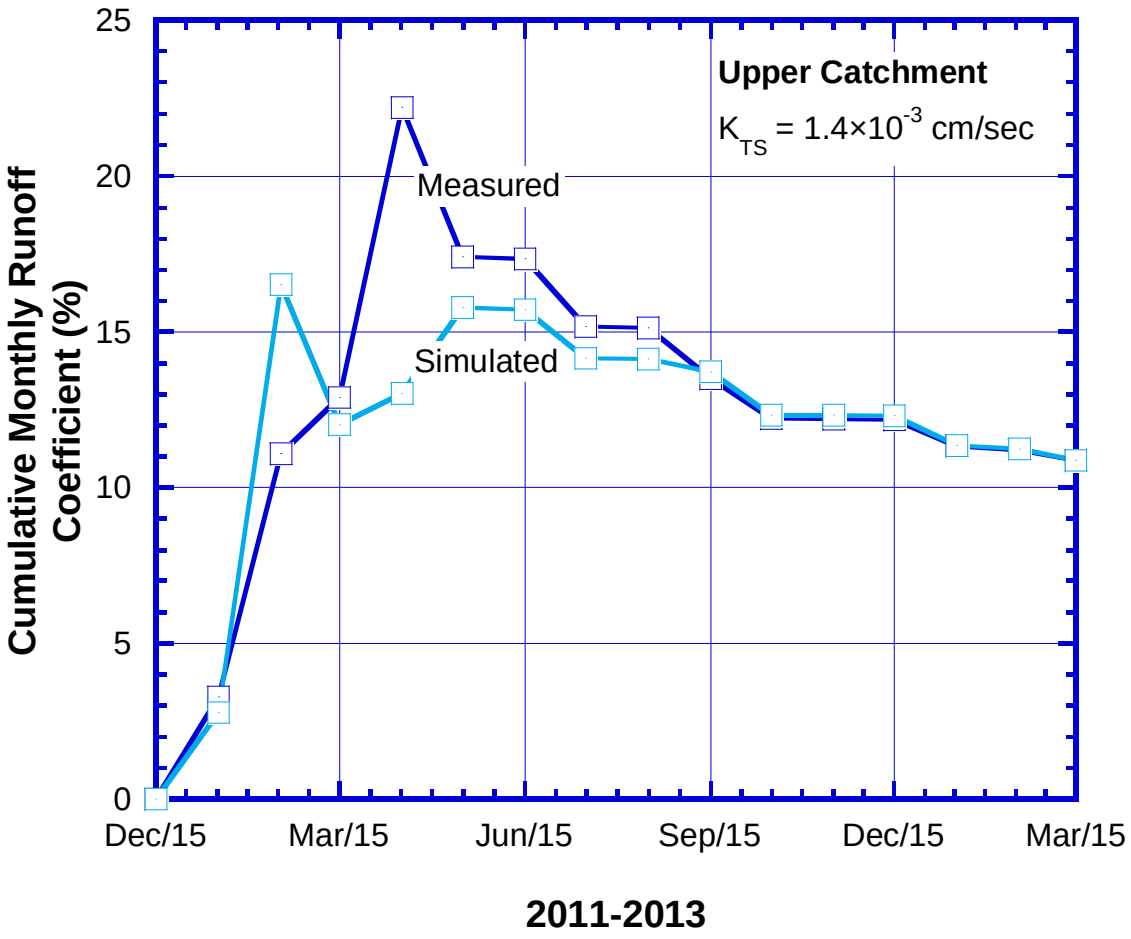

Figure 2-12. Measured and UNSAT-H predicted cumulative monthly runoff coefficient for upper catchment

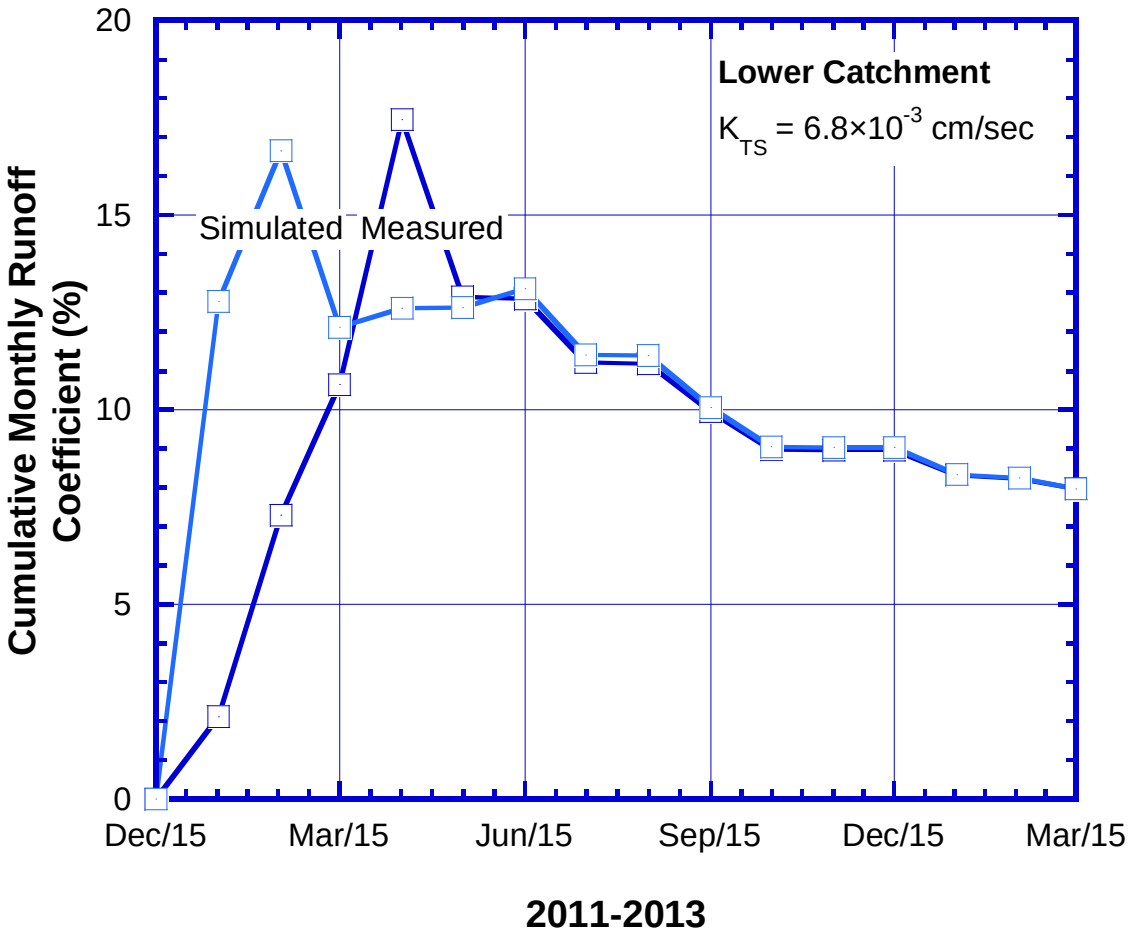

Figure 2-13. Measured and UNSAT-H predicted cumulative monthly runoff coefficient for lower catchment

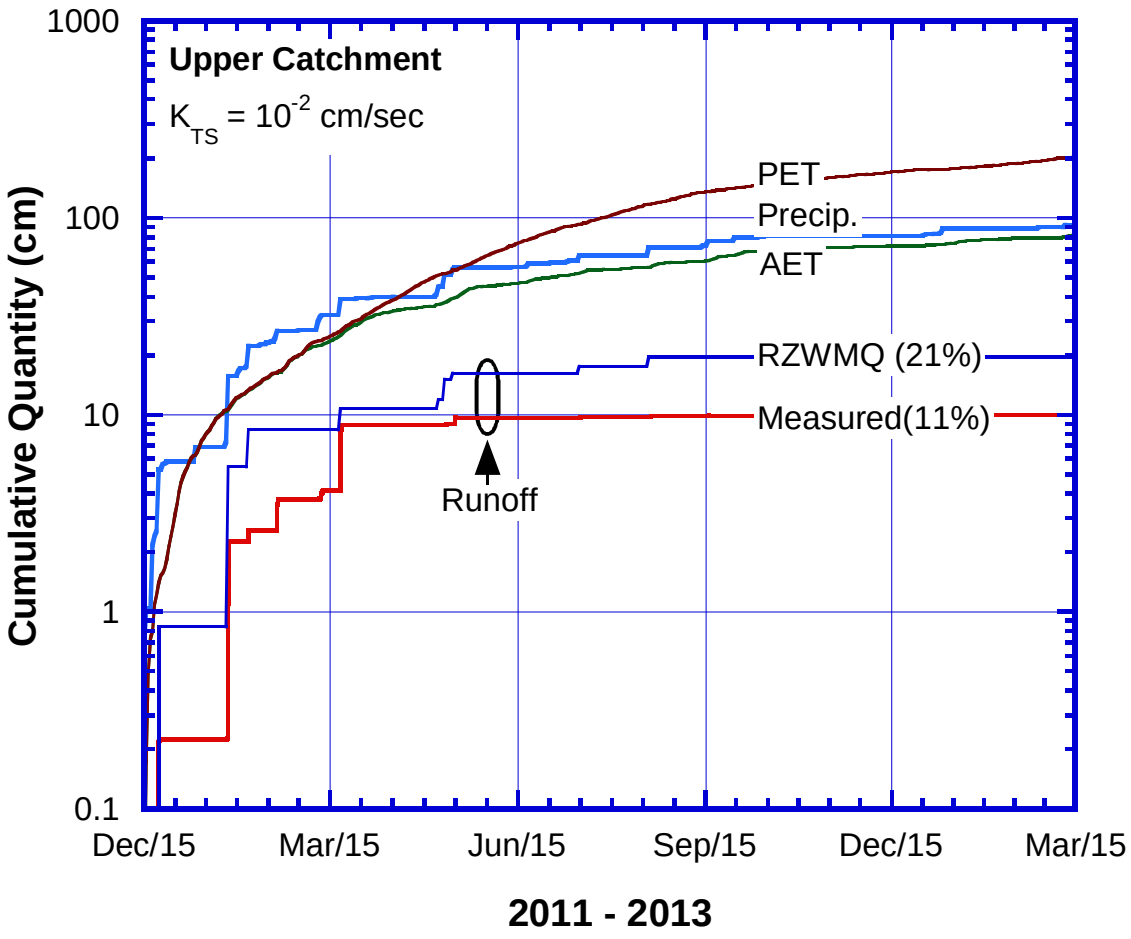

Figure 2-14. Comparison of measured and predicted runoff by RZWQM for upper catchment

runoff coefficients of 0.11 and 0.08 for upper and lower catchments respectively, with a high K_{TS} value of 10^{-2} cm/sec (Fig. 2-14). Similar observation was made by Ma et al. (2007), where RZWQM over predicted runoff from 26 plots near Nashua, Iowa. Measured surface runoff at Nashua, Iowa ranged from 0.1 cm/yr to 0.7 cm/yr while RZWQM predicted it to 0.9 cm/yr to 13.2 cm/yr. RZWQM does not incorporate surface roughness and surface detention storage and hence over predicted the runoff (Ma et al. 2007).

Runoff predicted by RZWQM (19.7 cm) was greater than UNSAT-H predicted runoff (5.2 cm) when $K_{TS} = 10^{-2}$ cm/sec was used for upper catchment. RZWQM also under predicted PET (204 cm) and ET (82 cm) compared to those predicted by UNSAT-H. RZWQM runoff and infiltration predictions were affected significantly by input hourly precipitation intensity as discussed in the next section.

RZWQM: Effect of Input Precipitation Intensity on Simulated Water Balance

Although ACL upper catchment field-scale runoff processes could not be closely represented by 1-D simulations of RZWQM, upper catchment was used to compare the effect of input precipitation intensity on RZWQM predicted runoff because soil water content readings necessary to accurately define the initial conditions were available only for upper catchment. In order to quantify the effect of precipitation intensity on RZWQM predicted runoff, upper catchment was simulated in RZWQM with a uniform steady precipitation intensity of 1 cm/hr and compared to RZWQM predictions using measured unsteady hourly precipitation intensity at ACL. Daily precipitation was applied continuously at the rate of 1 cm/hr for successive hours starting midnight until the remainder precipitation was less than 1 cm for the next hour, which was distributed over the last hour. RZWQM predicted 19 cm total runoff (runoff coefficient = 0.21) with measured hourly precipitation intensity. However, the predicted total runoff of 9 cm (runoff

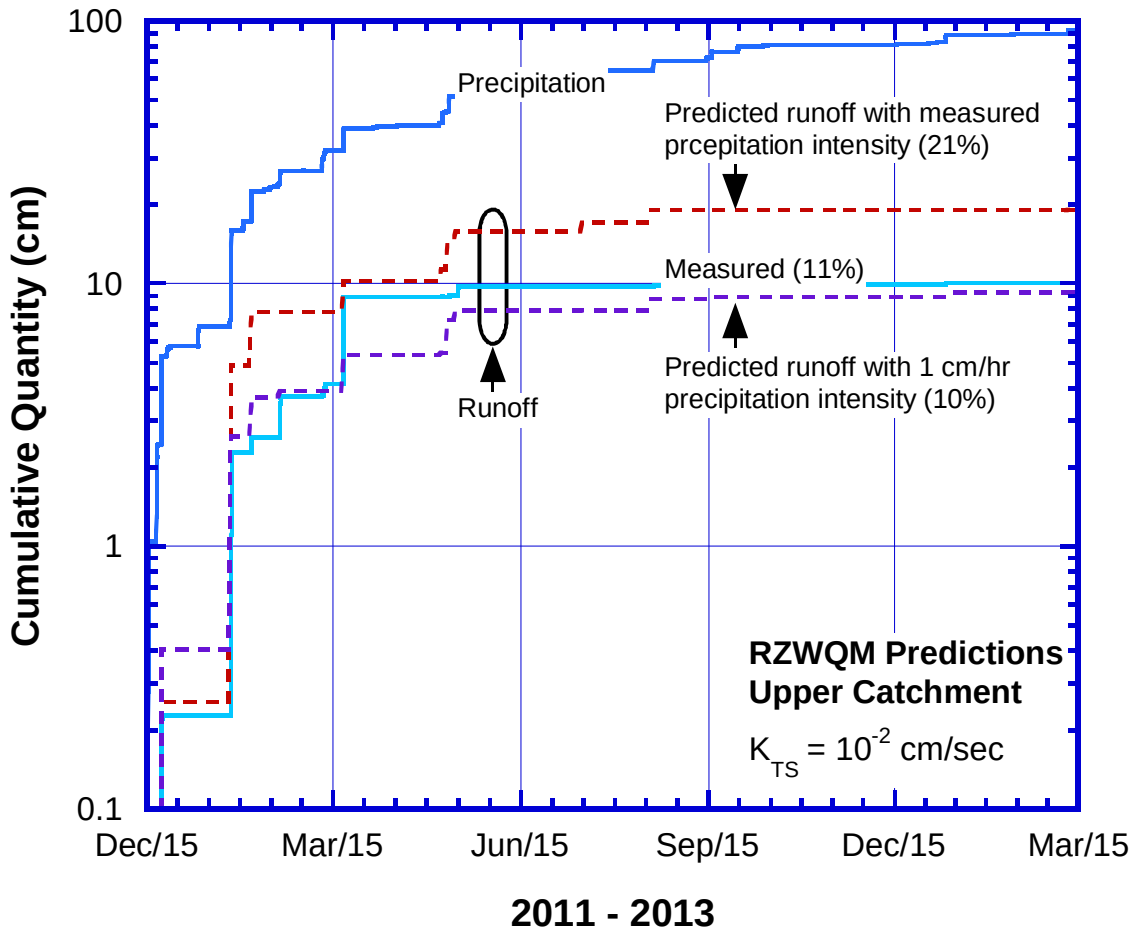

Figure 2-15. Effect of input precipitation intensity on RZWQM predicted runoff for upper catchment

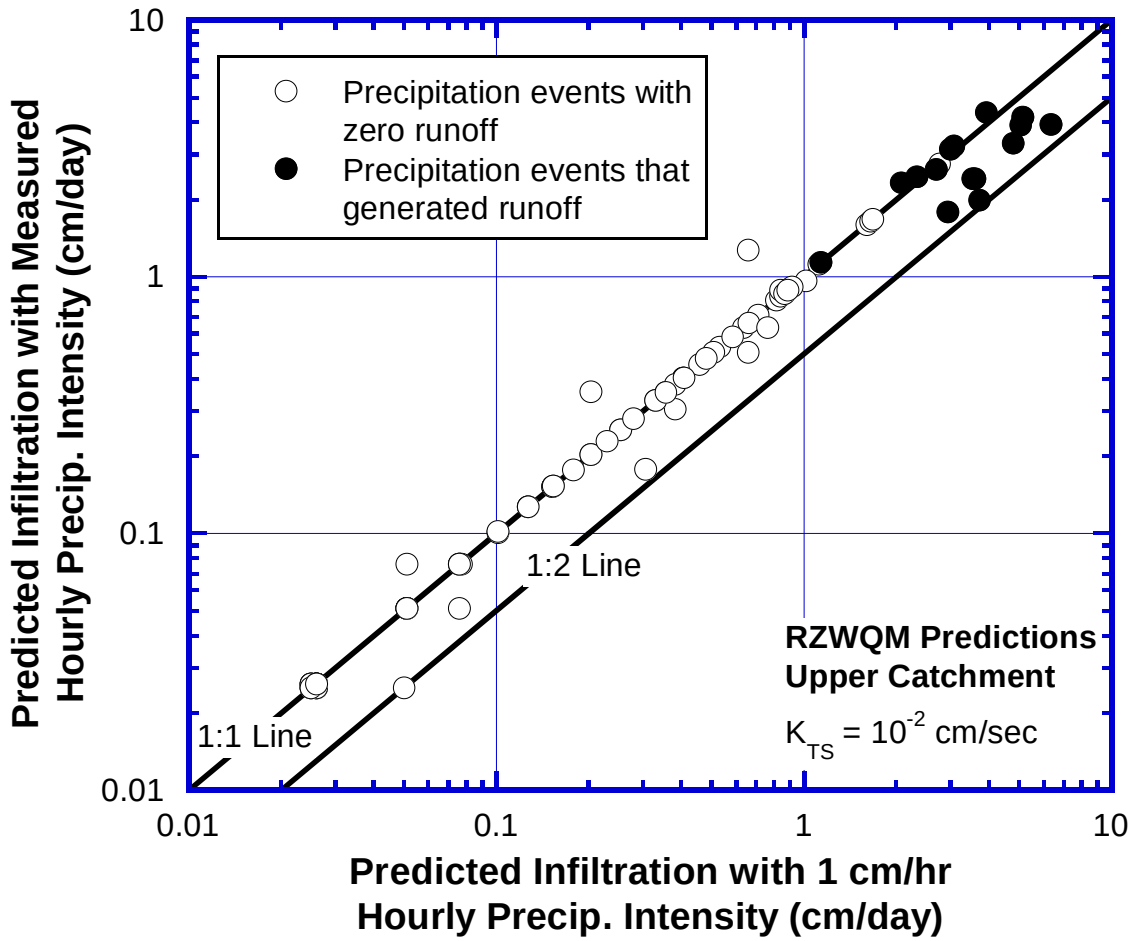

Figure 2-16. Effect of input precipitation intensity on RZWQM predicted infiltration for upper catchment

coefficient = 0.10) was relatively accurate with respect to the measured runoff value of 10 cm (runoff coefficient = 0.11) for RZWQM simulations with input precipitation intensity of 1 cm/hr (Fig. 2-15). RZWQM uses Green-Ampt (1911) model to evaluate infiltration and sheds off excess precipitation as runoff. Richards' equation is used by RZWQM to model unsaturated flow only in between the consecutive precipitation hours. Water balance predictions from such infiltration formulation of RZWQM were found to be dependent on the input of precipitation intensity. RZWQM predicted daily infiltration values were up to two times higher for simulations with 1 cm/hr precipitation intensity than for simulations with the measured hourly precipitation intensity as input (Fig. 2-16). The difference in predicted daily infiltration between the two simulations was relatively more pronounced for runoff predicting precipitation events than zero runoff predicting precipitation events. Higher infiltration resulted in less predicted cumulative runoff with 1 cm/hr precipitation intensity. Hence, Green-Ampt infiltration model implemented in RZWQM was unable to model unsteady hourly ACL water balance processes accurately.

Measured and Predicted Soil Water Contents with RZWQM and UNSAT-H

Upper catchment soil water contents predicted by RZWQM and UNSAT-H were compared with the measured soil water contents (Fig. 2-17). RZWQM simulations with K_{TS} value of 10^{-2} cm/sec and UNSAT-H simulations with K_{TS} value of 1.4×10^{-3} cm/sec from simulation set 2 are presented to maintain continuity with the corresponding runoff simulations discussed earlier in the paper. UNSAT-H simulated water contents for upper catchment with simulation set 1 and simulation set 3 behaved in the similar fashion as UNSAT-H simulations with simulation set 2 as presented in Fig. 2-17.

RZWQM and UNSAT-H were unable to accurately predict daily soil water contents accurately. But seasonal variations in measured water content at all depths were predicted

relatively accurately by both models (Fig. 2-17). Similar to the measured data, higher soil water contents were predicted in Winter 2012 which dropped to relatively low predicted values in the subsequent seasons and never reached the high values observed in Winter 2012 for both models. Several authors had reported similar finding while simulating soil water contents of engineered clay soils of EFCs and natural soils. Khire et al. (1997), Mijares and Khire (2012) and Scanlon et al. (2002) successfully used UNSAT-H to predict seasonal variation in the soil water storage across United States in semiarid climate of Wenatchee, sub-humid climate of Detroit, and semiarid climate of west Texas. Ghidey et al. (1999) used RZWQM to predict seasonal variation in soil water contents relatively accurately at depths equal to 15 cm, 60 cm, 75 cm and 90 cm with respect to the measured data at Missouri MSEA (Missouri Management Systems Evaluation Area).

Seasonal soil water contents were under predicted in Winter 2012 but over predicted by both models after winter season 2012 for shallow depth of 30 cm and deeper depth of 105 cm of the upper catchment (Fig. 2-17). Seasonal soil water content predictions in water balance codes is dependent on the accuracy of runoff predictions. Over prediction of cumulative runoff in Winter and Spring 2012 resulted in under prediction of soil water contents as less water was available for infiltration in UNSAT-H simulations. Similar observation of over estimation of runoff by water balance codes resulting in under estimation of infiltration and consequently lower predicted soil water storage was made by several authors (Fayer et al. 1992; Bohnhoff et al. 2009; Ma et al. 1999; Scanlon et al. 2002). Soil water storage was over predicted for Summer 2012 to Winter 2013 irrespective of relatively accurate prediction of cumulative runoff by UNSAT-H. Transpiration loss due to vegetation resulting in lower soil water storage was not simulated in UNSAT-H which resulted in over prediction of soil water storage.

At seasonal and annual temporal scale, soil water contents predicted by RZWQM closely

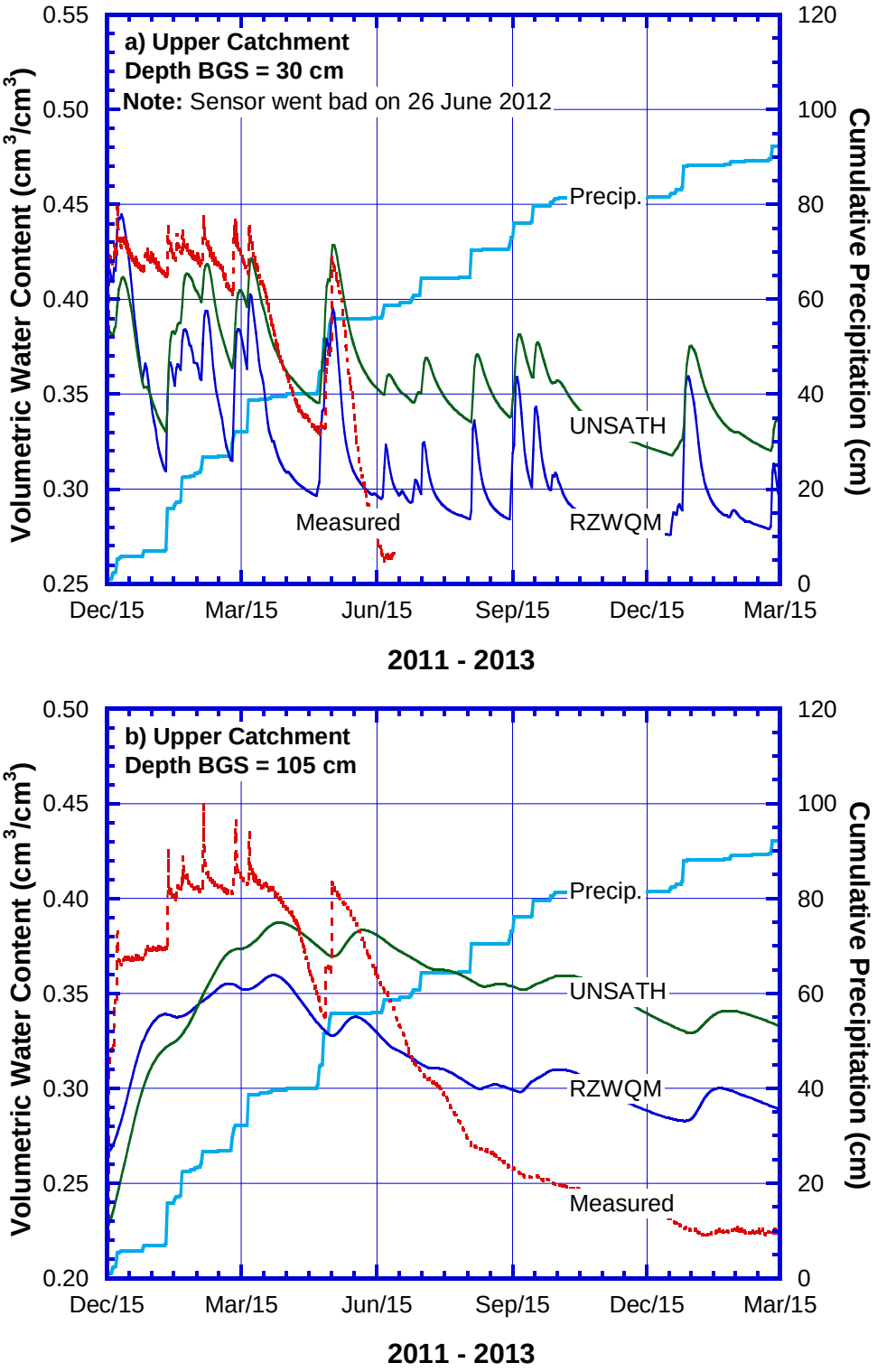

Figure 2-17. Measured versus predicted (UNSAT-H and RZWQM) soil water contents in upper catchment at 30 cm (a); and 105 cm (b) below ground surface

followed UNSAT-H predictions and were not significantly affected by inter-code differences in runoff calculations and initial conditions. RZWQM predicted higher soil water content than UNSAT-H at both shallow and deep depths for the wet season until Winter 2012, which was due to relatively wetter initial conditions simulated by RZWQM. However, RZWQM consistently under predicted soil water contents for rest of the simulated period after Winter 2012. The difference in the daily predicted runoff by UNSAT-H and RZWQM resulted in relative difference in daily infiltration and evaporation predictions which consequently led to the difference in soil water content predictions.

Event Scale Analysis UNSAT-H Results

Runoff ratio was defined as the ratio of UNSAT-H predicted runoff to measured runoff. Hence, runoff ratio greater than one indicated over prediction of runoff by UNSAT-H and vice versa. A comparison of runoff ratios for the individual storm events with the measured runoff was done for upper catchment (Fig. 2-18). UNSAT-H predicted lower catchment runoff generally followed the upper catchment runoff trends and is not discussed further. UNSAT-H predicted 9 runoff events compared to 17 runoff events measured for the upper catchment. UNSAT-H generally under predicted daily runoff. Runoff ratio histogram was sorted in ascending order respect runoff ratio and compared with the corresponding measured runoff to establish a possible correlation. No correlation could be established between the measured runoff and runoff ratio. UNSAT-H predict zero runoff on 8 January 2013 (measured runoff = 0.07 cm) but relatively accurately predicted runoff on 18 August 2012 (measured runoff = 0.08 cm) and 7 May 2012 (measured runoff = 0.04 cm) for similar measured runoff. Hence, UNSAT-H predicted runoff was not correlated to the measured runoff. However cumulatively over the 15 month period, runoff predicted by UNSAT-H was relatively accurate.

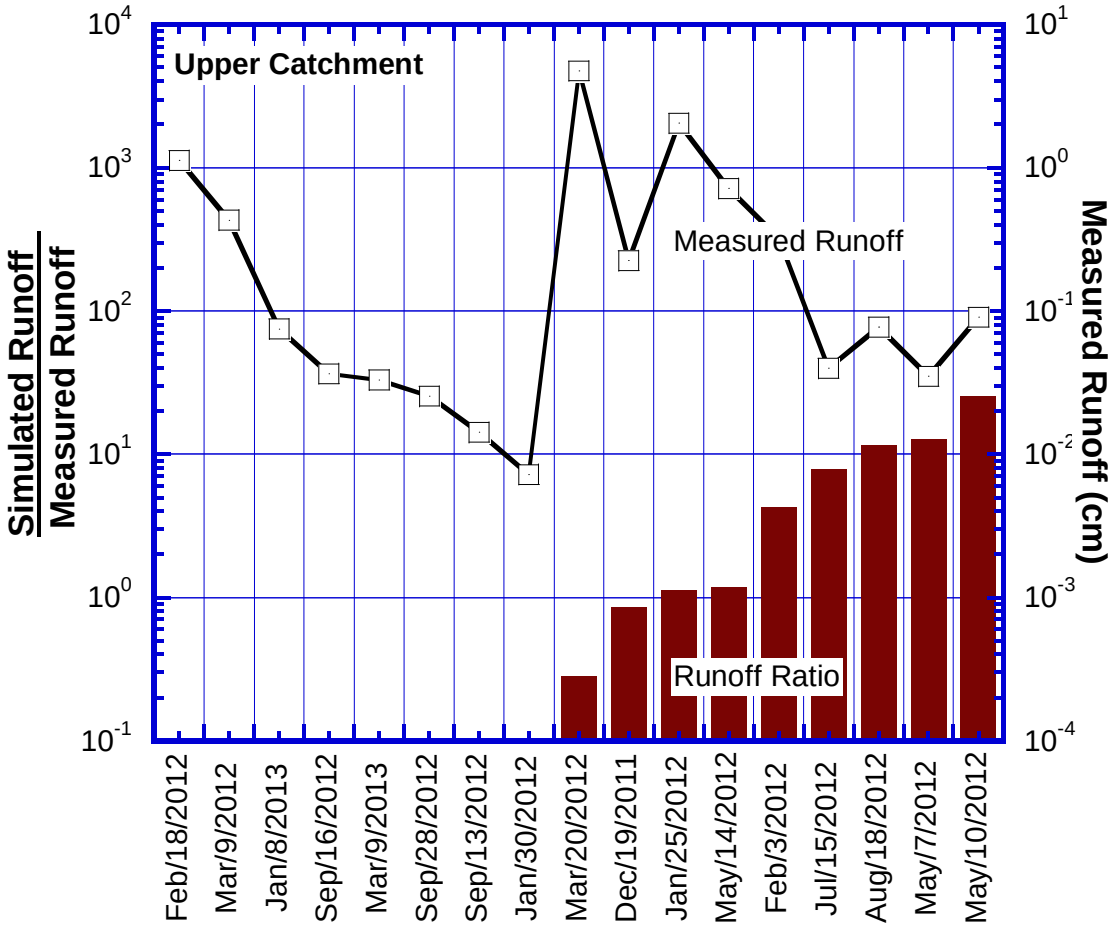

Figure 2-18. Event wise measured and UNSAT-H predicted runoff for upper catchment

Hill slope runoff usually consists of both infiltration excess runoff and saturation excess runoff components (Beven and Kirkby 1979; Freeze 1980; Beven 1986; Wood et al. 1988; Binley et al. 1989). UNSAT-H is primarily an infiltration excess capillary flow model (Fayer 2000) and spatial processes such as lateral subsurface flow, macro-pore flow, slope inclination, local depression storage, vegetation canopy, runoff flow connectivity and rainfall distribution which govern hill slope overland runoff (Hewlett and Hibbert 1967; Dunne and Black 1970b; Weyman 1973; Dunne et al. 1991; Abrahams et al. 1994; Gomi et al. 2008) were not simulated by UNSAT-H. Further, process based models such as UNSAT-H cannot always predict event-dependent hydrologic response of heterogeneous catchments with mean soil parameters and mean initial soil water conditions (Merz and Plate 1997). Hence, UNSAT-H predicted runoff values for individual storm events were inaccurate but catchment scale annual and cumulative monthly runoff values predicted by UNSAT-H were relatively accurate.

SUMMARY AND CONCLUSIONS

An existing landfill EFC was instrumented in semiarid climate of Austin, Texas to measure catchment scale runoff. Runoff, soil water contents and soil suctions were measured for the monitoring period of fifteen months. UNSAT-H and RZWQM were used to simulate 1-D unsaturated zone hydrology and water balance of the two test catchments using the hydraulic properties estimated from three instrumented nests located in different catchments at different elevations along the same vertical transect.

UNSAT-H predicted runoff was significantly affected by input top soil saturated hydraulic conductivity and UHCF. Laboratory measured UHCF did not represent the catchment scale hydraulic properties of top soil to model EFC hydrology accurately with UNSAT-H. However, at annual time scale, UNSAT-H predicted EFC runoff relatively accurately with K_{TS} value ranging

from 1.4×10^{-3} cm/sec to 6.8×10^{-3} cm/sec. RZWQM grossly over predicted runoff with measured hourly precipitation. However, RZWQM predicted runoff was relatively accurate when daily precipitation was applied at a uniform precipitation intensity of 1 cm/hr. Green-Ampt infiltration model implemented in RZWQM was unable to simulate unsteady hourly water balance at ACL.

None of the numerical models were able to predict soil water contents of the storage layer accurately. RZWQM and UNSAT-H under predicted soil water contents during Winter 2012 but over predicted soil water contents in Summer 2012. UNSAT-H was also unable to accurately predict event scale runoff hydrology at ACL.

The current study was able to verify the use of 1-D water balance models for predicting runoff from catchment scale EFCs. UNSAT-H performed relatively accurate at the annual scale than RZWQM. Additional data if collected to study the spatiotemporal effects of vegetation and macro-pore flow on runoff connectivity and infiltration can help in quantification of the physical processes governing catchment scale runoff which can be subsequently used to modify numerical models to better predict EFC hydrology.

PAPER 3: PREDICTED SURFACE RUNOFF FOR EARTHEN COVERS IN TEXAS

ABSTRACT

Numerical models are routinely used to design earthen final covers (EFCs) to cap municipal solid waste landfills. Several studies over the last two decades have highlighted the importance of calibrated numerical models in predicting long term hydrology of EFCs. A regional scale numerical modeling study for Texas was undertaken to assess the influence of soil depth, soil type and climatic conditions on the landfill cover hydrology. UNSAT-H, a water balance and unsaturated flow model was used for the regional scale hydrology modeling. A total of twenty four stations located in Texas were identified with high quality meteorological data for about fifty years or more (1961-2011). Multi-year average precipitation year (APY) simulation followed by a wet precipitation year (WPY) were deemed to represent the critical scenario for simulating long term EFC hydrology. WPY annual runoff was generally higher than APY annual runoff for all stations. Annual runoff for both APY and WPY generally increased from west to east Texas consistent with the annual precipitation. Daily and annual runoff correlated positively with precipitation for the entire Texas for both APY and WPY climates. Daily runoff-precipitation relation generally correlated better than annual runoff-precipitation relation for both APY and WPY climates. Daily and annual runoff was highly variable in drier regions (west Texas) and correlated poorly with precipitation as compared to wet regions (east Texas). The statistical correlation of WPY annual runoff with APY annual runoff was poor. UNSAT-H simulations did not consider ground surface roughness, runoff connectivity, vegetation cover, soil water hysteresis, macro-pore flow, spatial and temporal variation in soil hydraulic properties, slope inclination and slope length of landfill covers which can significantly affect catchment scale EFC runoff generation and soil water balance.

INTRODUCTION

Earthen final covers (EFCs) or alternative final covers are used for isolating municipal solid waste (MSW) in landfills depending on the liner system below. EFCs when designed properly minimize both the percolation to the landfills and the fugitive greenhouse gas emissions from escaping landfills (Nyhan et al. 1990; Börjesson and Svensson 1997; Hauser et al. 2001; Madalinski et al. 2003; Scheutz et al. 2003; Mijares et al. 2012). EFCs are engineered earthen layers designed to store infiltration and release it back as evapotranspiration (ET). However, permitting of EFCs often requires field-scale demonstration to evaluate its hydraulic equivalency with the conventional covers [CFR 258.60(b) (1), United States Government 2002]. Several field-scale studies had been conducted in last two decades to identify design variables governing performance of EFCs (Nyhan et al. 1990; Khire et al. 1997, 1999; Scanlon et al. 2002; Scanlon et al. 2005, Albright et al. 2004; Mijares et al. 2012). As these field-scale studies are expensive and extend only for a few years, numerically calibrated models are often used to estimate the long term performance of EFCs (Scanlon et al. 2005; Khire et al. 2000).

Design and performance of EFCs is primarily controlled by thickness of soil layers, soil hydraulic properties and climate (Khire et al. 2000). Soil water storage layer thickness and soil type (i.e., soil hydraulic properties) can be varied to meet design criterion. However, limited modeling studies have been done to study EFC water balance at a regional scale.

A regional scale water balance mapping and analysis generally consist of one or more of the arithmetic averaging, area weighted averaging, statistical interpolation, empirical water balance equations and process based water balance modeling techniques (Arnell 1995). Algebraic and statistical interpolation techniques become constrained at a regional scale due to limited data on catchment scale hydrology of EFCs. Consequently, process based water balance modeling is

an alternative for regional scale runoff and hydrology analysis of EFCs. Similar approach was used by Keese et al. (2005) to predict annual ground water recharge for thirteen aquifer regions in Texas.

The primary objective of the current water balance modeling study is to simulate runoff for EFCs located in Texas and map runoff at a regional scale for Texas.

STUDY AREA

The west south central state of Texas (US Census Bureau classification) is characterized with diverse hydro-geologic settings. With an area of approximately 700,000 km^2, the elevation in Texas ranges from sea level along the coast line in southern part to 2,700 m in Guadalupe Peak in west Texas. The mean annual precipitation in Texas ranges from 147 cm in east to 36 cm in the west part of the state. North America Cordillera (more popularly known as Rocky Mountains) acts as a barrier to the east-west flow of air across United States and provides an ideal pathway for cold winds from Canada travelling south to Texas which results in relatively cold temperatures in north Texas. Gulf of Mexico serves as the primary source of east-west variation in precipitation with high precipitation in the east than west Texas. Thus, generally the precipitation in Texas increases from west to east and the temperature increases from north to south (Nielsen-Gammon 2011). Texas with a wide geologic, climate and soil diversity presents an ideal setting to understand regional scale water balance of EFCs.

NUMERICAL MODEL

HYDRUS, Vadose/W, UNSAT-H, LEACHM, HELP are several public domain and commercial codes routinely used to model EFC hydrology (Khire et al. 1997; Mijares et al. 2012; Bohnhoff et al. 2009; Ogorzalek et al. 2008; Albright et al. 2013). UNSAT-H (Fayer 2000) is a public domain unsaturated flow and water balance model and has been validated to closely

simulate lysimeter water balance of EFCs (Scanlon et al. 2002; Mijares and Khire 2012). UNSAT-H was also able to successfully predict catchment scale runoff from EFC in semiarid climate of Austin as presented in paper 2. Keese et al. (2005) used UNSAT-H for regional scale studies to simulate natural aquifer recharge of Texas and Khire et al. (2000) used UNSAT-H to predict long term design variables for capillary barrier MSW landfill cover in semiarid climate of Wenatchee. Hence, UNSAT-H has been successfully used for both regional scale study and long term water balance simulations and consequently was chosen for the current study.

UNSAT-H is a finite-difference code and can simulate 1-D heat and liquid flow through unsaturated soils under different meteorological conditions. However, only isothermal simulations were carried out in this study. The numerical algorithm of UNSAT-H can be divided in two parts: (1) water balance computations and (2) unsaturated flow. Water balance part of the code is represented as:

$$\Delta S = P - R_O - ET - D \tag{3-1}$$

where, P is precipitation, R_O is runoff, ET is evapotranspiration, D is deep drainage or percolation, and ΔS is change in soil water storage. Unsaturated flow within a soil layer is simulated by UNSAT-H with Richards' equation (Richards 1931)

$$\frac{\partial \theta}{\partial t} = \frac{\partial}{\partial z} K(\theta)\left(\frac{\partial h}{\partial z} + 1\right) - S_t(z,t) \tag{3-2}$$

where, θ is volumetric water content, $K(\theta)$ is unsaturated hydraulic conductivity dependent on volumetric water content, h is suction head, z is vertical distance below the ground surface, t is time and S_t is source or sink term.

Upper boundary of the soil domain in UNSAT-H can be simulated as a constant head or variable flux boundary. Under climate loading, the upper boundary in UNSAT-H loses water to

ET at a maximum potential flux if the suction at top node is smaller than pre-specified maximum suction. This maximum suction h_{dry} was set to 10,000 m for all simulations in the current analysis. The maximum potential ET flux evaluated by UNSAT-H is computed with Penman equation (Doorenbos and Pruitt 1977).The top boundary changes to a constant head boundary condition (equal to h_{dry}) when the suction at top node rose above the maximum suction. ET in such condition is calculated based on water flux across lower nodes below the soil surface. The bottom boundary of in-situ landfill covers is usually soil-waste interface. The waste layer underlying the landfill cover was not simulated in UNSAT-H and the bottom boundary of EFC was idealized to have unit gradient allowing free gravitational water flow (Fayer et al. 1992; Khire et al. 1997). Mijares and Khire (2012) also used unit gradient bottom boundary condition for UNSAT-H modeling and predicted percolation relatively accurately for an instrumented EFC in Detroit. No explicit subroutine is available in UNSAT-H to model runoff. However, excess precipitation which is unable to infiltrate the soil is lost from the upper soil boundary as runoff.

INPUT PARAMETERS

Meteorological data, soil hydraulic properties and soil layer thickness were among several variables needed as input to UNSAT-H. Precipitation, air temperature, dew point and wind speed were sourced from National Climate Data Centre (NCDC) of NOAA (http://www.ncdc.noaa.gov/). Solar radiation data was retrieved from National Solar Radiation Database (NSRDB) (Wilcox 2007). The number of simulated stations in Texas was constrained to twenty four due to the limited availability of high quality climate data necessary as input to UNSAT-H. No transpiration loss due to vegetation cover was assumed and all the simulations were done for bare ground conditions. Such an assumption was expected to predict worst case runoff in field conditions with minimal

water loss due to surface roughness, plant canopy abstraction and opportunistic infiltration due to root penetration.

Soil hydraulic parameters were modeled in UNSAT-H with van Genuchten (1980) functions. Soil water characteristic curve (SWCC) was defined as follows:

$$\theta = \theta_r + \frac{\theta_s - \theta_r}{\left(1 + \left|\alpha h\right|^n\right)^m} \tag{3-3}$$

where, θ is volumetric water content, θ_r is residual volumetric water content, θ_s is saturated volumetric water content, h is matric suction while α, n, and m are curve fitting parameters. Unsaturated hydraulic conductivity function (van Genuchten 1980) was defined as follows

$$K(h) = K_{sat} \frac{\left\{1 - (\alpha h)^{nm}[1 + (\alpha h)^n]^{-m}\right\}^2}{[1 + (\alpha h)^n]^{ml}} \tag{3-4}$$

where, K_{sat} is saturated hydraulic conductivity, K(h) is unsaturated hydraulic conductivity at suction h and *l* is pore-interaction term usually assumed equal to 0.5.

SOIL TYPES

CH, SM-ML and SM were three soil types simulated for all stations to closely replicate the range of soil types that can be used as storage layer of EFC in Texas. These soils have been tested by Kaushik et al. (2014), CEC (1997) and Khire et al. (1994), respectively. Vegetative layer was assumed to be made up of a top soil tested by Kaushik et al. (2014) for an EFC located in Austin, Texas. The unsaturated properties of top soil were measured in laboratory with centrifuge and dewpoint potentiometer (Kaushik et al. 2014). Field measured water content and suction data was used to evaluate CH unsaturated hydraulic properties because in-service properties were necessary for water balance models to accurately predict evapotranspiration and runoff from EFCs

(Ogorzalek et al. 2008; Bohnhoff et al. 2009; Mijares and Khire 2012; Albright et al. 2013). Unfortunately, unsaturated properties of SM-ML and SM were limited to laboratory measurements due to lack of field data. SM-ML and SM soil properties were identical to the properties used by Khire et al. (2000) to simulate long term water balance of capillary barrier MSW covers in arid and semiarid climates of United States. A summary of soil hydraulic properties used in UNSAT-H simulations is presented in Table 3-1 while the respective plots are presented in Fig. 3-1.

METEOROLOGICAL DATA

The precipitation data collected over 50 years (1961-2011) was used to evaluate average annual precipitation and 95 percentile annual precipitation at twenty four weather stations. Average precipitation year (APY) and wet precipitation year (WPY) were defined as the climate year which received average (arithmetic mean) 50 year precipitation and 95 percentile or higher precipitation, respectively for the water balance modeling. Once the magnitude of APY and WPY precipitation were calculated, a specific year that represented APY precipitation and a specific year that represented WPY precipitation were identified such that all other climatic data (solar radiation, air temperature, etc.) were available for the chosen years, from NOAA to create UNSAT-H climate input.

INITIAL CONDITIONS

The initial condition was assigned as suction corresponding to 60% saturation of the cover. Water balance of simulated EFCs reached a steady-state within twenty years of successive APY loading. Final degree of saturation of EFC at the end of twenty years of APY loading was used as initial condition for WPY simulations. WPY was simulated only for one year and was assumed to represent twenty year climate return period.

Table 3-1. Hydraulic soil properties for UNSAT-H simulations

Soil Water Characteristic Curve Parameters				
Parameters	**θ_s (cm3/cm3)**	**θ_r (cm3/cm3)**	**α (1/cm)**	**n (-)**
Top soil[1]	0.0	0.5326	0.05	1.22
CH soil[1]	0.454	0.04	0.0095	1.08
SM-ML soil[2]	0.35	0.02	0.012	1.123
SM soil[3]	0.02	0.42	0.005	1.48
Unsaturated Hydraulic Conductivity Parameters				
Parameters	**K_{sat} (cm/sec)**	**α (1/cm)**	**n (-)**	***l* (-)**
Top soil[1]	10^{-2}	0.05	1.22	-3.0
CH soil[1]	10^{-6}	0.015	2.2	-2.8
SM-ML soil[2]	10^{-5}	0.012	1.123	0.5
SM soil[3]	2.7×10^{-4}	0.005	1.48	0.5

Note: 1. Kaushik et al. (2014)
2. CEC (1997)
3. Khire et al. (1994)

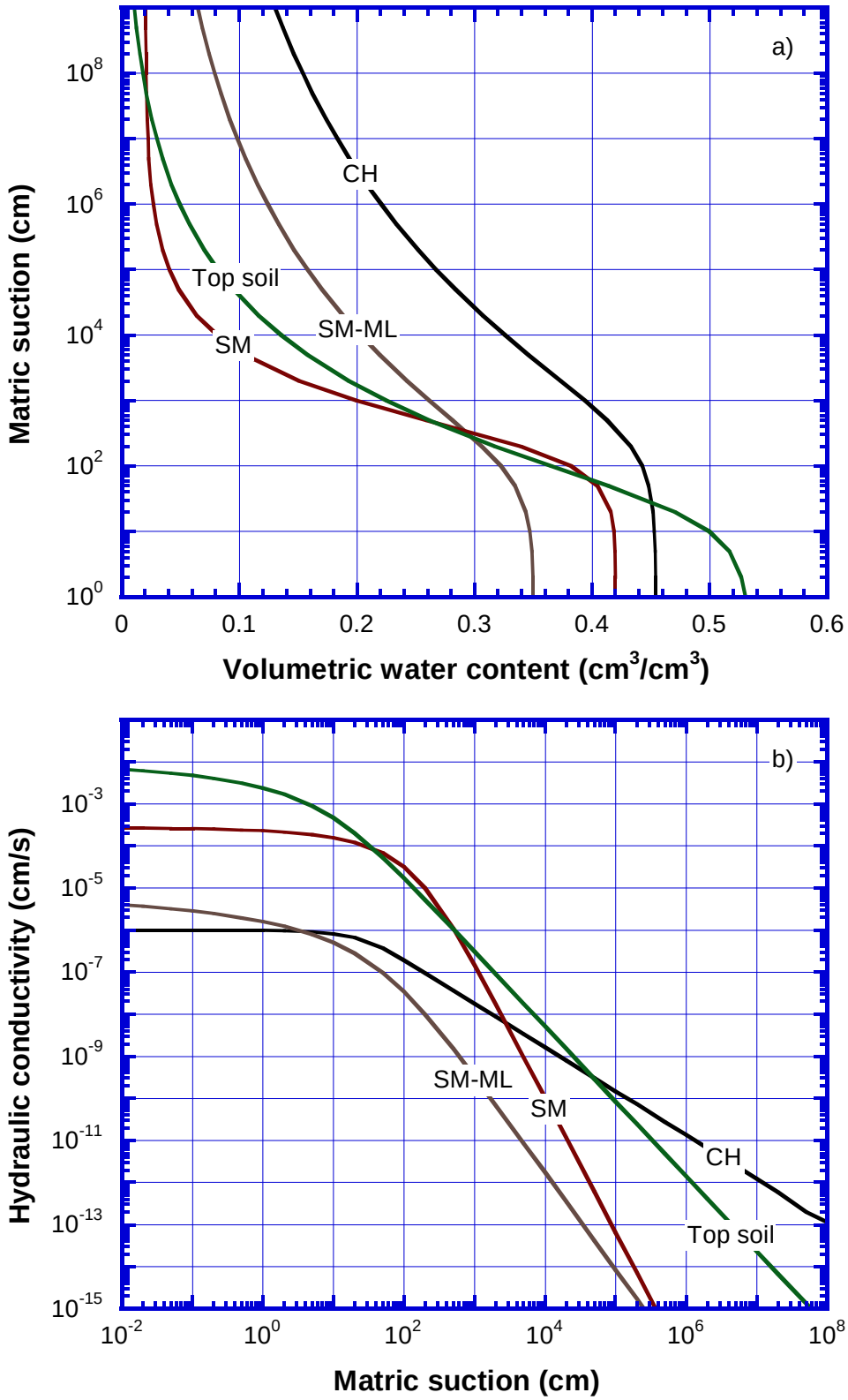

Figure 3-1. Soil water characteristic curves (a); and unsaturated hydraulic conductivity functions (b) for top soil, CH, SM-ML and SM soils

NUMERICAL PARAMETERS

A typical cross-section of the simulated vertical profile is presented in Fig. 3-2. The top soil was assumed to have a constant thickness equal to 15 cm (0.5 ft) for all simulations. Top soil was underlain by a monolithic storage layer of variable thickness. The thickness of the storage layer was varied from 30 cm (1 ft) to 240 cm (8 ft) to simulate different EFC designs. Nodal spacing was adjusted to ~1 mm near the upper boundary, lower boundary and at the interface of top soil and storage layer. Time stepping was chosen so as not to exceed the overall mass balance error of 1%. Daily precipitation was applied at the default intensity of 1 cm/hr.

EFFECT OF PRECIPITATION INTENSITY

Several studies have highlighted the importance of precipitation intensity for accurately modeling the measured runoff from landfill covers. Ogorzalek et al. (2008) predicted approximately three times more runoff with default precipitation of 1 cm/hr in UNSAT-H as compared to average precipitation intensity of 0.51 mm/hr, for capillary barrier cover in sub-humid climate of Polson, Montana. The predicted runoff decreased approximately by a factor of two when average precipitation rate of 0.68 mm/hr was used instead of 1 cm/hr for simulating water balance of monolithic cover in semiarid climate of Altamont, California. However, Scanlon et al. (2002) did not notice appreciable change in predicted runoff due to modeled precipitation intensity in UNSAT-H. Meyer (1993) highlighted over prediction of runoff due to hourly precipitation values as compared to daily precipitation values for South Carolina climate. Thus, the available literature offers conflicting observations with respect to the effect of precipitation intensity on UNSAT-H predicted runoff. Hence, to correctly assess the effect of precipitation intensity on water balance modeling of Texas, an independent validation of UNSAT-H predictions was done for Austin Community Landfill (ACL) in semiarid climate of Austin, Texas (Kaushik et al. 2014).

UNSAT-H simulations were carried out with as measured precipitation intensity (ACL-H) and with UNSAT-H default precipitation intensity of 1 cm/hr (ACL-D) for an instrumented catchment scale test section located in Austin, Texas (Kaushik et al. 2014). Both simulations had identical initial conditions as measured at the site and identical hydraulic soil properties. UNSAT-H under predicted runoff for both ACL-H (7.5% of precipitation) and ACL-D (6.6% of precipitation) simulations as compared to measured runoff (8% of precipitation) as presented in Fig. 3-3. Fig. 3-4 presents the histogram of number of hourly precipitation events which had predicted runoff versus the corresponding hourly precipitation bins for ACL-D and ACL-H simulations. All runoff generating precipitation events concentrated to a single precipitation intensity bin of 0.0254-1.0 cm/hr giving a single histogram bar for ACL-D simulations due to a uniform hourly simulated precipitation intensity. However, ACL-H simulations used field precipitation intensities and hence predicted runoff for several precipitation intensities. ACL-D predicted runoff was lower than ACL-H predicted runoff as ACL-D was unable to simulate several high intensity storm events of intensity greater than 1 cm/hr (Fig. 3-4). Hence, the importance of measured hourly precipitation to improve UNSAT-H runoff predictions cannot be ignored. Nonetheless, the default precipitation intensity of 1 cm/hr introduced an error of less than 1% in predicted runoff with respect to precipitation at ACL and was hence deemed good for the regional scale modeling. Further, high quality hourly precipitation data is not readily and consistently available at all twenty four stations. Hence, it is acknowledged that measured runoff due to localized climate conditions can significantly deviate from the predicted runoff presented in the current study.

Steeper slopes had been reported to generate more runoff than gentle slopes (Hewlett and Hibbert 1967; Nyhan 2005). However, UNSAT-H being 1-D model does not consider the effect

of EFC slope. However, UNSAT-H was able to predict the annual runoff at ACL with relative good accuracy and introduced an error of only 0.5% with respect to precipitation against measured runoff (Fig. 3-3). UNSAT-H predictions were thus deemed suitable for predicting runoff from EFCs sloped at 1V:4H at several sites in Texas.

RESULTS

Texas receives a wide range of precipitation ranging from an annual average of 36 cm to 147 cm (Fig. 3-5). The 95 percentile annual precipitation ranges from 57 cm to 207 cm (Fig. 3-6). PET for twenty four stations was evaluated for APY and WPY based on Penman equation (Penman 1940) as programmed in UNSAT-H (Fayer 2000). The average annual PET/P for APY ranged from 1.1 to 7.5 (Fig. 3-7) while PET/P based on WPY ranged from 0.7 to 4.6 (Fig. 3-8). WPY with greater annual precipitation generally resulted in lower PET/P than APY. The precipitation and PET/P generally followed longitudinal pattern from east to west. Texas represented by twenty four climate stations was divided in ten geo-climatic regions for the purpose of this water balance study on EFCs (Fig. 3-9). However, region #10 was precluded from the foregoing discussions because water balance simulations for region #10 yielded relatively high percolation rendering very large storage layer thickness (> 3 m) for EFCs which may be of little practical value. Similar to Albright et al. (2004), PET/P was used to define the climate type as per United Nations Educational, Scientific and Cultural Organization (UNESCO 1979). Texas has diverse climate types which ranged from arid ($PET/P \geq 5$), semiarid ($5.0 > PET/P \geq 2.0$), sub-humid ($2.0 > PET/P \geq 1.3$) to humid ($PET/P < 1.3$). Simulation results for 20 years of APY simulation were deemed to present APY climate while WPY results were representative of 20 APY years followed by one WPY year.

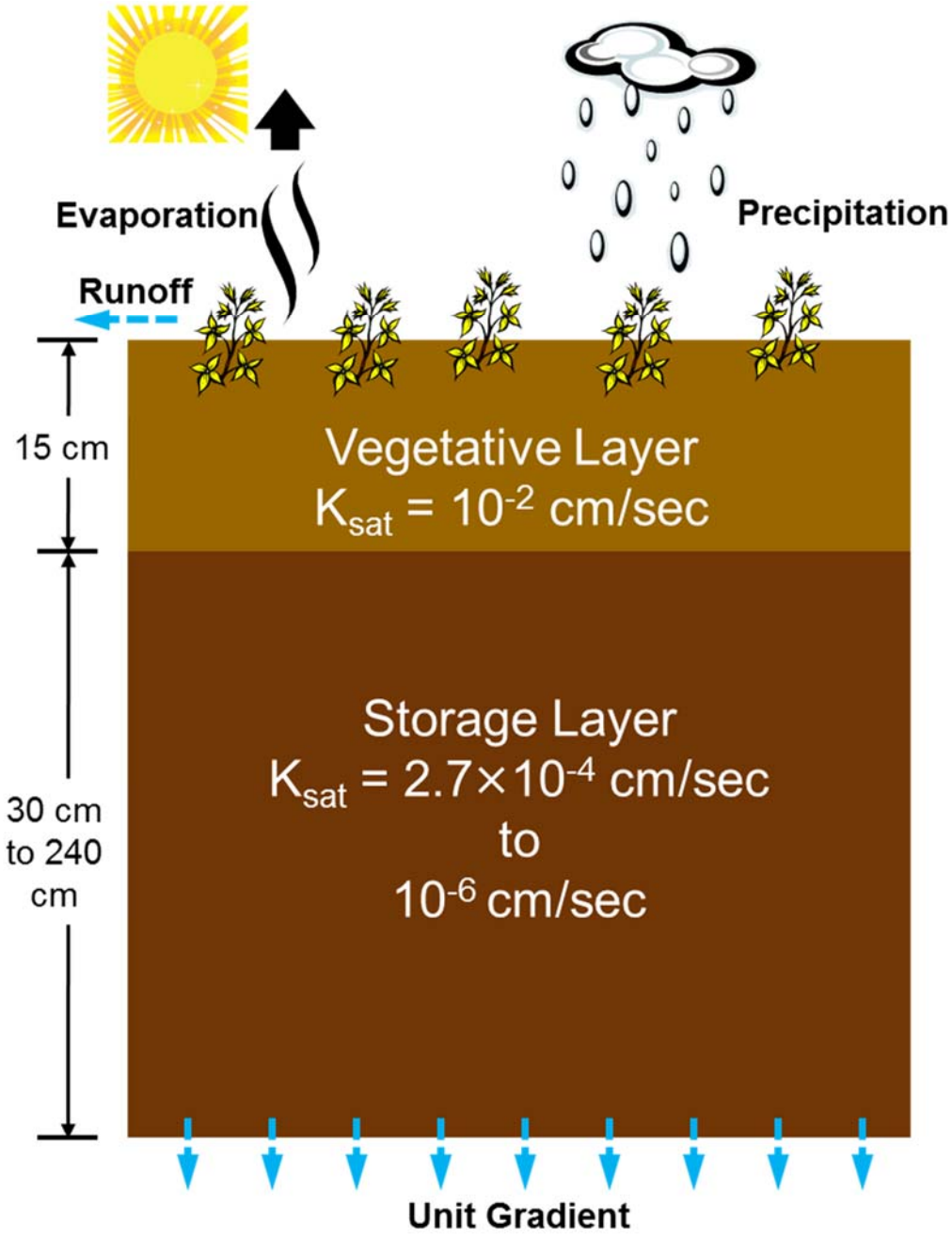

Figure 3-2. Simulated 1-D verticle profile of earthen final covers (EFCs) with UNSAT-H

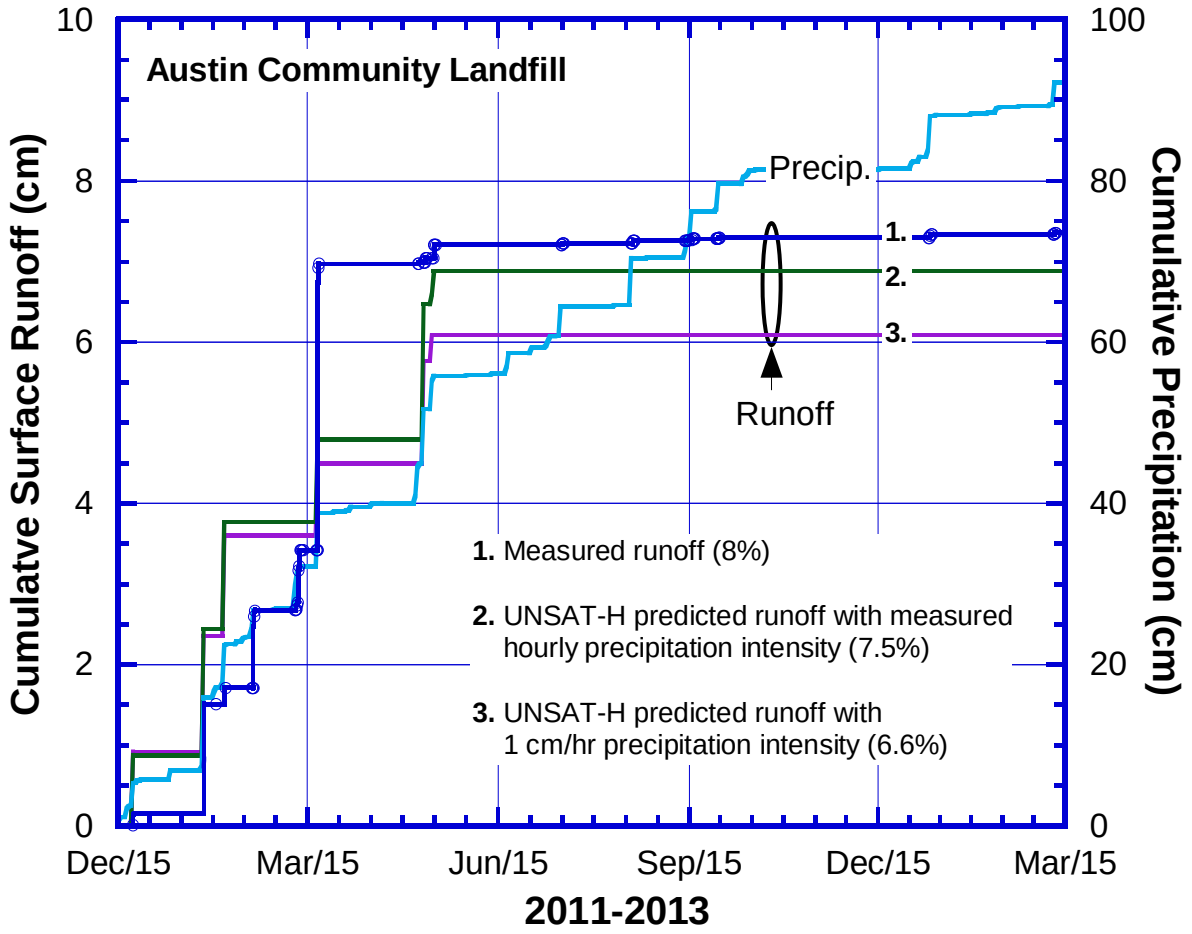

Figure 3-3. Comparison of UNSAT-H predicted runoff due to measured hourly precipitation intensity and default precipitation intensity

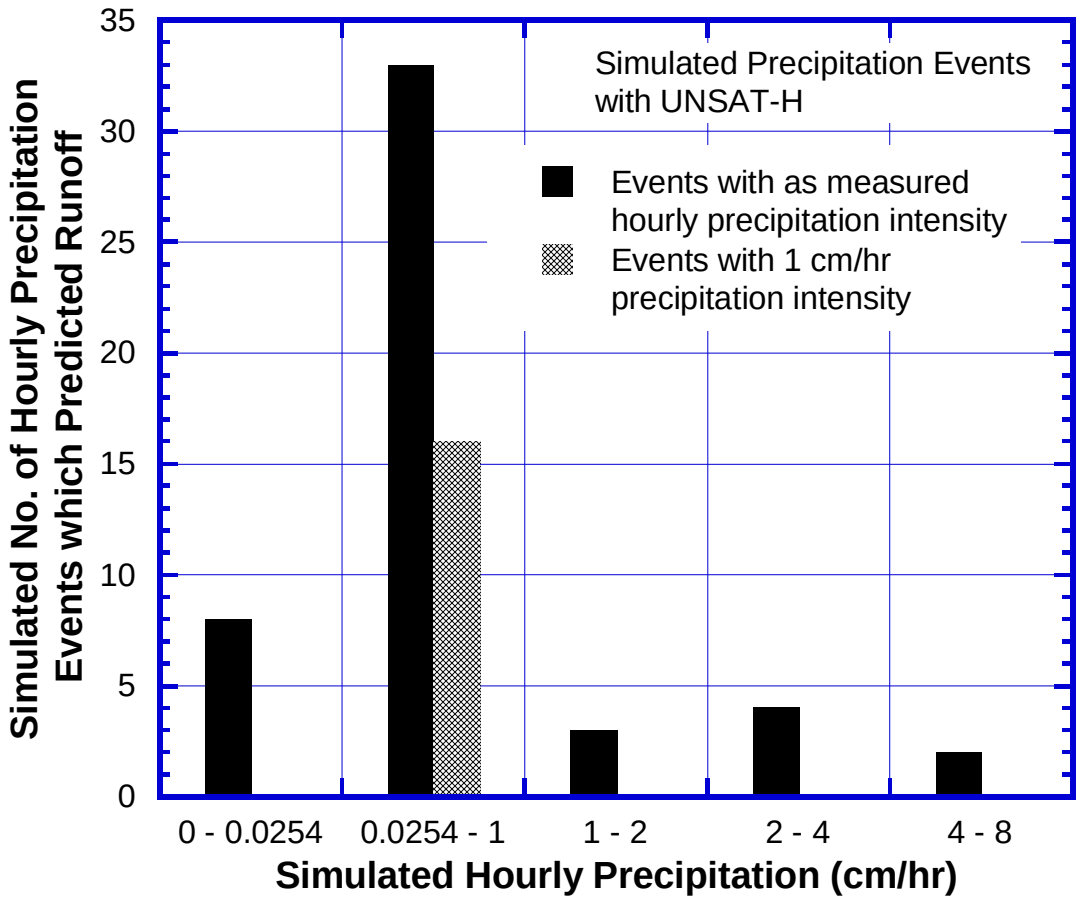

Figure 3-4. Distribution of hourly precipitation events which predicted runoff with UNSAT-H simulations

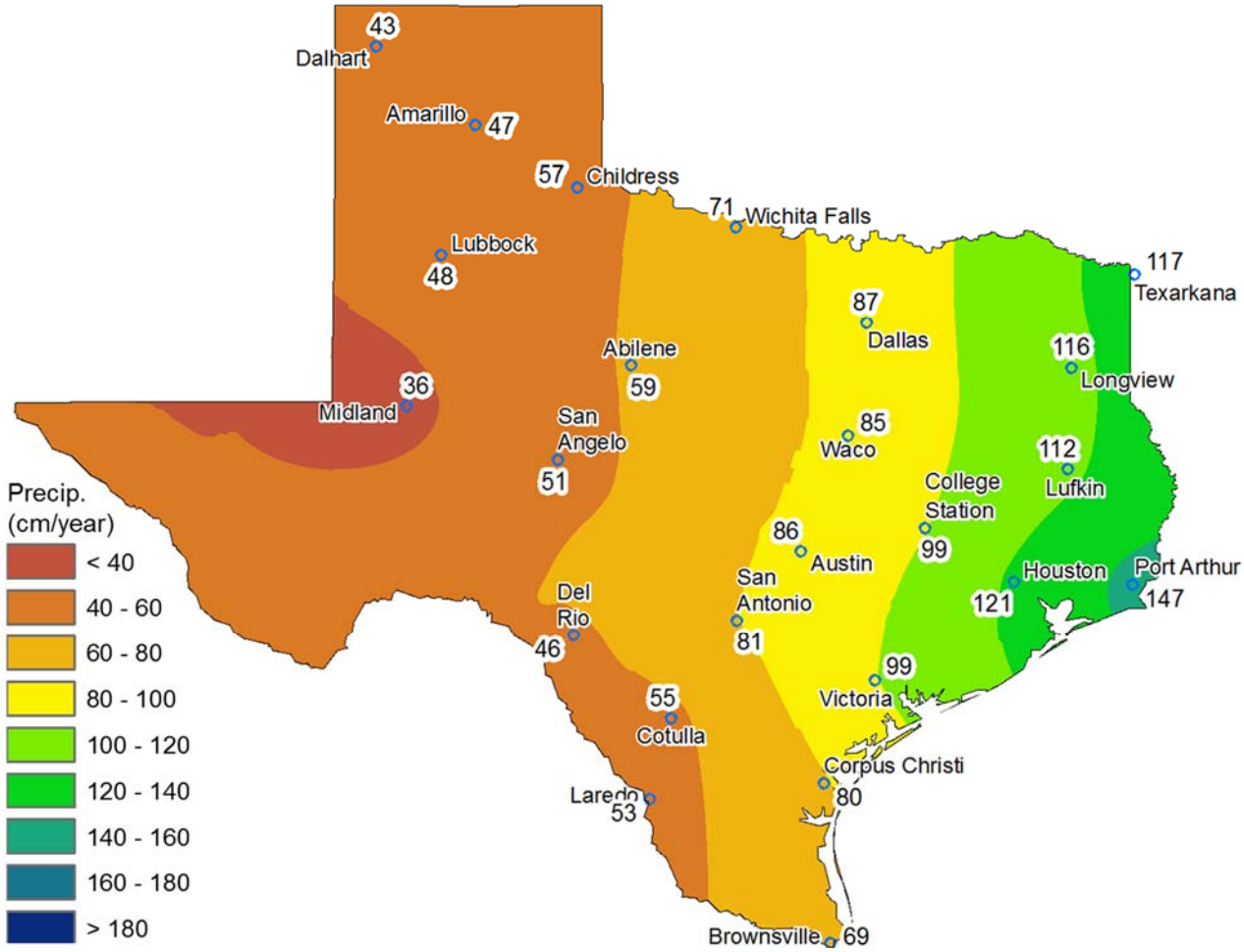

Figure 3-5. Annual precipitation contours for 50 year average precipitation

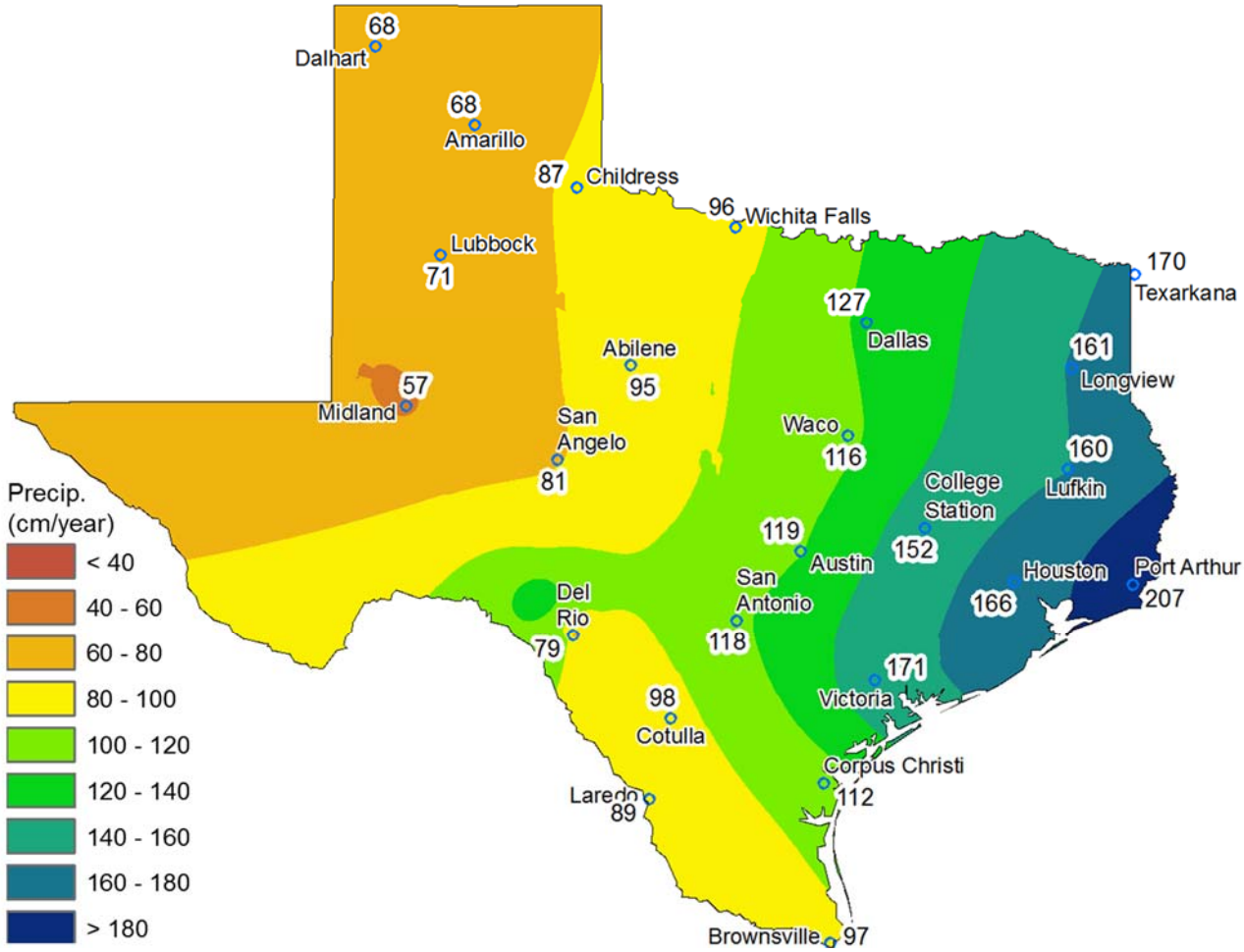

Figure 3-6. Annual precipitation contours for 50 year 95 percentile precipitation

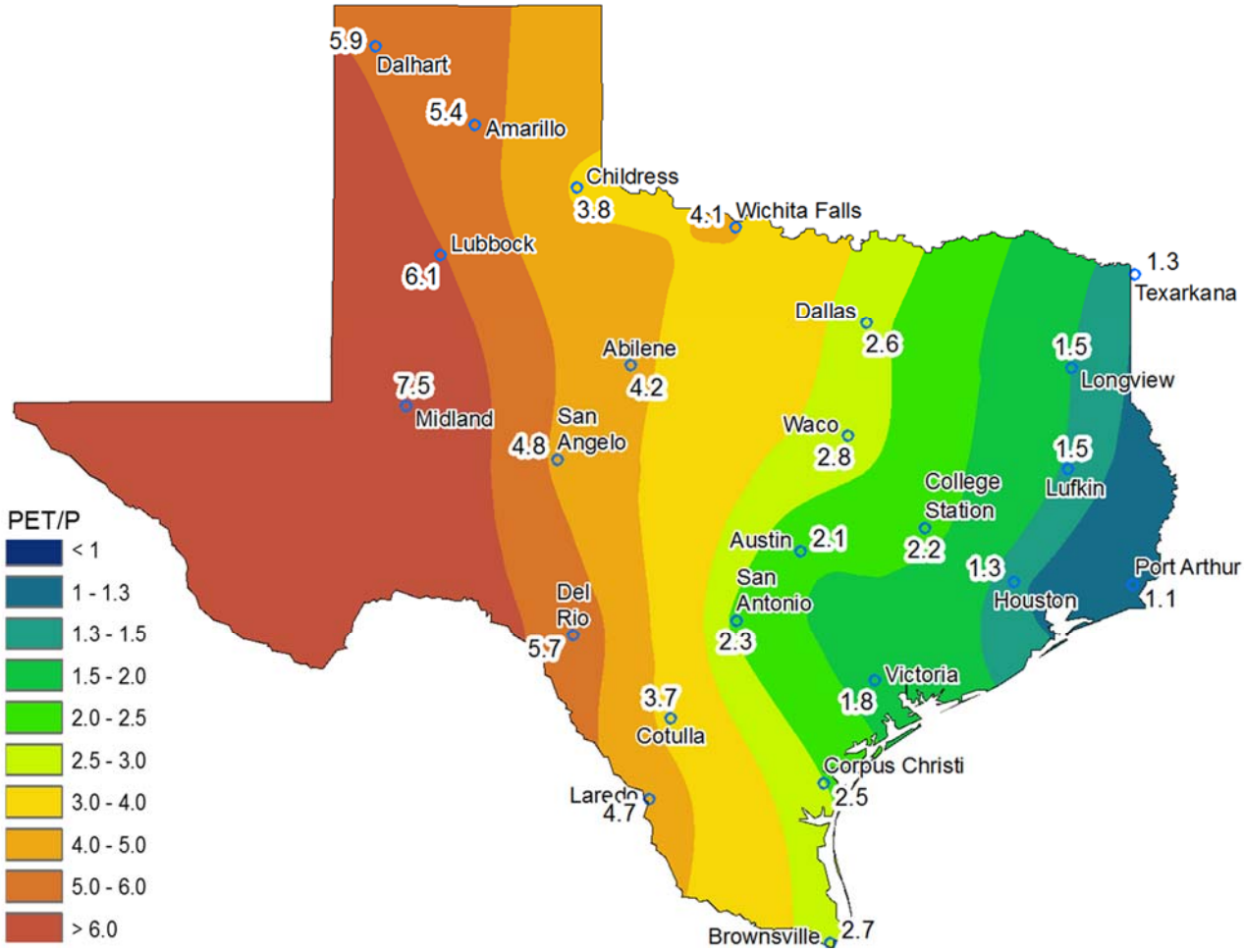

Figure 3-7. Annual PET/P for an average precipitation year

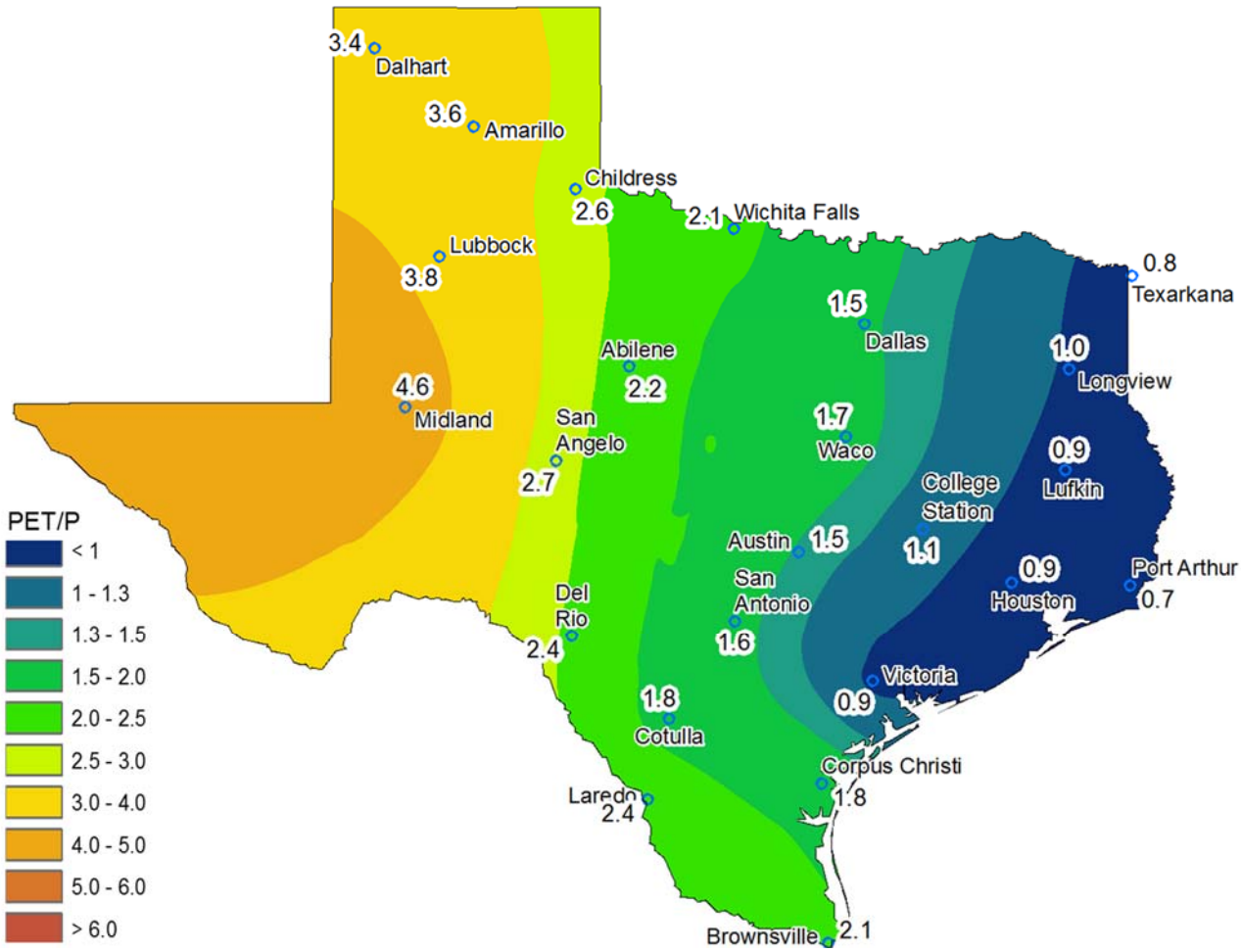

Figure 3-8. Annual PET/P for a 50 year 95 percentile precipitation year

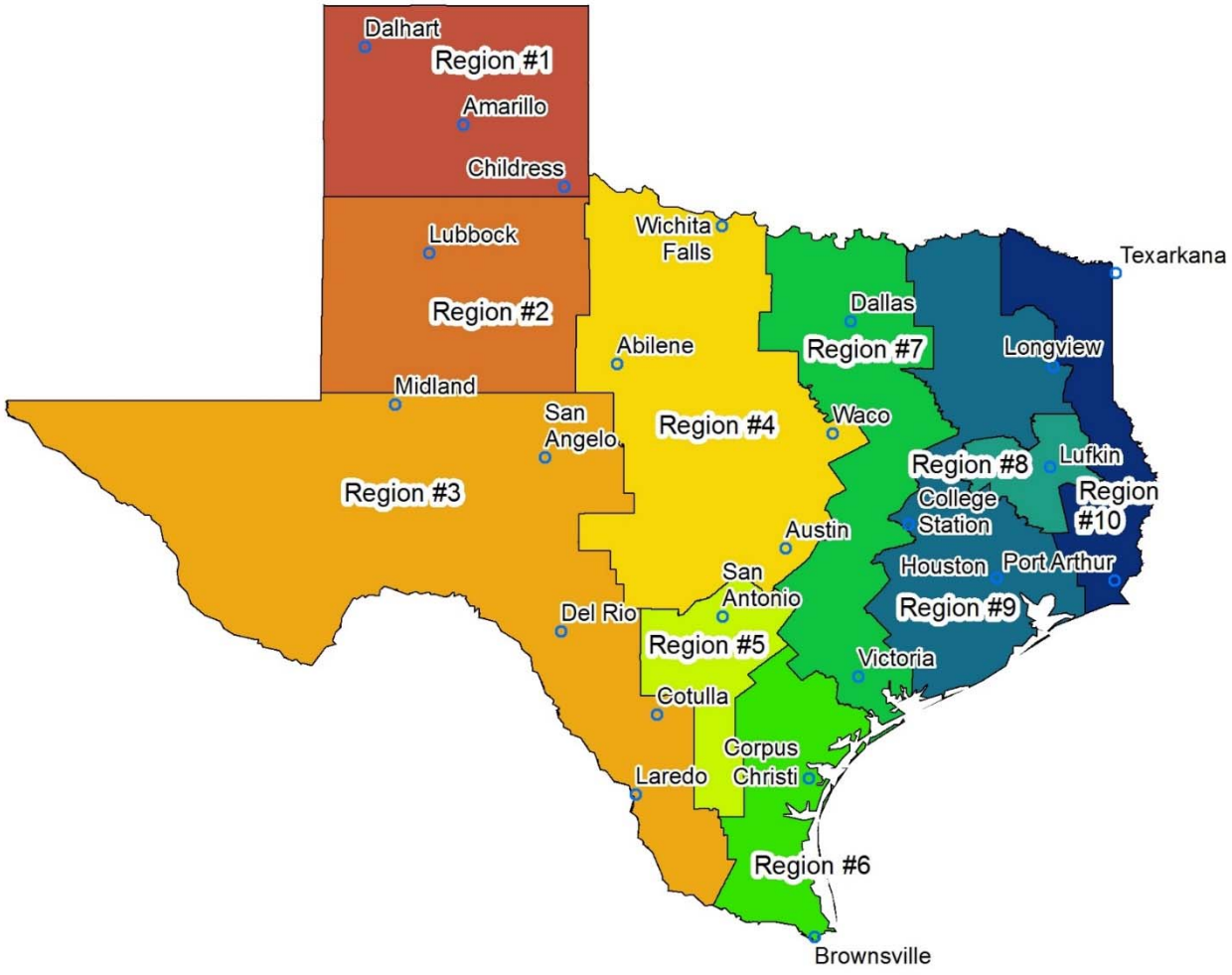

Figure 3-9. Geo-climatic regions for regional scale water balance modeling of EFCs in Texas

Control Water Balance Simulations

Climate data used in the current study consisted of measured meteorological variables except solar radiation, which was modeled by NOAA for different sites (Wilcox 2007). Hence, to assess the effect of modeled solar radiation on UNSAT-H predictions, Austin site with NOAA data (U-AUS) was compared against instrumented EFC at Austin Community Landfill (U-ACL) where solar radiation was measured with an onsite pyranometer. Kaushik et al. (2014) instrumented a catchment scale EFC at Austin Community Landfill (ACL) in Austin, Texas to measure runoff and soil water contents. UNSAT-H predicted the measured runoff at ACL relatively accurately compared to other numerical codes as presented in paper 2. The simulated climate years for U-ACL and U-AUS simulations were chosen so as to have close to 50 year average annual precipitation of Austin.

U-ACL with 81 cm annual precipitation had potential evapotranspiration (PET) of 189 cm (PET/P = 2.3) while U-AUS with 86 cm annual precipitation had PET of 181 cm (PET/P = 2.1). U-ACL was initialized with in-situ measured water contents while U-AUS was initialized with 60% degree of saturation. U-ACL predicted 8.6% runoff was close to U-AUS predicted runoff of 7.4% (Fig. 3-10a). The initial soil water storage, precipitation and PET for U-ACL were similar to U-AUS and consequently predicted runoff was not significantly affected by initial conditions and climate parameters (Fig. 3-10b). However, predicted percolation at U-ACL (0.2 cm) was an order higher than U-AUS (0.03 cm). The peak daily runoff was conservatively over predicted for U-AUS than U-ACL with majority of runoff taking place on Julian day 150. Hence, annual scale hydrology was relatively accurately simulated by UNSAT-H than daily scale hydrology.

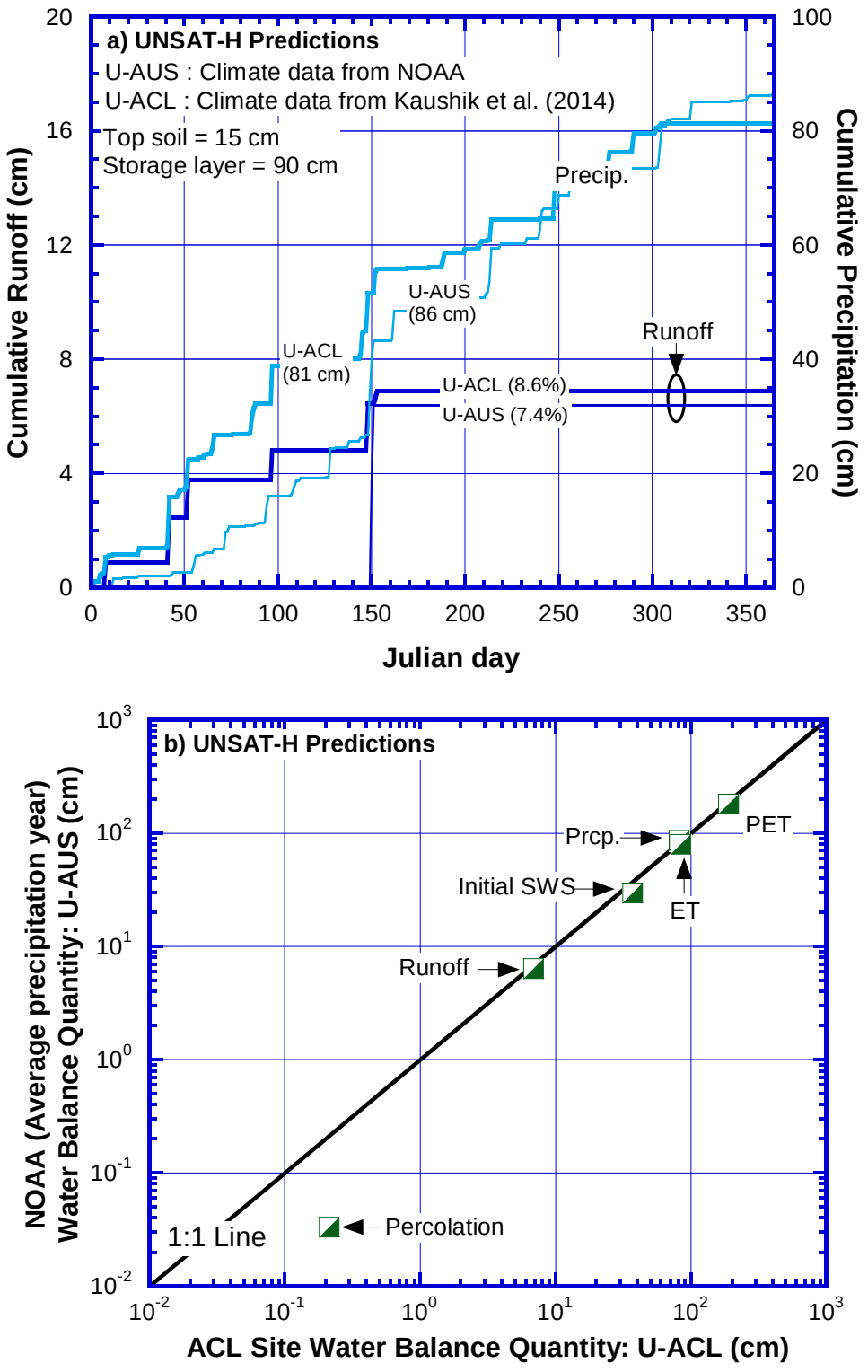

Figure 3-10. Predicted runoff for ACL (U-ACL) and Austin (U-AUS) (a); and comparison of water balance parameters from NOAA climate at Austin (U-AUS) to measured climate at ACL (U-ACL) (b)

Effect of Soil Type on Predicted Runoff

Saturated hydraulic conductivity (K_{sat}) of the three soils evaluated in the study ranged from 10^{-6} cm/sec to 2.7×10^{-4} cm/sec (Table 3-1). SM soil had highest saturated hydraulic conductivity ($K_{sat} = 2.7\times10^{-4}$ cm/sec) which was comparable to the default precipitation intensity of 1 cm/hr used for UNSAT-H simulations. Consequently, simulated rainfall intensity rarely exceeded infiltration capacity of SM soil and minimal water was shed as runoff for all stations in Texas by UNSAT-H. Runoff predicted by UNSAT-H for 30 cm SM soil underlain with 75 cm thick SP soil of a capillary barrier landfill cover was also zero (Khire et al. 2000). Hence, SM soil predictions were excluded in the foregoing analysis and discussions.

Runoff predicted by UNSAT-H using SM-ML soil ($K_{sat} = 10^{-5}$ cm/sec) as the storage layer was marginally higher than CH ($K_{sat} = 10^{-6}$ cm/sec) storage layer for both 90 cm (3 ft) and 180 cm (6 ft) thick storage layers (Fig. 3-11). SM-ML with lower unsaturated hydraulic conductivity for same suction resulted in lower infiltration and higher runoff than CH soil (Fig. 3-1b). The effect of storage layer soil type on the predicted runoff was however dampened by identical 15 cm (0.5 ft) thick top soil layer which resulted in similar infiltration capacities of the top 15 cm soil for both CH and SM-ML storage layer simulations.

Effect of Storage Layer Thickness on Predicted Runoff

Predicted annual and peak daily runoff from CH and SM-ML storage layers are plotted in Fig. 3-12. Predicted annual runoff from 90 cm (3 ft) thick storage layer was almost the same as that from 180 cm (6 ft) storage layer for APY and WPY (Fig. 3-12a). UNSAT-H runoff prediction was primarily influenced by the upper soil layers and it was not significantly affected by deeper soil layers. Similar observation was made by Sharpley (1985), where the precipitation and runoff interaction on Houston black clay was also primarily a surface phenomenon with the interaction

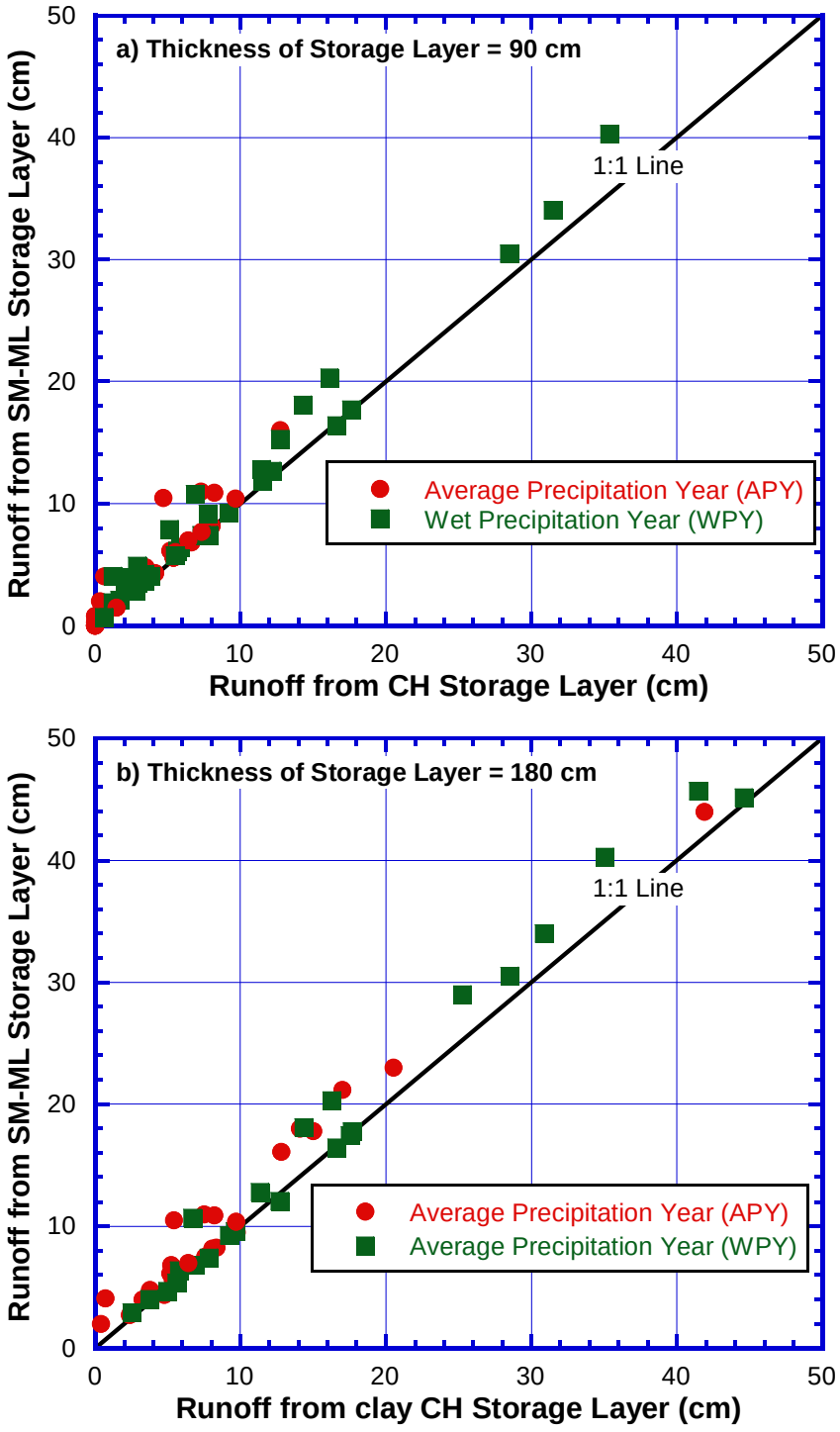

Figure 3-11. Effect of storage layer soil type on predicted runoff for 90 cm thick storage layer (a); and 180 cm thick storage layer (b)

depth of less than 2 cm for 20% soil slope. Albright et al. (2004) also attributed the measured runoff from earthen and conventional landfill covers primarily to soil-atmosphere interactions with minimal impact due to low conductivity soil layers at deeper depths below the ground surface. Similar to the predicted annual runoff, no significant effect of the storage layer thickness was observed on the predicted peak daily runoff (Fig. 3-12b).

Regional Scale Runoff and ET

UNSAT-H predicted runoff was found not to be significantly affected by the storage layer soil type (hydraulic conductivity properties) when saturated hydraulic conductivity was less than or equal to 10^{-5} cm/sec and the storage layer thickness. Hence, the forgoing discussion on the regional scale water balance of Texas was limited to 90 cm thick CH storage layer unless specified otherwise (Fig. 3-13 to Fig. 3-16). Other combinations of storage layer soil type and thickness were assumed to follow similar trends without the loss of generality as long as saturated hydraulic conductivity of the storage layer was less than or equal to 10^{-5} cm/sec. Runoff coefficient and ET coefficient were defined as the ratio of annual (or daily) runoff and ET, respectively to the annual (or daily) precipitation for the ease of discussion.

Predicted runoff generally followed the precipitation variations at the regional scale of Texas. For APY, higher precipitation in east Texas generally resulted in higher predicted runoff (and higher annual runoff coefficient) than west Texas which receives lower precipitation (Fig. 3-13). However, local anomalies in predicted APY runoff were observed for Brownsville (region #6), Lufkin (region #8) and College Station (region #9). Brownsville received lower annual APY precipitation of 69 cm than Corpus Christi (80 cm/yr), both with similar longitude but lost 99% precipitation as ET resulting in lower predicted runoff (Fig. 3-14). Predicted runoff was 6% for Lufkin compared to 17% for Houston and 14% for Longview as 94% of precipitation was lost as

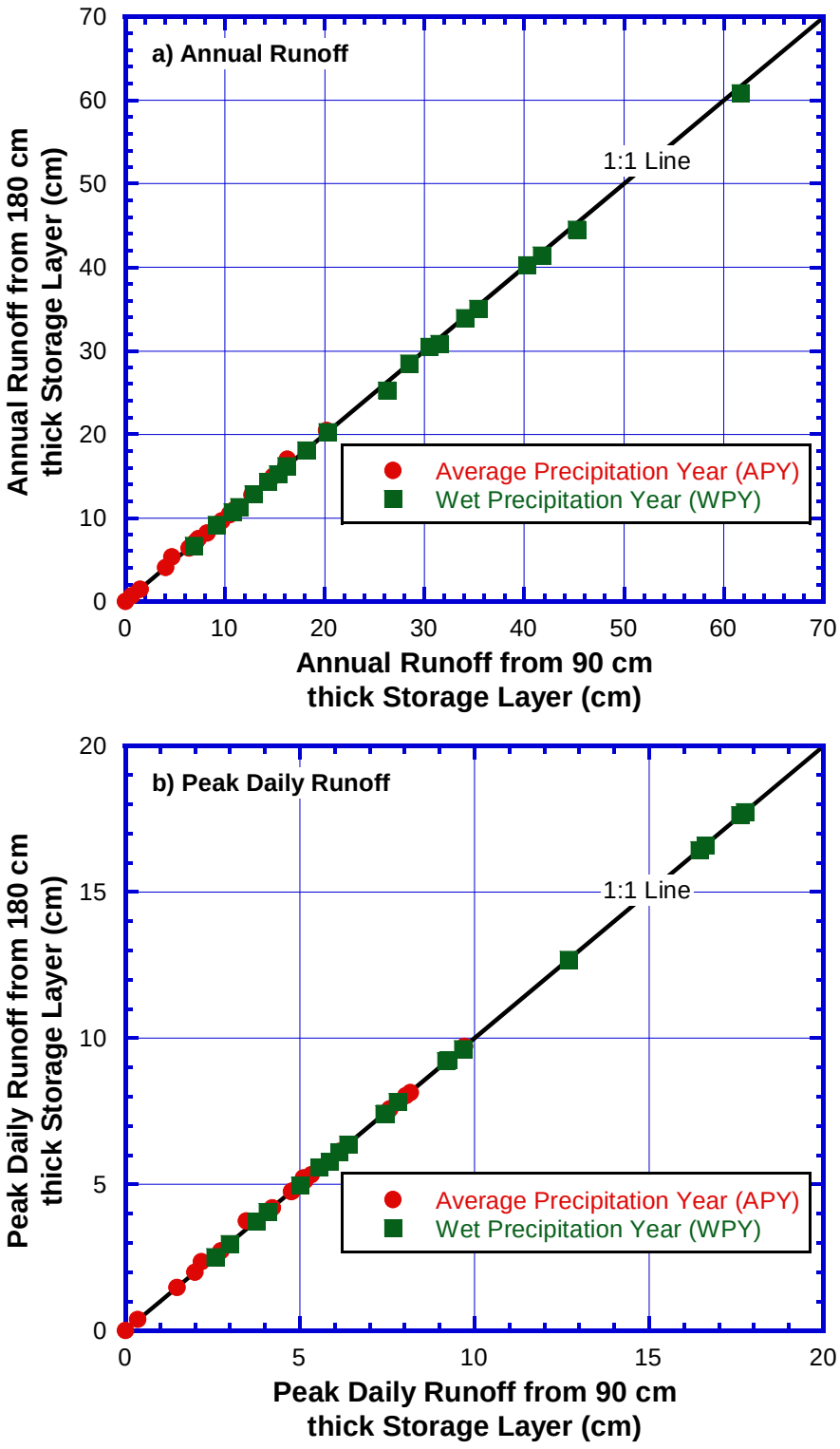

Figure 3-12. Effect of storage layer thickness on predicted annual runoff (a); and peak daily runoff (b)

ET at Lufkin compared to only 83% and 85% for Houston and Longview, respectively. Similarly, College Station received lower APY precipitation (99 cm/yr) than Houston (121 cm/yr) in the same region #9 but lost 95% precipitation as ET which was larger than 83% ET loss predicted for Houston.

Similar to APY runoff predictions, localized islands of large and small predicted runoffs due to local climate conditions were observed for WPY climate (Fig. 3-15). The observed anomalies in WPY runoff were explained with predicted ET for WPY (Fig. 3-16). Predicted runoff coefficients for Lubbock and Victoria were higher (0.17 and 0.36, respectively) due to smaller ET coefficient (0.82 and 0.64, respectively) while they were lower for Austin and Houston (0.06 and 0.16, respectively) due to larger ET coefficient (0.86 and 0.84). Similar effect of ET on predicted runoff was observed for Wenatchee (semiarid site in Washington) where simulations with lowest ET predicted highest runoff (Khire et al. 2000). Lower precipitation and higher ET also resulted in lower predicted runoff from water balance simulations of landfill covers at Albuquerque, New Mexico than Sierra Blanca, Texas (Scanlon et al. 2005). Effect of predicted ET on predicted runoff by water balance models has been reported by several authors (Khire et al. 1997, 2000; Scanlon et al. 2005; Bohnhoff et al. 2009; Ogorzalek et al. 2008; Albright et al. 2013).

Comparison of Predicted versus Measured Runoff from Landfill Covers

Albright et al. (2004) measured runoff from eleven lysimeters of EFCs in seven states across United States as part of Alternative Cover Assessment Project (ACAP) funded by USEPA. ACAP project sites represented an exhaustive measured data set for diverse climatic conditions from arid (PET/P > 5) to humid (PET/P < 1.3) and were thus used for validating the runoff predicted in this study for Texas. Predicted APY runoff for EFCs in arid to humid regions of Texas and the measured runoff from ACAP sites showed similar behavior of increased annual

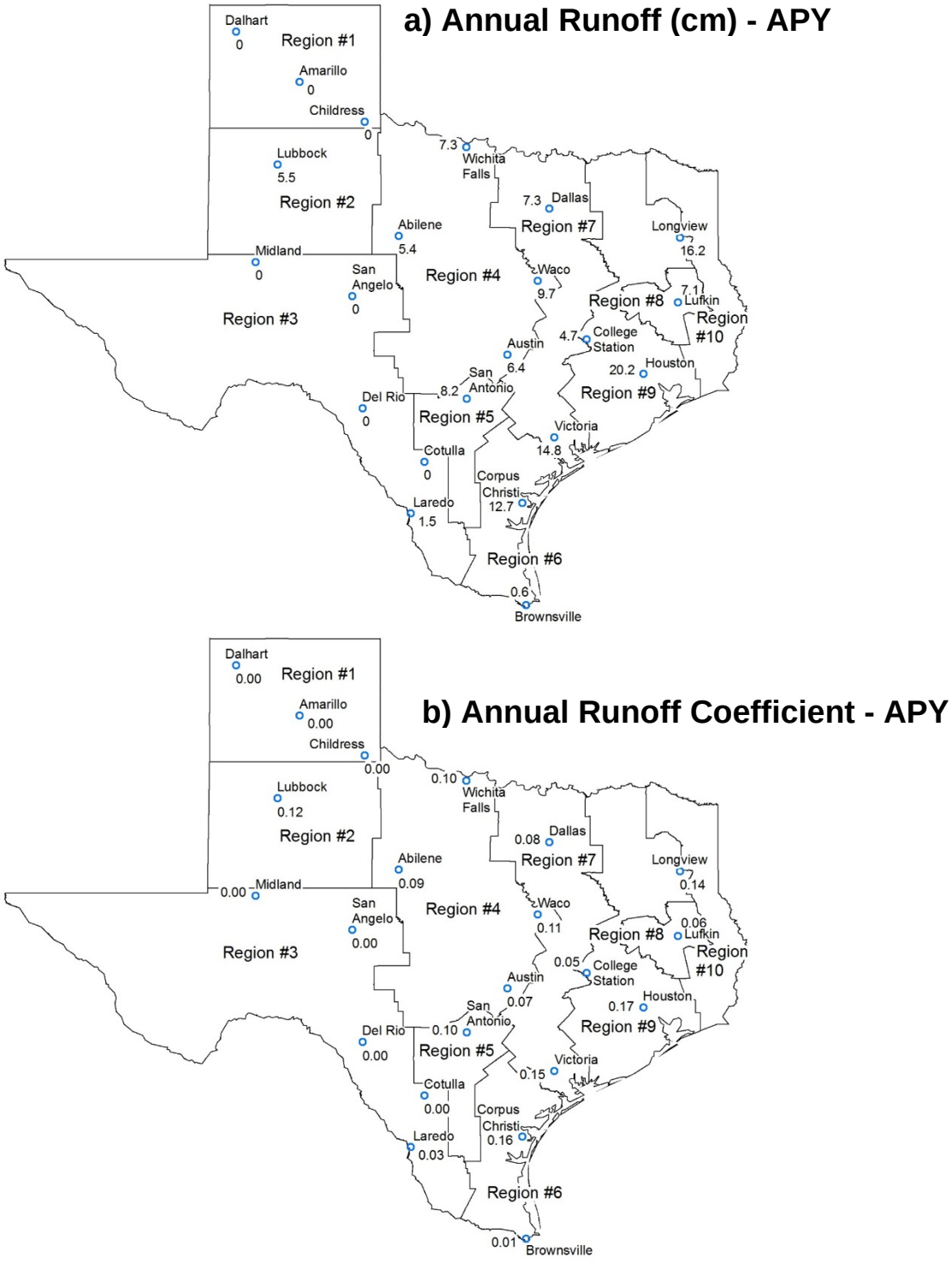

Figure 3-13. Regional scale predicted annual runoff (a); and annual runoff coefficient (b) for Texas for average precipitation year (APY)

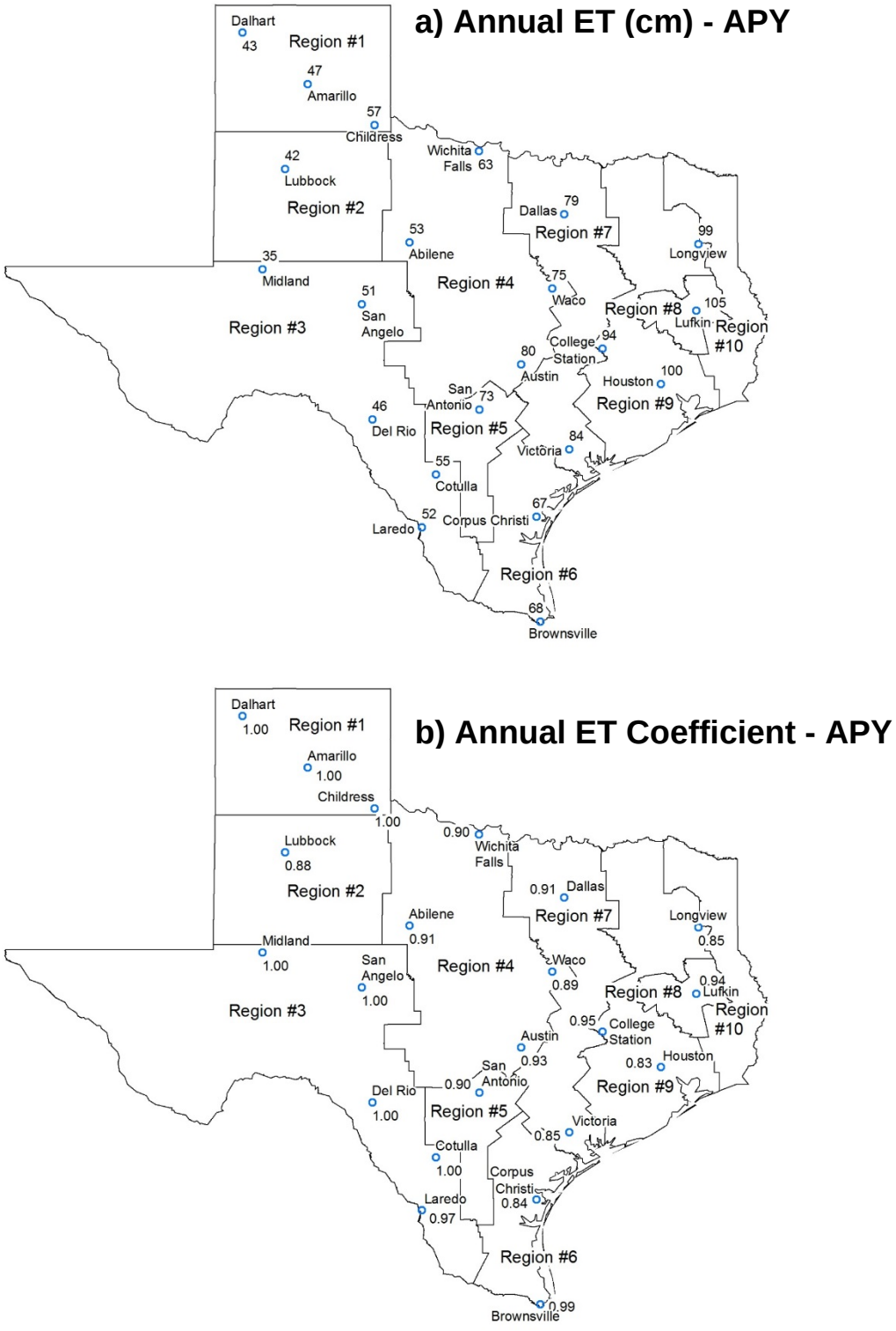

Figure 3-14. Regional scale predicted annual evapotranspiration (ET) (a); and annual evapotranspiration coefficient (b) for Texas for average precipitation year (APY)

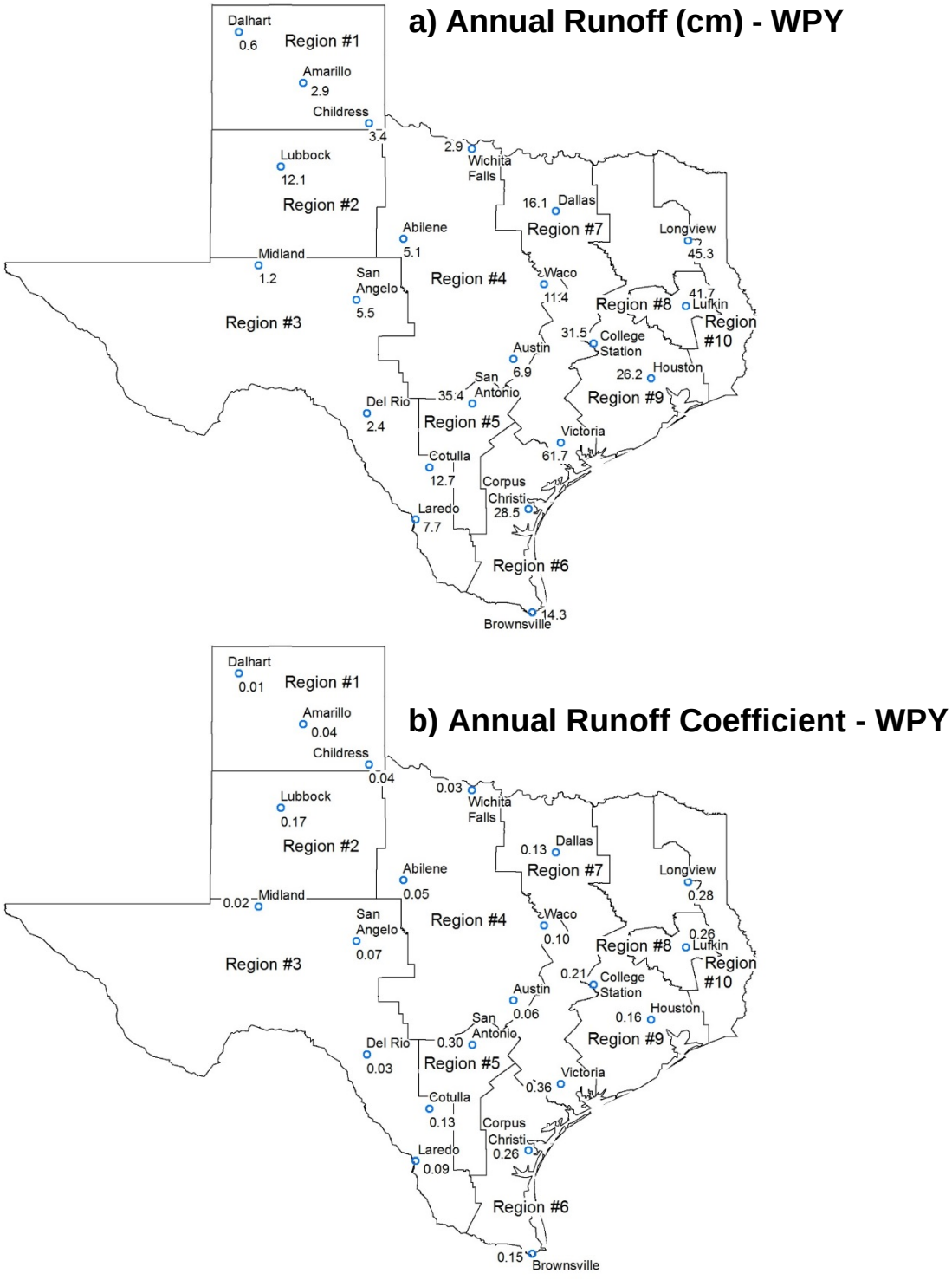

Figure 3-15. Regional scale predicted annual runoff (a); and annual runoff coefficient (b) for Texas for wet precipitation year (WPY)

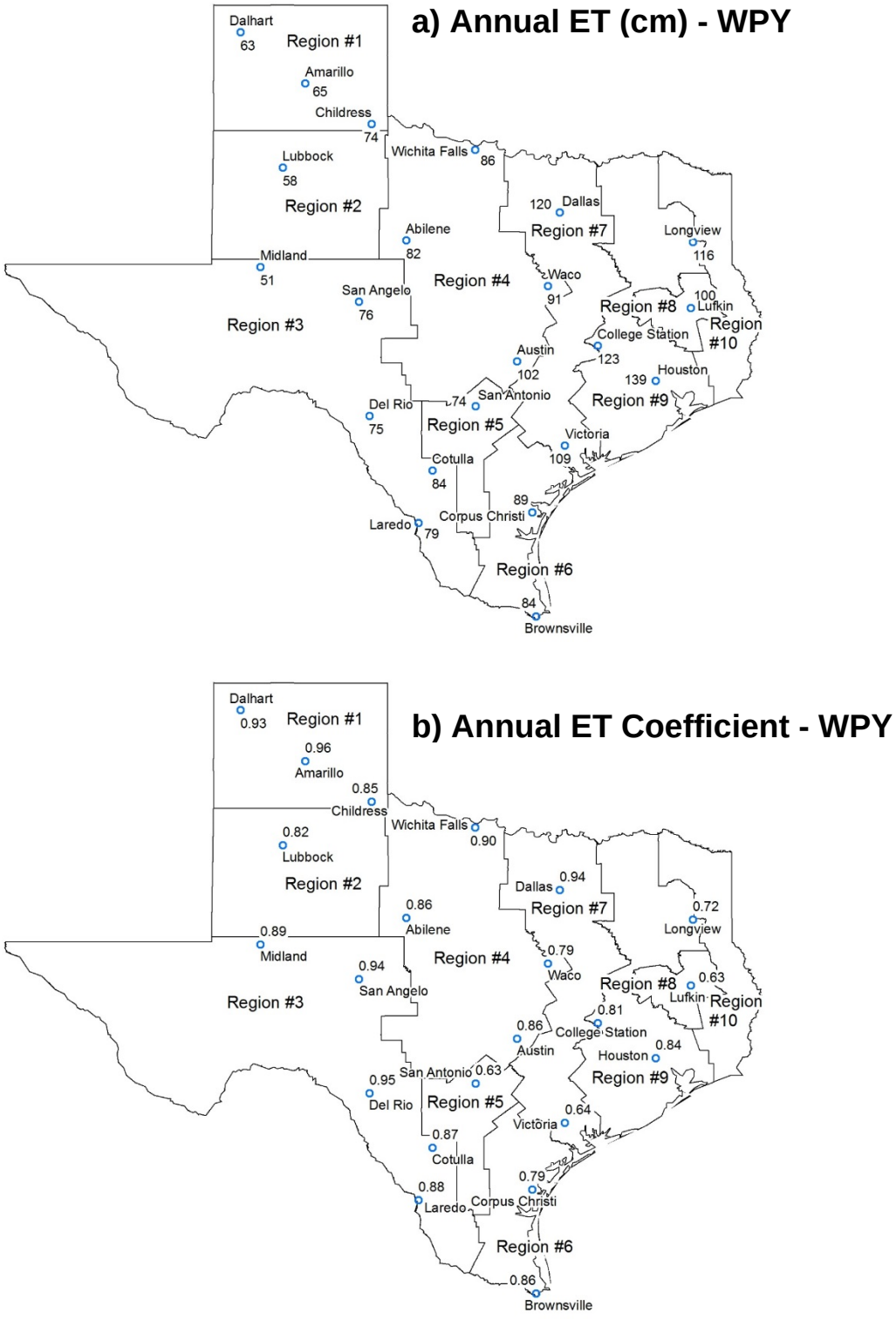

Figure 3-16. Regional scale predicted annual evapotranspiration (ET) (a); and annual evapotranspiration coefficient (b) for Texas for wet precipitation year (WPY)

runoff with increase in annual precipitation (Fig. 3-17). Predicted and measured EFC runoff was 1% to 20% of the annual precipitation. Although predicted APY runoff-precipitation relationship generally followed the measured runoff-precipitation trends, UNSAT-H did not simulate the measured runoff-precipitation relation very accurately. Soil surface parameters and local climate conditions including precipitation intensity are known to significantly influence predicted ET and consequently predicted runoff (Khire et al. 2000; Ogorzalek et al. 2008). Evapotranspiration from a monolithic cover in semiarid climate of Altamont, California was also not accurately predicted by UNSAT-H and consequently UNSAT-H under predicted runoff (Bohnhoff et al. 2009). Alternate wetting and drying cycles over several seasons can alter the pore structure of soil layers resulting in extensive clay desiccation and altering the water balance of landfill covers wherein the governing water flow occurs through highly conductive macro-pores instead of capillary pores as modeled by UNSAT-H (Hawkins and Horton 1967; Benson and Daniel 1990; Corser and Cranston 1991; Albrecht and Benson 2001; Albright et al. 2006a, b). Such time dependent evolution of hydraulic conductivity of soils is not implemented in UNSAT-H, resulting in poor correlation of predicted and measured runoff.

Vegetation was another important variable influencing runoff generation and transport on the surface of EFC hill slopes which did not form part of the current analysis. Conventional cover at Albany with native grass vegetation and leaf area index (LAI) of 0.2 measured a high 10% runoff compared to only 0.5% runoff from adjacent monolithic cover (LAI = 2.2) of relatively dense vegetation (Albright et al. 2004). Different vegetation cover and density resulted in different soil hydraulic conductivity and surface roughness resulting in different runoff. UNSAT-H cannot model dynamic change in hydraulic conductivity and surface roughness due to vegetation. Further, transpiration loss due to vegetation was also not simulated in the current analysis owing to the data

unavailability on different plant species used on EFCs over MSW landfills in different geographical parts of Texas. Lastly, hysteresis in unsaturated soil hydraulic properties due to wetting and drying of soil can also affect predicted water balance of landfill covers but was not simulated in this study due to lack of soil properties with hysteresis (Fayer et al. 1992; Fayer and Gee 1997). Hence, although predicted runoff does not exactly match the measured runoff, the predicted runoff is within the same order of magnitude as measured runoff and relatively accurate for carrying out preliminary designs at a regional scale.

Regional Scale Precipitation-Runoff Relationship

The predicted runoff from CH and SM-ML covers was used to establish runoff-precipitation correlations for average and wet year climates in Texas. A second order polynomial regression function was fitted to predict annual runoff from annual precipitation as follows:

$$y = px^2 + qx + r \tag{3-5}$$

where, y is predicted runoff (cm) and x is precipitation (cm). The curve fit parameters p, q and r were estimated to yield highest correlation coefficient (R^2). Different sets of curve fit parameters were derived for APY and WPY climates (Table 3-2).

The predicted runoff from dry regions (regions #1 to #3) was observed to behave distinctly different from wet regions (regions #4 to #9). The annual runoff-precipitation correlated poorly for both wet and dry regions in both APY and WPY climates. However, WPY predicted runoff and precipitation correlated better than APY. Annual runoff-precipitation correlated better for wet regions (regions #4 to #9) than for dry regions (regions #1 to #3) in both APY and WPY (Table 3-2). Dry regions generally received less than 60 cm average annual precipitation and greater than

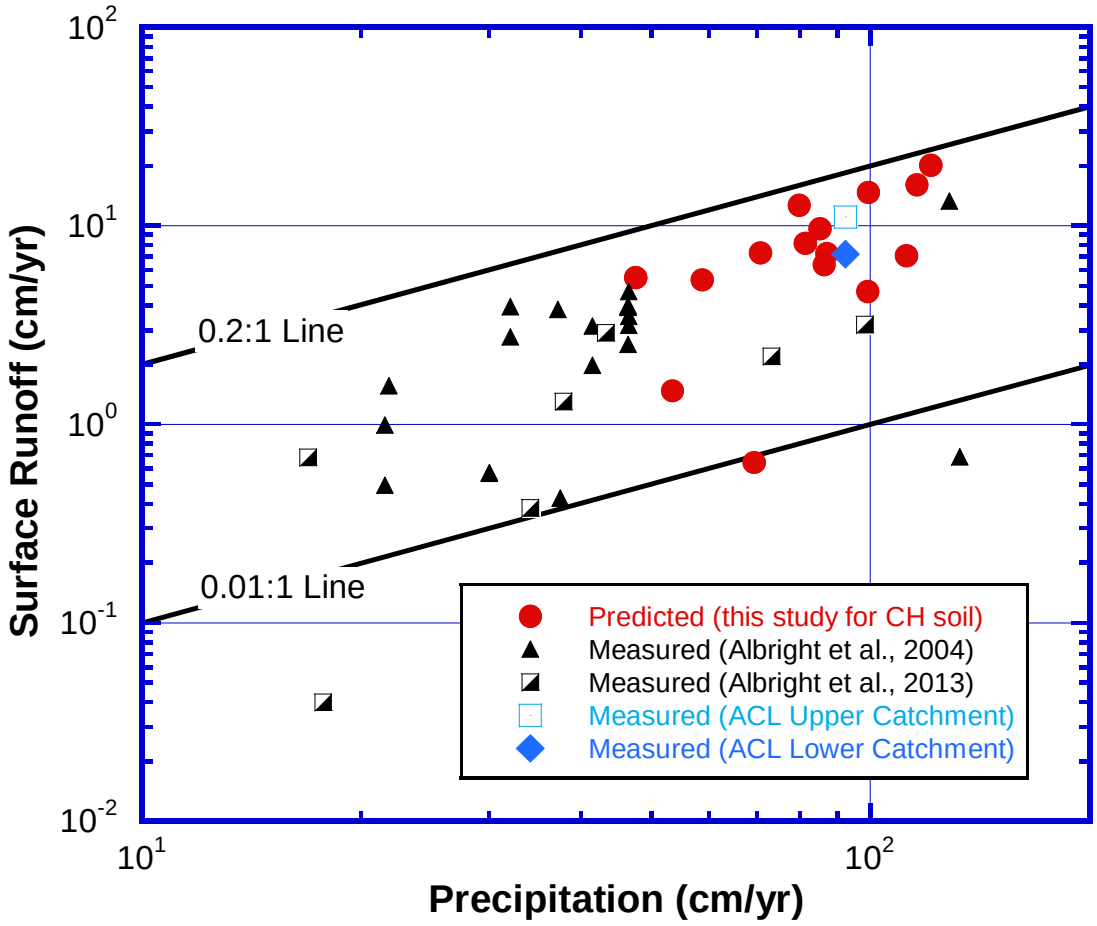

Figure 3-17. Measured and predicted annual surface runoff for landfill covers

200 cm average annual PET (Fig. 3-5 to Fig. 3-8) resulting in generally low predicted runoff and poor runoff-precipitation correlation. Similar observation was also made by Reed et al. (1997) where stream runoff-precipitation relationship changed at the threshold precipitation of 80.1 cm in Texas as follows:

$$y = 0.00064x\exp(0.061x) \qquad \text{for } x < 80.1 \qquad (3\text{-}6)$$

$$y = 0.51x - 33.91 \qquad \text{for } x \geq 80.1 \qquad (3\text{-}7)$$

where, y is runoff (cm/yr) and x is precipitation (cm/yr). Reed et al. (1997) equation generally over predicted average annual runoff for all regions of Texas in both APY and WPY climates of the current analysis (Fig. 3-18 to Fig. 3-19).

Predicted Peak Daily Runoff

Peak daily runoff is defined as the predicted maximum daily runoff in a climate year. Predicted peak daily runoff for APY ranged from 0 cm/day to 9.7 cm/day and had a peak runoff coefficient that ranged from 0 to 0.97. Peak daily runoff for WPY ranged from 0.62 cm/day to 17.7 cm/day and had a peak runoff coefficient that ranged from 0.08 to 0.93. It was interesting to observe a higher maximum daily runoff coefficient for APY than WPY considering APY received relatively lower maximum daily runoff than WPY. Such an observation was the artifact of a localized uneven daily precipitation distribution and consequent runoff generation.

A polynomial curve was fitted for peak daily runoff against daily precipitation as per equation 3-5. The curve fit coefficients are summarized in Table 3-3. Similar to annual runoff-precipitation relationship, dry regions (regions #1 to #3) were grouped separately from the other regions for both APY and WPY (Fig. 3-20 and Fig. 3-21). Peak daily runoff-precipitation for dry regions for APY correlated marginally better (R^2=0.73) than wet regions (R^2=0.56). However, the correlation of peak daily runoff-precipitation of wet regions (R^2=0.84) was better than dry regions

Table 3-2. Curve fit coefficients for annual runoff-precipitation analysis

Precipitation Year	Regions	p	q	r	R^2
APY	1 to 3	-0.0152	1.42	-31.7	0.13
	4 to 9	0.0022	-0.19	9.01	0.46
WPY	1 to 3	0.0085	-1.09	37.9	0.48
	4 to 9	0.0027	-0.25	11.65	0.57

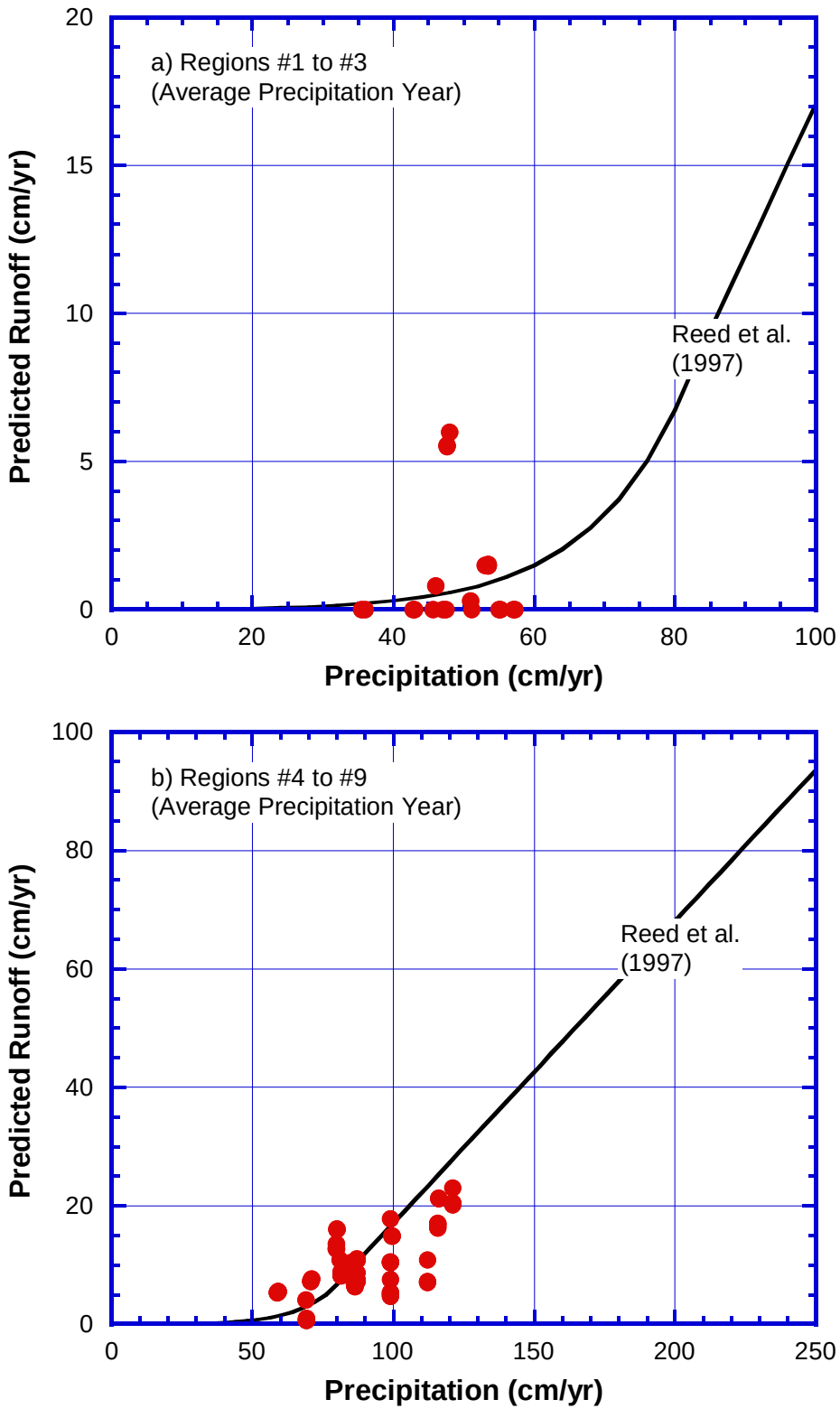

Figure 3-18. Predicted annual runoff versus annual precipitation for APY for regions #1 to #3 (a); and regions #4 to #9 (b) for various storage layer thicknesses of CH and SM-ML soil types

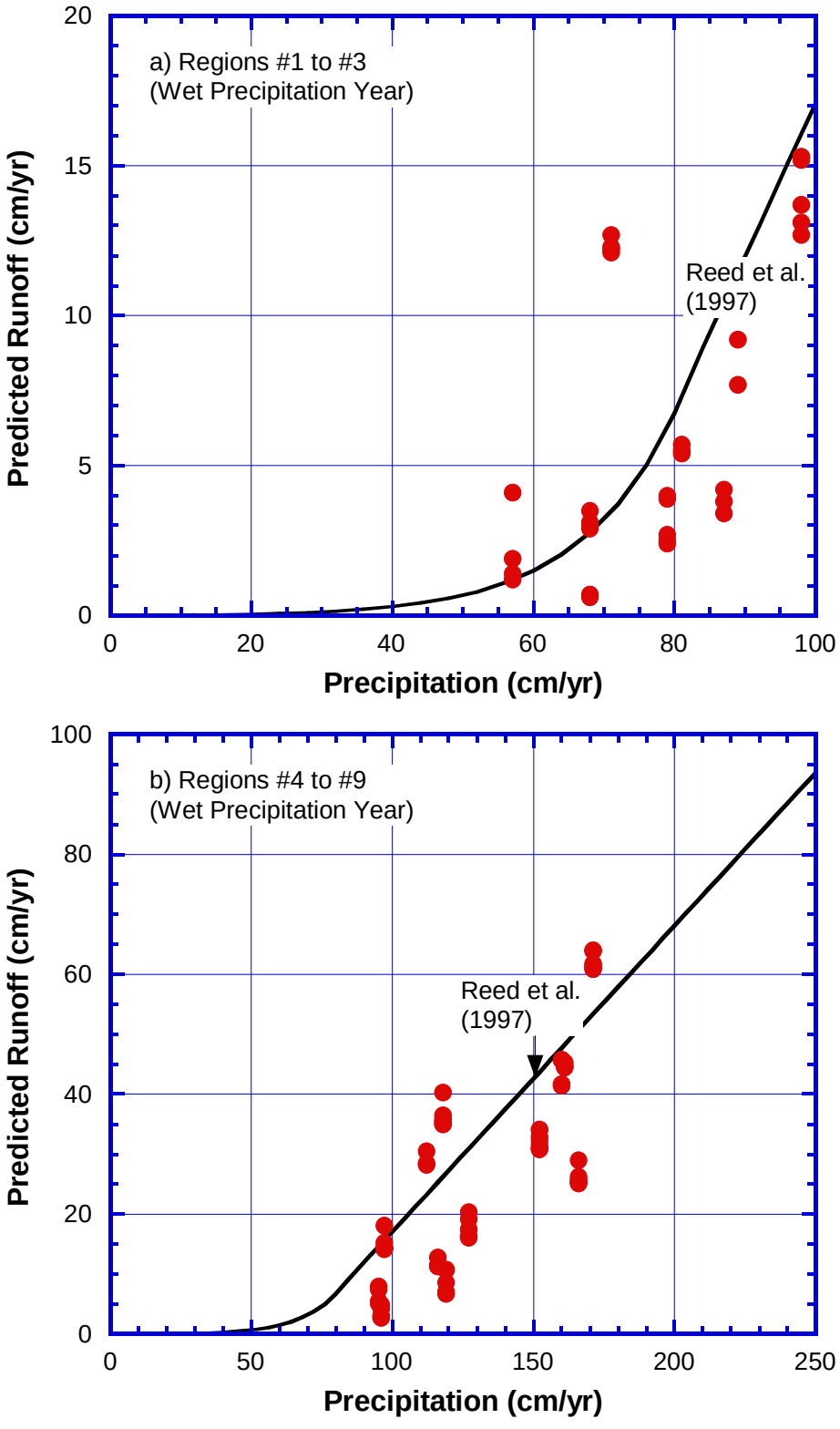

Figure 3-19. Predicted annual runoff versus annual precipitation for WPY for regions #1 to #3 (a); and regions #4 to #9 (b) for various storage layer thicknesses of CH and SM-ML soil types

(R^2=0.76) for WPY climate. Generally, peak daily runoff-precipitation correlated better for WPY than APY. Also, peak daily runoff-precipitation was found to generally correlate better than annual runoff-precipitation.

Storm water systems for EFCs are usually designed based on peak daily runoff values. Hence, a global peak daily runoff contour map for Texas was generated from peak daily runoff values of APY and WPY (Fig. 3-22). Global peak daily runoff generally followed precipitation contours and increased from west to east Texas. Drier regions with low precipitation generally had lower runoff than wet regions. However, similar to annual runoff local islands of global peak daily runoff were prominent at several locations within the general regional trend. Such anomalies were attributed to localized daily precipitation intensity and other local meteorological variables. A regression analysis of global peak daily runoff and corresponding daily precipitation showed good correlation for both dry regions (R^2 = 0.72) and wet regions (R^2 = 0.73). However, global peak daily runoff-precipitation correlation from WPY had higher slope than APY, due to relatively more predicted runoff in WPY than APY from similar daily precipitation (Fig. 3-23). Although peak daily runoff-precipitation correlation was poor, yet global peak daily runoff-precipitation correlated relatively much better which can therefore be used with more confidence for storm water system design of landfill covers.

Water Balance Correlation of WPY and APY

Khire et al. (2000) made first attempt in analyzing the effect of extreme precipitation on the water balance performance of EFCs. They used "wettest ten year period" at Wenatchee to simulate long term conditions with UNSAT-H. They also simulated thirty six year annual precipitation applied consecutively for three years at Wenatchee site to simulate extreme event conditions with UNSAT-H. The approach used by Khire et al. (2000) required significant number

of years of climatic data. Such data is often not available for all weather stations. In addition it is labor intensive to use such data in UNSAT-H. Hence, for this regional scale study, average precipitation year and wet precipitation year corresponding to 95 percentile year were simulated in UNSAT-H.

Water balance variables of WPY and APY were correlated with the following equation:

$$y = \beta x^{\gamma} \tag{3-7}$$

where, y is WPY water balance variable, x is APY water balance variable, β and γ are curve fit coefficients to yield maximum correlation coefficient (R^2). The summary of WPY water balance variables versus APY water balance variables correlation coefficients is presented in Table 3-4. WPY precipitation correlated linearly with APY precipitation with a correlation coefficient (R^2) value of 0.95 (Fig. 3-24). WPY precipitation was 1.35 to 1.8 times higher than APY precipitation of Texas. Annual PET was 0.7 to 1.1 times for WPY compared to APY and had a correlation coefficient (R^2) value of 0.69 (Fig. 3-25). WPY annual PET/P and APY annual PET/P had a correlation coefficient (R^2) value of 0.92. Annual PET/P was 0.4 to 0.8 times for WPY compared to APY (Fig. 3-26). Annual evaporation was generally greater for WPY compared to APY. WPY annual evaporation and APY evaporation correlation had a correlation coefficient (R^2) value of 0.83 (Fig. 3-27).

Unlike precipitation, WPY annual runoff correlated poorly to APY annual runoff and no correlation was identified to quantify change in annual runoff from APY to WPY (Fig. 3-28). Higher annual precipitation in WPY than APY generally resulted in greater predicted annual runoff for WPY compared to APY (Fig. 3-28). Albright et al. (2004) also observed higher runoff from humid climates than arid climate for conventional and earthen landfill covers. Abilene and Wichita Falls stations however, in contrast to the general trend, had lower runoff for WPY than APY.

Table 3-3. Curve fit coefficients for peak daily runoff-precipitation analysis

Precipitation Year	Region	p	q	r	R^2
APY	1 to 3	0.0	0.45	-2.27	0.73
	4 to 9	0.0	0.47	1.1	0.56
WPY	1 to 3	0.004	0.53	0.25	0.76
	4 to 9	0.0	0.73	0.22	0.84
Global peak daily runoff	1 to 3	0.014	0.29	1.31	0.72
	4 to 9	0.007	0.47	2.29	0.73

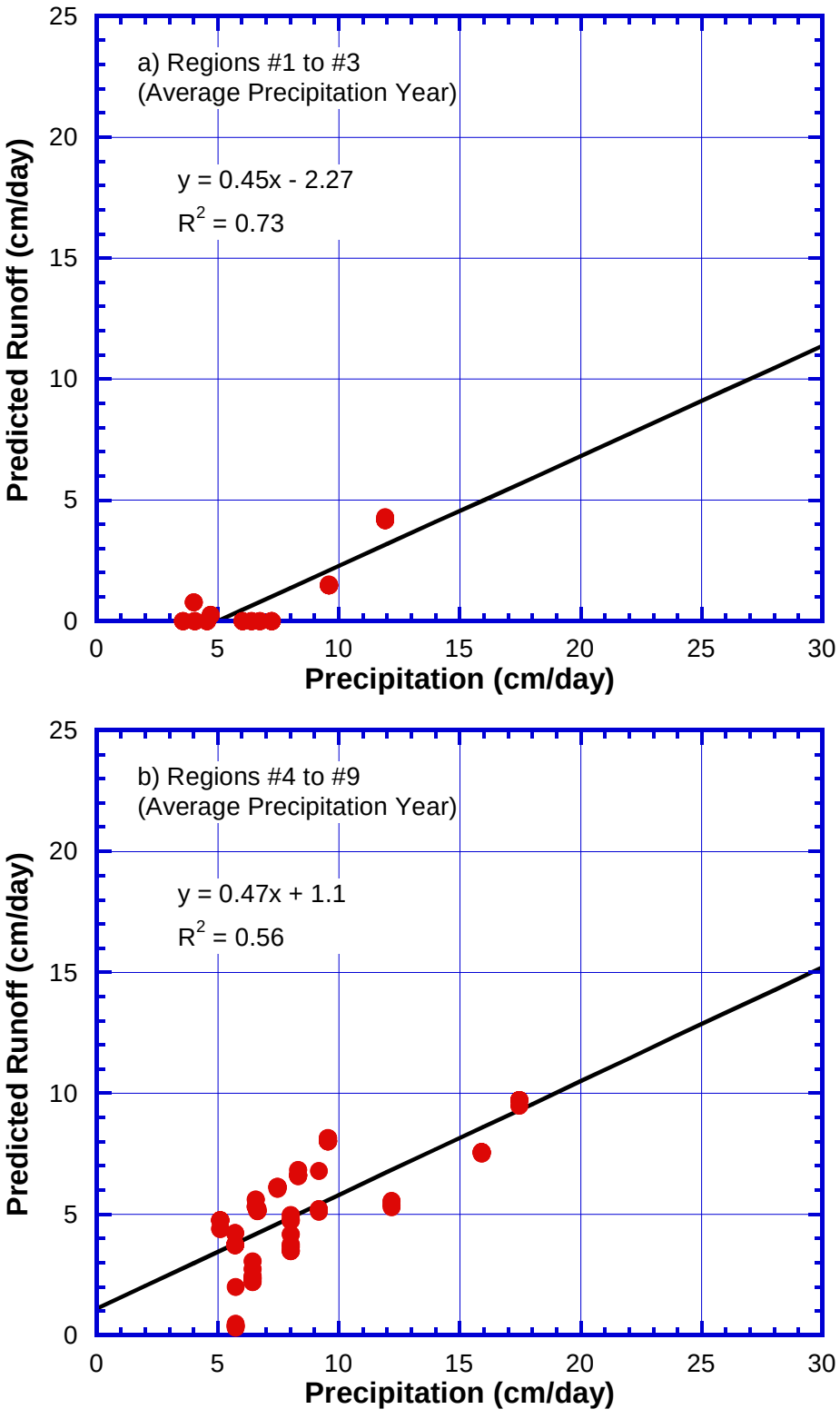

Figure 3-20. Predicted daily runoff versus daily precipitation for APY for regions #1 to #3 (a); and regions #4 to #9 (b)

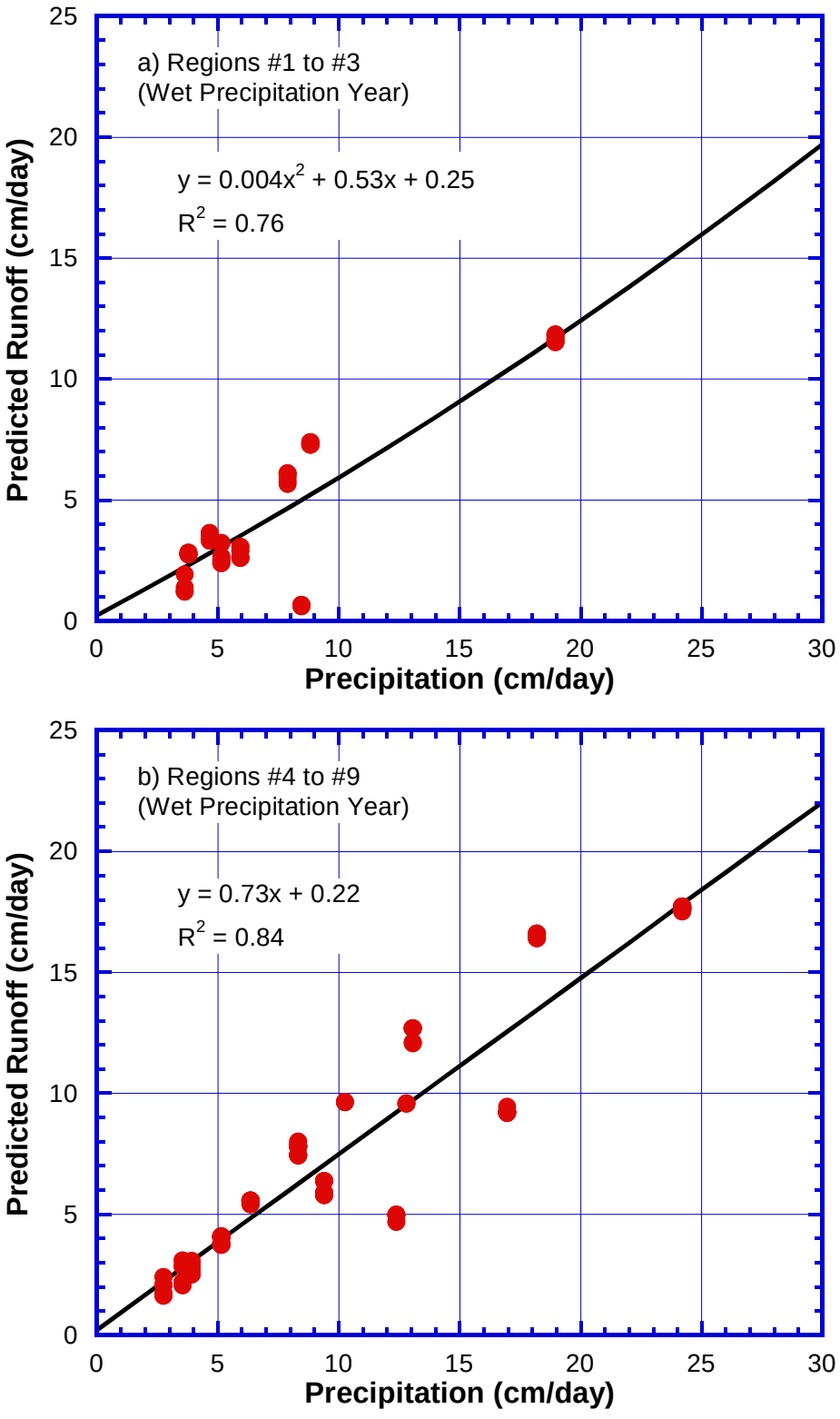

Figure 3-21. Predicted daily runoff versus daily precipitation for WPY for regions #1 to #3 (a); and regions #4 to #9 (b)

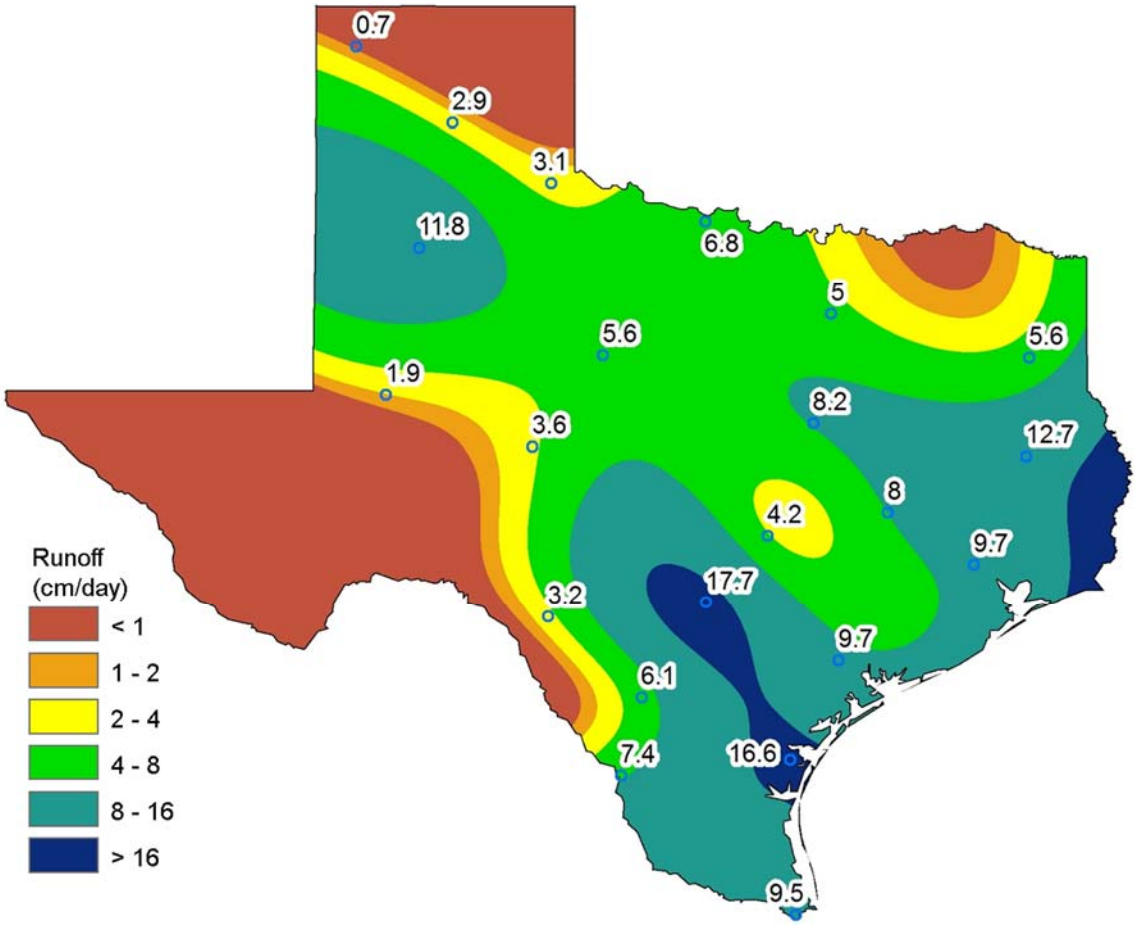

Figure 3-22. Global peak daily runoff (cm/day) contour map

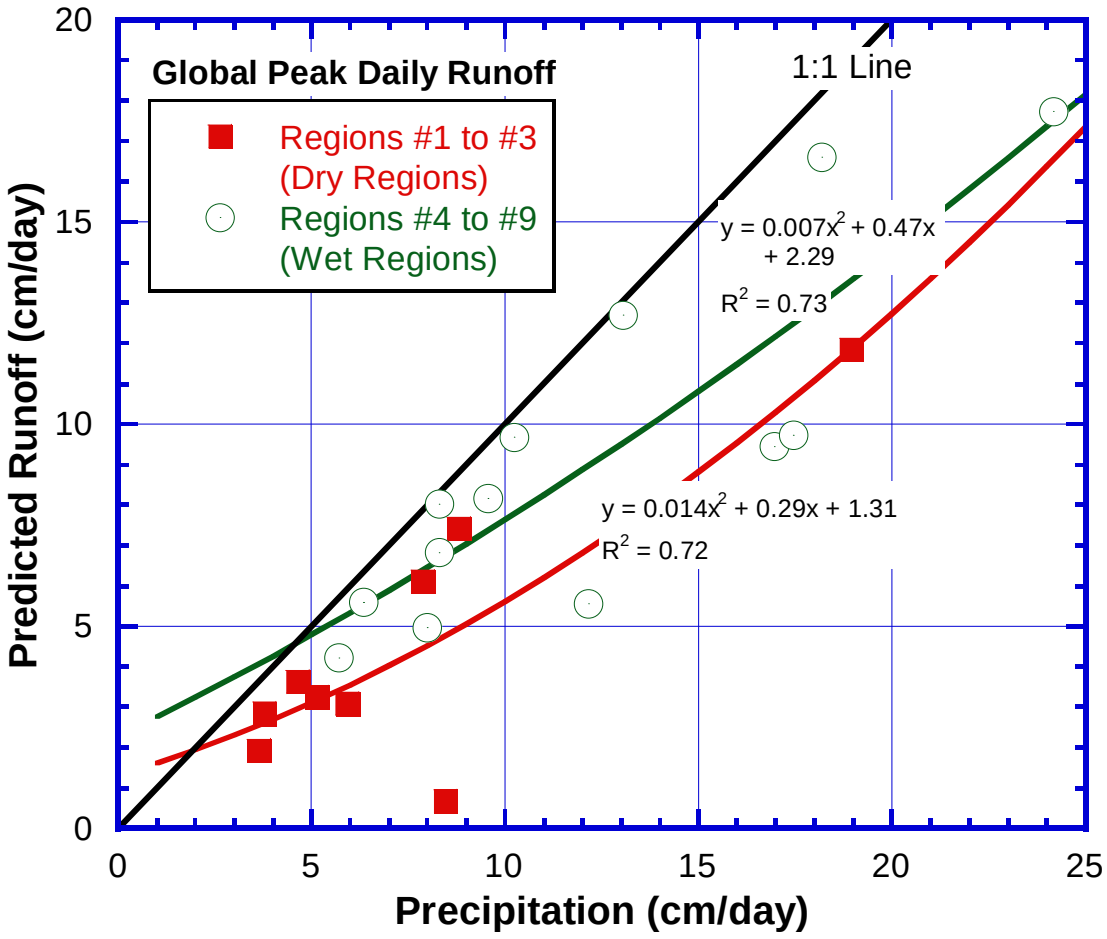

Figure 3-23. Precipitation and global peak daily runoff correlation for dry regions (regions #1 to #3) and wet regions (regions #4 to #9)

Abilene received high intensity storm in APY which generated more runoff than three relatively small intensity precipitation events in WPY (Fig. 3-29). Wichita Falls had lower runoff in WPY (2.9 cm/yr) than APY (7.3 cm/yr) although same percentage of annual precipitation was lost as annual ET (90%). APY at Wichita Falls received two runoff producing storm events and three runoff producing events in WPY. However, APY daily runoff producing precipitation events had almost three times greater storm intensity than the runoff producing events in WPY (Fig. 3-29). Nyhan (2005) observed approximately two orders of change in daily runoff due to change in daily precipitation intensity for landfill covers in New Mexico over several years of monitoring period. WPY percolation correlated to annual APY annual percolation with a high correlation coefficient (R^2) value of 0.91 (Fig. 3-30). Annual percolation for WPY was 1.3 to 8.7 times greater than APY.

PRACTICAL IMPLICATIONS AND CONCLUSION

USEPA guidelines stipulate the design of runoff control systems for a minimum 24-hour, 25-year storm as specified in 40 CFR 258.26 (USEPA 1992). In order to control water pollution from storm water runoff, US Congress recently passed strict requirements under Section 438 of Energy Independence and Security Act (Sissine 2007). In order to comply with Section 438, USEPA proposed several green infrastructure (GI) and low impact development (LID) practices depending on the peak design runoff (USEPA 2009). However, in spite of extensive climate data availability at several sites in United States from NCDC, very little guidance on runoff values for landfill storm water management systems for EFCs exists. Water balance model validated for a catchment scale study was used in this study to predict annual and peak daily runoff from EFCs. The current study presents simulated water balance hydrology that encompasses various climate regions of Texas ranging from arid to humid.

Table 3-4. Curve fit coefficients for annual water balance correlation of WPY and APY

Water balance variable	**β**	**γ**	**R^2**	**Upper bound slope**	**Lower bound slope**
Precipitation	2.51	0.88	0.95	1.8	1.35
Potential Evapotranspiration	2.51	0.81	0.69	1.1	0.7
PET/P	0.66	0.91	0.92	0.8	0.4
Evaporation	3.87	0.74	0.83	1.7	0.95
Runoff	-	-	-	7.0	0.39
Percolation	4.07	1.08	0.91	8.7	1.3

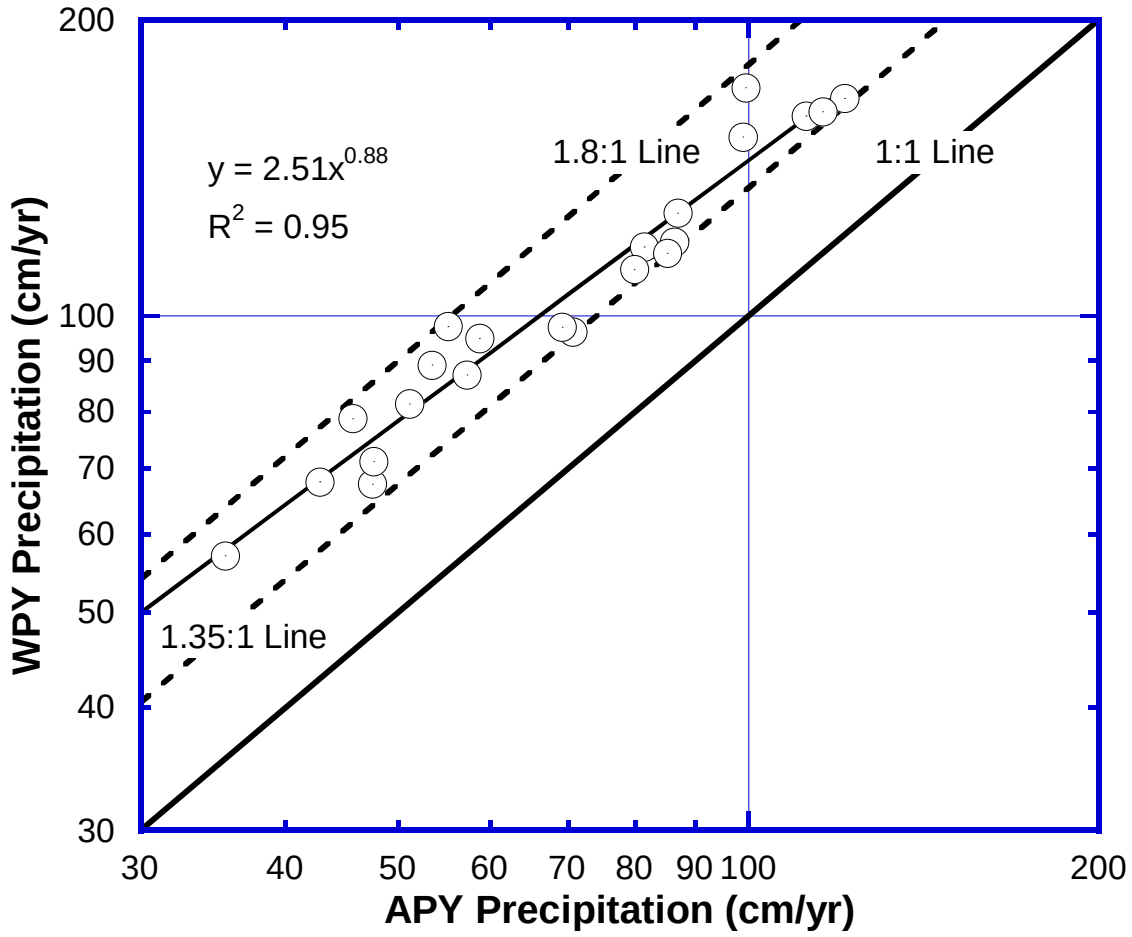

Figure 3-24. Annual WPY precipitation versus annual APY precipitation for Texas

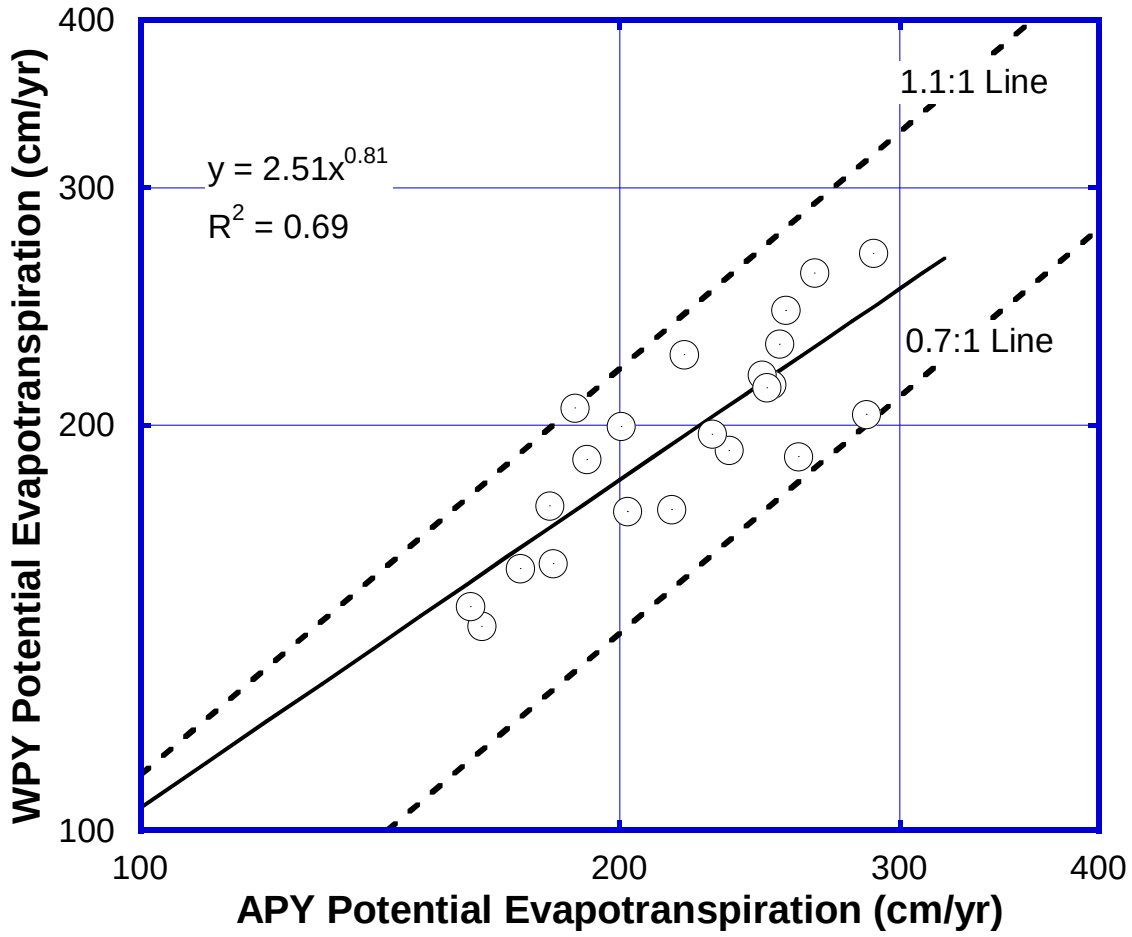

Figure 3-25. Annual WPY potential evapotranspiration versus annual APY potential evapotranspiration for Texas

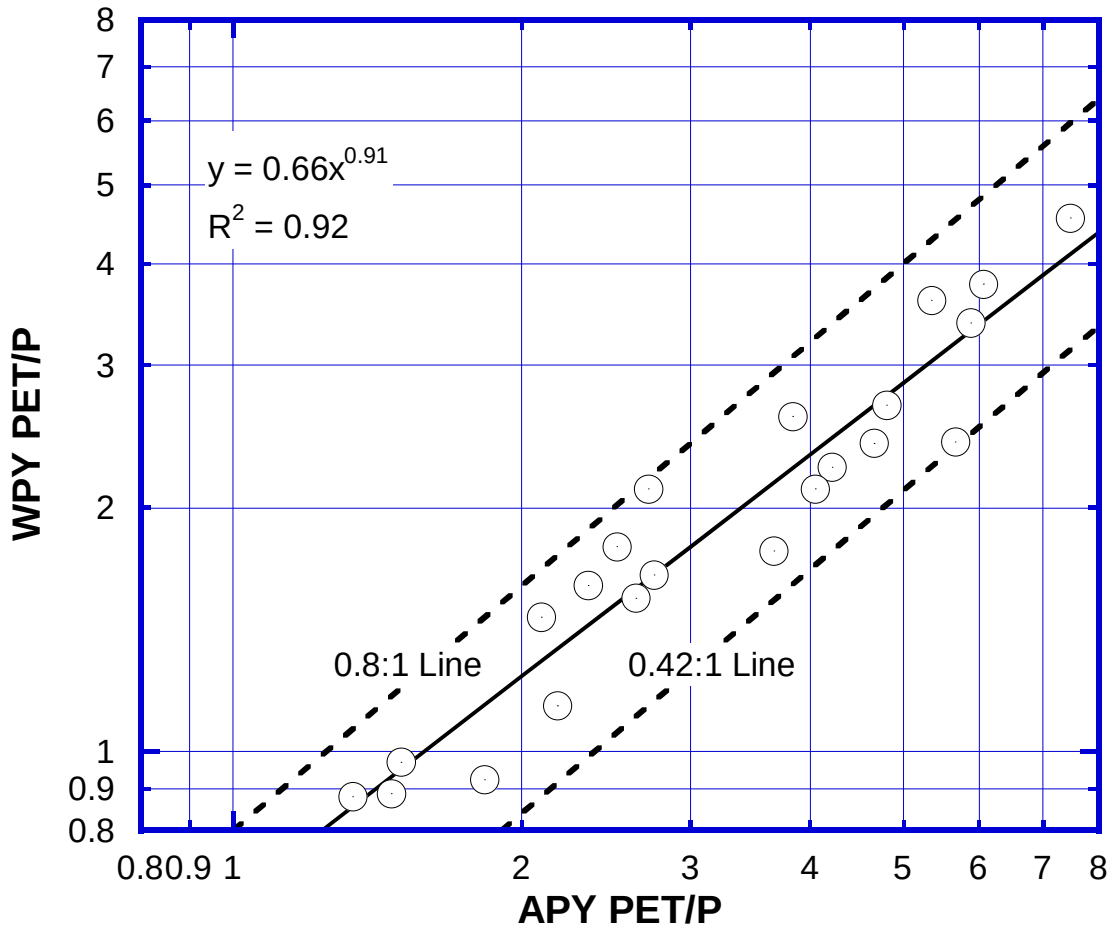

Figure 3-26. Annual WPY PET/P versus annual APY PET/P for Texas

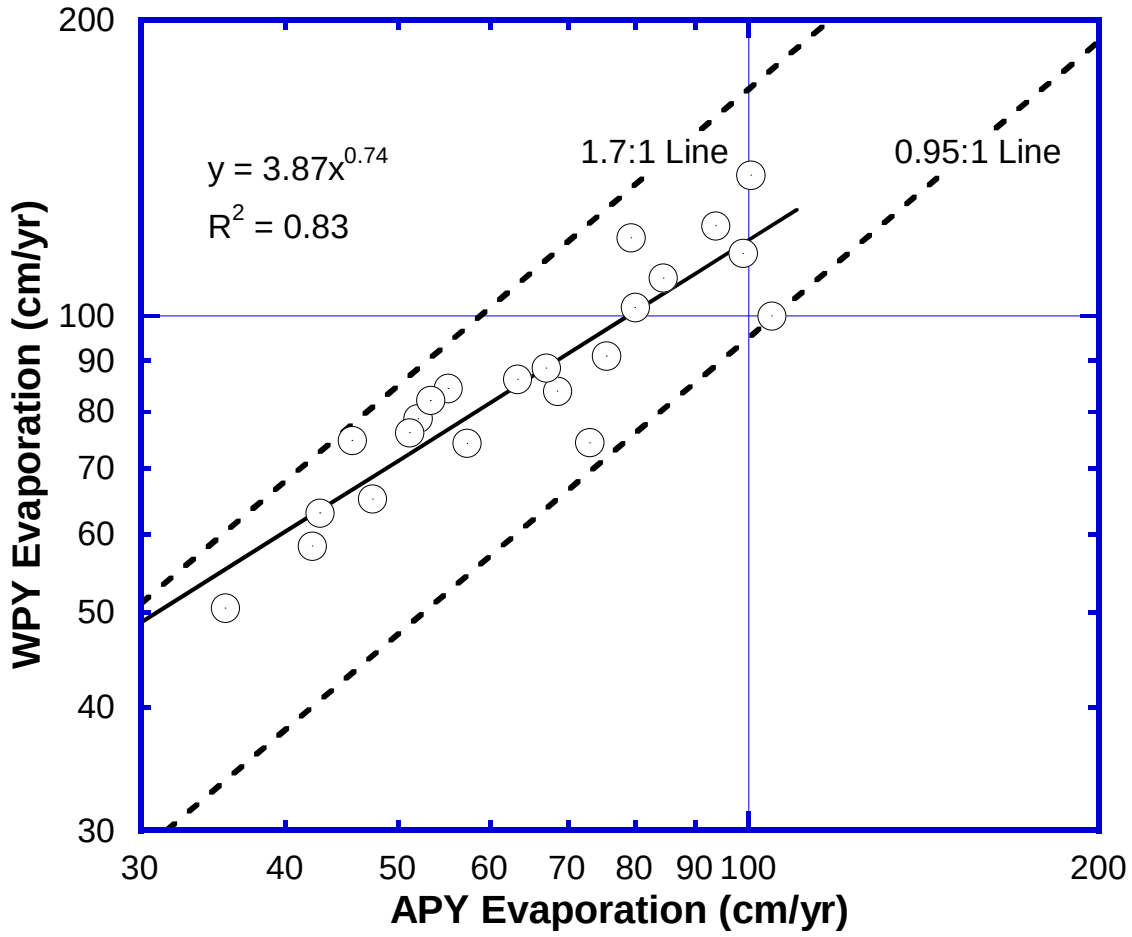

Figure 3-27. Predicted annual WPY evaporation versus predicted annual APY evaporation for Texas

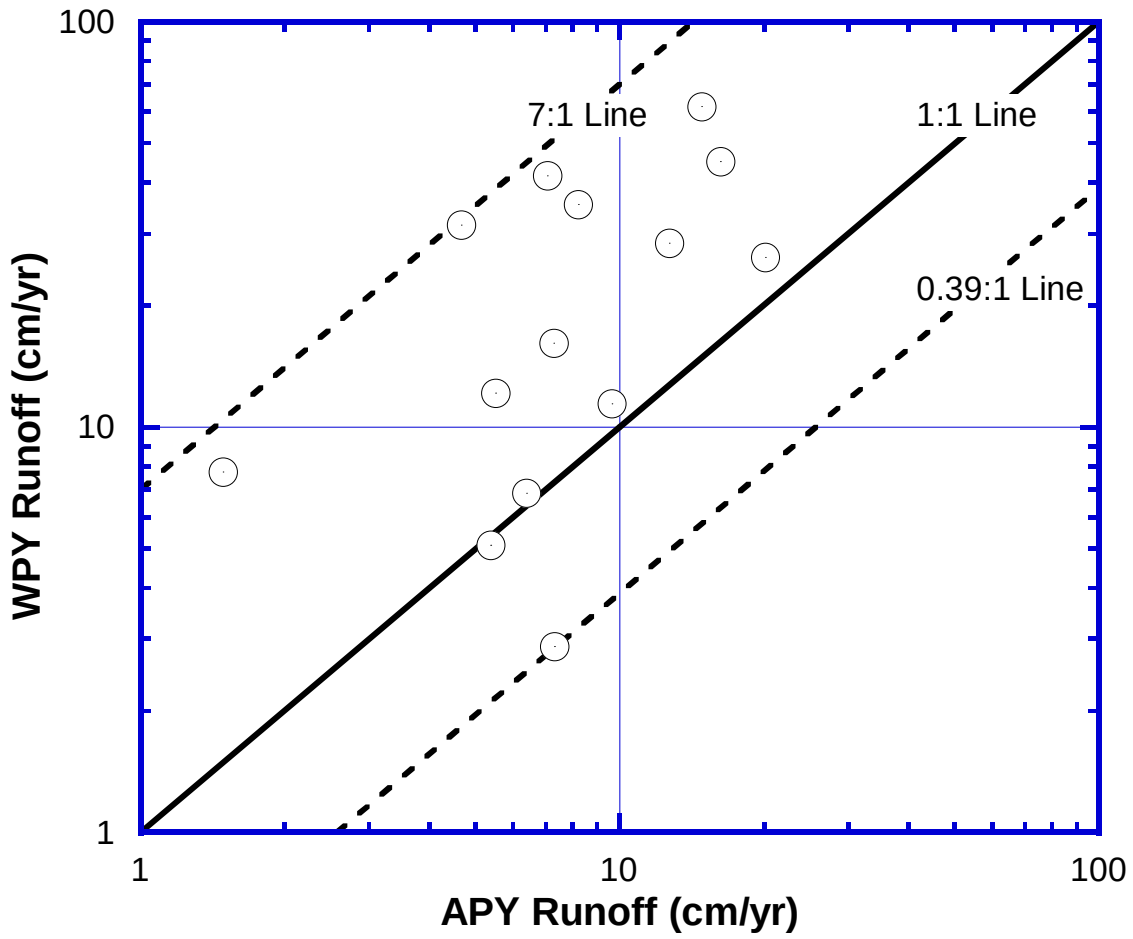

Figure 3-28. Predicted annual WPY runoff versus predicted annual APY runoff for Texas

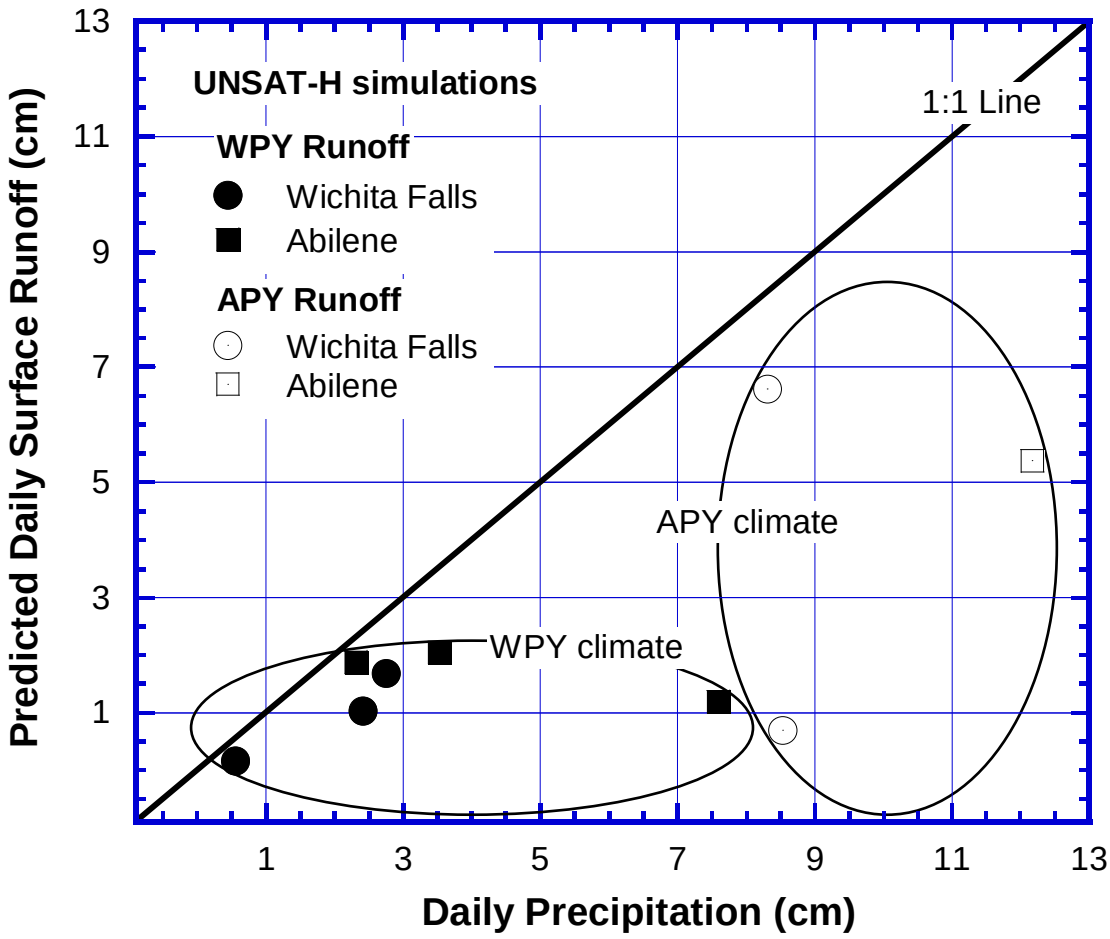

Figure 3-29. Predicted daily runoff versus daily precipitation for APY and WPY climate at Wichita Falls and Abilene

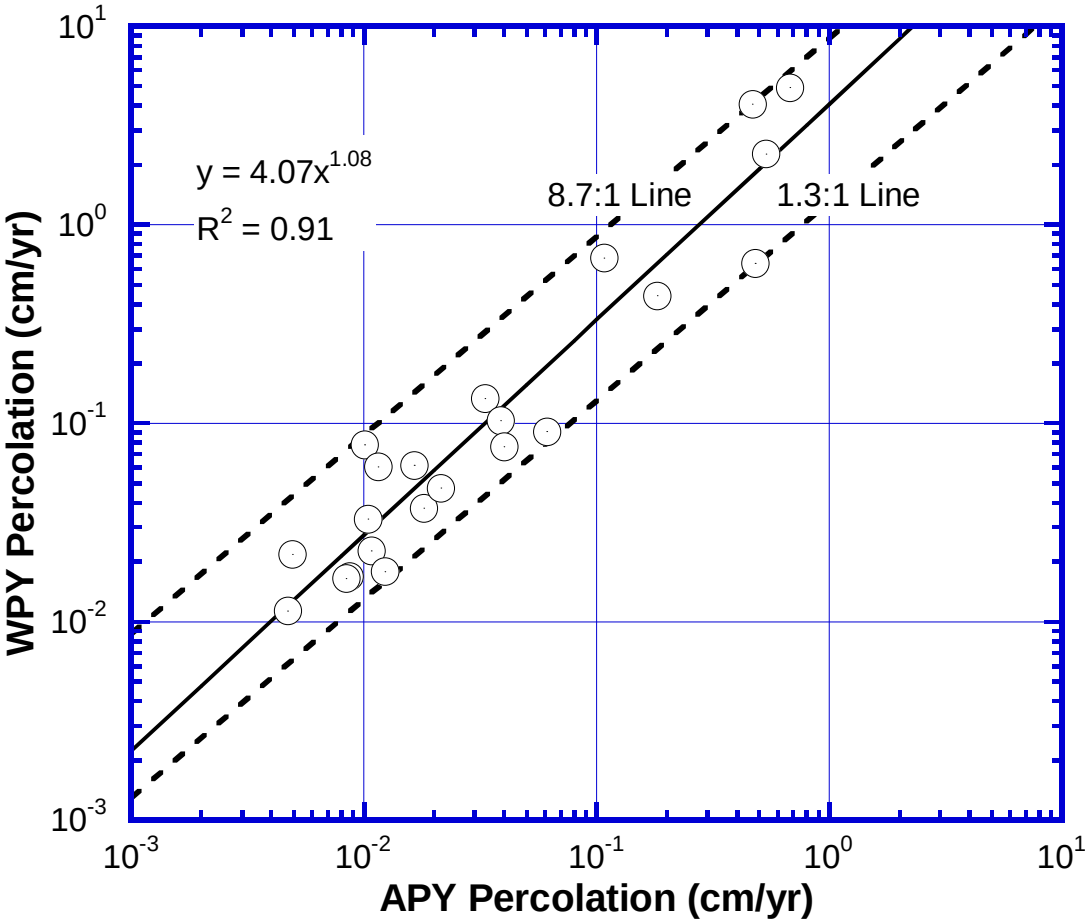

Figure 3-30. Predicted Annual WPY percolation versus predicted annual APY percolation for Texas

Following conclusions can be drawn from this study:

1) Annual and peak daily predicted runoff generally followed the precipitation contours and increased from west to east Texas. WPY climate generally had greater predicted runoff than APY climate.
2) Annual runoff-precipitation relationship had poor correlation for both dry and wet regions of Texas for APY and WPY climates as compared to daily runoff-precipitation correlation.
3) Annual and daily runoff was affected by local climatic conditions. Hence, site specific hydrologic analysis is necessary to accurately predict runoff from EFCs while the water balance values presented in this study can be used as a guidance.

SUMMARY AND CONCLUSIONS

Two catchment scale landfill covers were instrumented in semiarid climate of Austin, Texas. Surface runoff, soil water content and soil suction were measured from the instrumented landfill for twenty three months. The measured data helped to identify several variables governing surface runoff from engineered hill slopes. Larger catchment with longer runoff length generated lower surface runoff. Surface runoff correlated positively with the precipitation intensity during wet seasons (Season 1 and Season 3) but no correlation was observed for dry season when water contents were low. Total precipitation, average precipitation intensity, precipitation return period, antecedent water content, PET/P and vegetation cover resulted in non-linear seasonal variation of measured runoff. The measured EFC hydrology data was used to validate UNSAT-H and RZWQM water balance and unsaturated flow numerical models. UNSAT-H accurately predicted total surface runoff for a calibrated top soil saturated hydraulic conductivity and unsaturated hydraulic conductivity function. RZWQM grossly over predicted surface runoff with measured hourly precipitation intensity as Green-Ampt infiltration model of RZWQM was unable to accurately model unsteady hourly water balance. Measured surface runoff was dependent on the overland flow path connectivity, surface roughness, abstraction loss due to vegetation canopy, opportunistic infiltration due to vegetation roots, etc. Hence, UNSAT-H being 1-D numerical model did not accurately predict daily surface runoff from engineered hill slopes of landfill covers which is primarily a 2-D phenomenon.

UNSAT-H was subsequently used to predict surface runoff for engineered earthen final covers for several regions of Texas. Wet precipitation year predicted surface runoff was generally greater than runoff predicted for average precipitation year. Predicted annual and daily surface

runoff correlated poorly for dry regions but correlation was relatively good for wet regions of Texas. Local climate conditions significantly affected the predicted annual and daily surface runoff. Hence, site specific hydrology simulations are necessary to accurately predict EFC runoff.

REFERENCES

REFERENCES

Abrahams, A. D., Parsons, A. J., and Wainwright, J. (1994). "Resistance to overland flow on semiarid grassland and shrubland hillslopes, Walnut Gulch, southern Arizona." *Journal of Hydrology*, 156(1), 431-446.

Ahuja, L. R., Johnsen, K. E., and Rojas, K. W. (2000). "Water and chemical transport in soil matrix and macropores. Root Zone Water Quality Model. Modeling Management Effects on Water Quality and Crop Production." Water Resources Publications, LLC, Highlands Ranch, CO, 13-50.

Albrecht, B. A., and Benson, C. H. (2001). "Effect of desiccation on compacted natural clays." *Journal of Geotechnical and Geoenvironmental Engineering*, 127(1), 67-75.

Albright, W. H., Benson, C. H., Gee, G. W., Roesler, A. C., Abichou, T., Apiwantragoon, P., Lyles, B. F. and Rock, S. A. (2004). "Field water balance of landfill final covers." *Journal of Environmental Quality*, 33(6), 2317-2332.

Albright, W. H., Benson, C. H., Gee, G. W., Abichou, T., Tyler, S. W., and Rock, S. A. (2006a). "Field performance of three compacted clay landfill covers." *Vadose Zone Journal*, 5(4), 1157-1171.

Albright, W. H., Benson, C. H., Gee, G. W., Abichou, T., McDonald, E. V., Tyler, S. W., and Rock, S. A. (2006b). "Field performance of a compacted clay landfill final cover at a humid site." *Journal of Geotechnical and Geoenvironmental Engineering*, 132(11), 1393-1403.

Albright, W. H., Benson, C. H., and Apiwantragoon, P. (2013). "Field Hydrology of Landfill Final Covers with Composite Barrier Layers." *Journal of Geotechnical and Geoenvironmental Engineering*, 139(1), 1-12.

Arnell, N. W. (1995). "Grid mapping of river discharge." *Journal of Hydrology*, 167(1), 39-56.

ASTM, Standard D698-12. "Standard Test Methods for Laboratory compaction characteristics of soil using Standard Effort (12400 ft-lbf/ft^3 (600 kNm/m^3))." ASTM International, West Conshohocken, PA.

ASTM, Standard D5084-10. "Standard test methods for measurement of hydraulic conductivity of saturated porous materials using a flexible wall permeameter." *Annual Book of ASTM Standards*, 4(8). ASTM International, West Conshohocken, PA.

ASTM, Standard D6836-02. "Standard test methods for determination of the soil water characteristic curve for desorption using a hanging column, pressure extractor, chilled mirror hygrometer, and/or centrifuge." *Annual Book of ASTM Standards*, 4(9). ASTM International, West Conshohocken, PA.

Benson, C. H., and Daniel, D. E. (1990). "Influence of clods on the hydraulic conductivity of compacted clay." *Journal of Geotechnical Engineering*, 116(8), 1231-1248.

Benson, C. H. (2007). "Modeling unsaturated flow and atmospheric interactions." *Theoretical and numerical unsaturated soil mechanics*. T. Schanz, ed., Springer Berlin Heidelberg, 187-201.

Benson, C. H., Sawangsuriya, A., Trzebiatowski, B., and Albright, W. H. (2007). "Postconstruction changes in the hydraulic properties of water balance cover soils." *Journal of Geotechnical and Geoenvironmental engineering*, 133(4), 349-359.

Beven, K. J., and Kirkby, M. J. (1979). "A physically based, variable contributing area model of basin hydrology/Un modèle à base physique de zone d'appel variable de l'hydrologie du bassin versant." *Hydrological Sciences Journal*, 24(1), 43-69.

Beven, K. (1986). "Runoff production and flood frequency in catchments of order n: an alternative approach." *Scale Problems in Hydrology*. Springer Netherlands, 107-131.

Binley, A., Elgy, J., and Beven, K. (1989). "A physically based model of heterogeneous hillslopes: 1. Runoff production." *Water Resources Research*, 25(6), 1219-1226.

Bochet, E., Poesen, J., and Rubio, J. L. (2006). "Runoff and soil loss under individual plants of a semi-arid Mediterranean shrubland: influence of plant morphology and rainfall intensity." *Earth Surface Processes and Landforms*, 31(5), 536-549.

Bohnhoff, G. L., Ogorzalek, A. S., Benson, C. H., Shackelford, C. D., and Apiwantragoon, P. (2009). "Field data and water-balance predictions for a monolithic cover in a semiarid climate." *Journal of Geotechnical and Geoenvironmental engineering*, 135(3), 333-348.

Börjesson, G., and Svensson, B. H. (1997). "Effects of a gas extraction interruption on emissions of methane and carbon dioxide from a landfill, and on methane oxidation in the cover soil." *Journal of Environmental Quality*, 26(4), 1182-1190.

Bringhurst, B., and Adams, J. (2011). "Innovative sensor design for prevention of bio-fouling." *OCEANS 2011* (pp. 1-8). IEEE.

Brooks, R. H., and Corey, A. T. (1964). "Hydraulic properties of porous media." *Hydrology Papers,* Colorado State University, Fort Collins, CO, 1-15 (March).

Buttle, J. M., and Turcotte, D. S. (1999). "Runoff processes on a forested slope on the Canadian Shield." *Nordic Hydrology*, 30(1), 1-20.

Campbell Scientific Inc. (2009). "229 Heat Dissipation Matric Water Potential Sensor Manual. Revision 5/09." Campbell Scientific Inc., Logan, UT, USA.

Campbell Scientific Inc. (2013). "OBS500 Smart Turbidity Meter with Clear Sensor Technology. Revision 8/13." Campbell Scientific Inc., Logan, UT, USA.

Civil Engineering Consultants (CEC) (1997). "Hydraulic characteristics of barrier soils for the alternative landfill cover demonstration, City of Glendale, AZ." *Rep. Prepared for City of Glendale, AZ*, Verona, Wis.

Corser, P., and Cranston, M. (1991). "Observations on long-term performance of composite clay-liners and covers." *Geosynthetic Design and Performance,* Vancouver Geotech. Soc., Vancouver, British Columbia.

Darboux, F., Davy, P., Gascuel-Odoux, C., and Huang, C. (2002). "Evolution of soil surface roughness and flowpath connectivity in overland flow experiments." *Catena*, 46(2), 125-139.

Doorenbos J and WO Pruitt. (1977). "Guidelines for predicting crop water requirements." *FAO Irrigation Paper No. 24, 2nd ed.*, Food and Agriculture Organization of the United Nations, Rome, Italy.

Duley, F. L., and Ackerman, F. G. (1934). "Runoff and erosion from plots of different lengths." *Journal of Agricultural Research*, 48, 505-510.

Dunne, T., and Black, R. D. (1970a). "An experimental investigation of runoff production in permeable soils." *Water Resources Research*, 6(2), 478-490.

Dunne, T., and Black, R. D. (1970b). "Partial area contributions to storm runoff in a small New England watershed." *Water Resources Research*, 6(5), 1296-1311.

Dunne, T., Zhang, W., and Aubry, B. F. (1991). "Effects of rainfall, vegetation, and microtopography on infiltration and runoff." *Water Resources Research*, 27(9), 2271-2285.

Eagleson, P. S. (1970). "Dynamic Hydrology." McGraw-Hill, New York.

El-Hassanin, A. S., Labib, T. M., and Gaber, E. I. (1993). "Effect of vegetation cover and land slope on runoff and soil losses from the watersheds of Burundi." *Agriculture, Ecosystems and Environment*, 43(3), 301-308.

Fayer, M. J., Rockhold, M. L., and Campbell, M. D. (1992). "Hydrologic modeling of protective barriers: Comparison of field data and simulation results." *Soil Science Society of America Journal*, 56(3), 690-700.

Fayer, M. J., and Gee, G. W. (1997). "Hydraulic model tests for landfill covers using field data." *Landfill capping in the semiarid west: Problems, perspectives, and solutions*, Environmental Science and Research Foundation, Idaho Falls, Idaho, 53-68.

Fayer, M. J. (2000). "UNSAT-H Version 3.0: unsaturated soil water and heat flow model, theory, user manual, and examples." *Pacific Northwest National Laboratory*, 13249.

Francis, C. F., and Thornes, J. B. (1990). "Runoff hydrographs from three Mediterranean vegetation cover types." *Vegetation and Erosion. Processes and Environments.*, 363-384.

Freeze, R. A. (1972). "Role of subsurface flow in generating surface runoff: 2. Upstream source areas." *Water Resources Research*, 8(5), 1272-1283.

Freeze, R. A. (1980). "A stochastic-conceptual analysis of rainfall-runoff processes on a hillslope." *Water Resources Research*, 16(2), 391-408.

Ghidey, F., Alberts, E. E., and Kitchen, N. R. (1999). "Evaluation of the Root Zone Water Quality Model using field-measured data from the Missouri MSEA." *Agronomy Journal*, 91(2), 183-192.

Godsey, S. E., Kirchner, J. W., and Clow, D. W. (2009). "Concentration–discharge relationships reflect chemostatic characteristics of US catchments." *Hydrological Processes*, 23(13), 1844-1864.

Golder Associates Inc. (2005). "CQA monitoring and testing services of the clay infiltration layer final cover at the Austin Community Landfill in Travis County, Texas," Report No. 043-4718, Report prepared for Waste Management Inc., Golder Associates Inc., Texas.

Gomi, T., Sidle, R. C., Miyata, S., Kosugi, K. I., and Onda, Y. (2008). "Dynamic runoff connectivity of overland flow on steep forested hillslopes: Scale effects and runoff transfer." *Water Resources Research*, 44(8).

Graham, C. B., Van Verseveld, W., Barnard, H. R., and McDonnell, J. J. (2010). "Estimating the deep seepage component of the hillslope and catchment water balance within a measurement uncertainty framework." *Hydrological Processes*, 24(25), 3631-3647.

Green, W. H., and Ampt, G. A. (1911). "Studies on soil physics, 1. The flow of air and water through soils." *J. Agric. Sci.*, 4(1), 1-24.

Hauser, V. L., Weand, B. L., and Gill, M. D. (2001). "Natural covers for landfills and buried waste." *Journal of Environmental Engineering*, 127(9), 768-775.

Hawkins, R. H., and Horton, J. H. (1967). "Bentonite as a Protective Cover for Buried Radioactive Waste." *Health Physics*, 13(3), 287-292.

Hewlett, J. D., and Hibbert, A. R. (1967). "Factors affecting the response of small watersheds to precipitation in humid areas." *Forest Hydrology*, 275-290.

Hewlett, J. D., Fortson, J. C., and Cunningham, G. B. (1977). "The effect of rainfall intensity on storm flow and peak discharge from forest land." *Water Resources Research*, 13(2), 259-266.

Hopp, L., McDonnell, J. J., and Condon, P. (2011). "Lateral Subsurface Flow in a Soil Cover over Waste Rock in a Humid Temperate Environment." *Vadose Zone Journal*, 10(1), 332-344.

Imeson, A. C., Verstraten, J. M., Van Mulligen, E. J., and Sevink, J. (1992). "The effects of fire and water repellency on infiltration and runoff under Mediterranean type forest." *Catena*, 19(3), 345-361.

Johnson, C. W., and Gordon, N. D. (1988). "Runoff and erosion from rainfall simulator plots on sagebrush rangeland." *Transactions of the ASAE,* 31(2), 421-427.

Julien, P. Y., and Moglen, G. E. (1990). "Similarity and length scale for spatially varied overland flow." *Water Resources Research*, 26(8), 1819-1832.

Kaushik, T., Khire, M. V., Johnson, T., & Caldwell, M. (2014). "Surface Runoff at an Instrumented Catchment Scale Water Balance Final Cover." *Proc., GeoCongress 2014, GSP 234,* ASCE, Reston, VA, 4125-4135.

Keese, K. E., Scanlon, B. R., and Reedy, R. C. (2005). "Assessing controls on diffuse groundwater recharge using unsaturated flow modeling." *Water Resources Research*, 41(6).

Khire, M., Benson, C., and Bosscher, P. (1994). "Final cover hydrologic evaluation, Phase III." *Environ. Geotechnics Rep. 94-4*, Department of Civil and Environmental Engineering, University of Wisconsin-Madison, Wis.

Khire, M. V., Benson, C. H., and Bosscher, P. J. (1997). "Water balance modeling of earthen final covers." *Journal of Geotechnical and Geoenvironmental Engineering*, 123(8), 744-754.

Khire, M. V., Benson, C. H., and Bosscher, P. J. (1999). "Field data from a capillary barrier and model predictions with UNSAT-H." *Journal of Geotechnical and Geoenvironmental Engineering*, 125(6), 518-527.

Khire, M. V., Benson, C. H., and Bosscher, P. J. (2000). "Capillary barriers: Design variables and water balance." *Journal of Geotechnical and Geoenvironmental Engineering*, 126(8), 695-708.

Khire, M. V., and Saravanathiiban, D. S. (2012). "Centrifuge Testing of Unsaturated Hydraulic Properties of Municipal Solid Waste." *GeoCongress 2012, State of the Art and Practice in Geotechnical Engineering*, ASCE, Reston, VA, 3487-3496.

La Torre Torres, I. B., Amatya, D. M., Sun, G., and Callahan, T. J. (2011). "Seasonal rainfall–runoff relationships in a lowland forested watershed in the southeastern USA." *Hydrological Processes*, 25(13), 2032-2045.

Leys, A., Govers, G., Gillijns, K., Berckmoes, E., and Takken, I. (2010). "Scale effects on runoff and erosion losses from arable land under conservation and conventional tillage: The role of residue cover." *Journal of Hydrology*, 390(3), 143-154.

Ma, Q. L., Hook, J. E., and Wauchope, R. D. (1999). "Evapotranspiration predictions: a comparison among GLEAMS, Opus, PRZM-2, and RZWQM models in a humid and thermic climate." *Agricultural Systems*, 59(1), 41-55.

Ma, L., Malone, R. W., Heilman, P., Karlen, D. L., Kanwar, R. S., Cambardella, C. A., Saseendran, S. A., and Ahuja, L. R. (2007). "RZWQM simulation of long-term crop production, water and nitrogen balances in Northeast Iowa." *Geoderma*, 140(3), 247-259.

Ma, L., Ahuja, L. R., Nolan, B. T., Malone, R. W., Trout, T. J., and Qi, Z. (2012). "Root Zone Water Quality Model (RZWQM 2): Model use, calibration, and validation." *Transactions of the ASABE*, 55(4), 1425-1446.

Madalinski, K. L., Gratton, D. N., and Weisman, R. J. (2003). "Evapotranspiration covers: An innovative approach to remediate and close contaminated sites." *Remediation Journal*, 14(1), 55-67.

Mayor, Á. G., Bautista, S., and Bellot, J. (2011). "Scale-dependent variation in runoff and sediment yield in a semiarid Mediterranean catchment." *Journal of Hydrology*, 397(1), 128-135.

Meyer, P. D. (1993). "Application of an infiltration evaluation methodology to a hypothetical low-level waste disposal facility." Division of Regulatory Applications, Office of Nuclear Regulatory Research, US Nuclear Regulatory Commission.

Meerdink, J. S., Benson, C. H., and Khire, M. V. (1996). "Unsaturated hydraulic conductivity of two compacted barrier soils." *Journal of Geotechnical Engineering*, 122(7), 565-576.

Merz, B., and Plate, E. J. (1997). "An analysis of the effects of spatial variability of soil and soil moisture on runoff." *Water Resources Research*, 33(12), 2909-2922.

Mijares, R. G., Khire, M. V., and Johnson, T. (2012). "Field-scale evaluation of lysimeters versus actual earthen covers." *Geotech. Testing Journal*, 35(1), 31-40.

Mijares, R. G., and Khire, M. V. (2012). "Field Data and Numerical Modeling of Water Balance of Lysimeter versus Actual Earthen Cap." *Journal of Geotechnical and Geoenvironmental Engineering*, 138(8), 889-897.

Miyata, S., Kosugi, K. I., Gomi, T., Onda, Y., and Mizuyama, T. (2007). "Surface runoff as affected by soil water repellency in a Japanese cypress forest." *Hydrological Processes*, 21(17), 2365-2376.

Moreno-de las Heras, M., Nicolau, J. M., Merino-Martín, L., and Wilcox, B. P. (2010). "Plot-scale effects on runoff and erosion along a slope degradation gradient." *Water Resources Research*, 46(4), W04503.

Mueller, E. N., Wainwright, J., and Parsons, A. J. (2007). "Impact of connectivity on the modeling of overland flow within semiarid shrubland environments." *Water Resources Research*, 43(9).

Mutchler, C. K., and Greer, J. D. (1980). "Effect of slope length on erosion from low slopes." *Transactions of the ASAE*, 23(4), 866-869.

Nielsen-Gammon, J. (2011). "The changing climate of Texas." *The impact of global warming on Texas*, University of Texas Press, Austin, 39-68.

Nyhan, J. W., Hakonson, T. E., and Drennon, B. J. (1990). "A water balance study of two landfill cover designs for semiarid regions." *Journal of Environmental Quality*, 19(2), 281-288.

Nyhan, J. W. (2005). "A seven-year water balance study of an evapotranspiration landfill cover varying in slope for semiarid regions." *Vadose Zone Journal*, 4(3), 466-480.

Ogorzalek, A. S., Bohnhoff, G. L., Shackelford, C. D., Benson, C. H., and Apiwantragoon, P. (2008). "Comparison of field data and water-balance predictions for a capillary barrier cover." *Journal of Geotechnical and Geoenvironmental Engineering*, 134(4), 470-486.

Palleiro, L., Rodríguez-Blanco, M. L., Taboada-Castro, M. M., and Taboada-Castro, M. T. (2014). "Hydrological response of a humid agroforestry catchment at different time scales." *Hydrological Processes*, 28(4), 1677-1688.

Passioura, J. (1977). "Determining soil water diffusivities from one-step outflow experiments." *Aust. J. Soil Res.*, 15(1), 1-8.

Penman, H. L. (1940). "Gas and vapour movements in the soil: I. The diffusion of vapours through porous solids." *The Journal of Agricultural Science*, 30(03), 437-462.

Reed, S. M., D. R. Maidment, and J. Patoux (1997). "Spatial water balance of Texas." *Tech. Rep. 97-1*, Cent. for Res. in Water Resour., Univ. of Tex. at Austin, Austin.

Richards, L. A. (1931). "Capillary conduction of liquids through porous mediums." *Journal of Applied Physics*, 1(5), 318-333.

Scanlon, B. R., Christman, M., Reedy, R. C., Porro, I., Simunek, J., and Flerchinger, G. N. (2002). "Intercode comparisons for simulating water balance of surficial sediments in semiarid regions." *Water Resources Research*, 38(12), 59-1.

Scanlon, B. R., Reedy, R. C., Keese, K. E., and Dwyer, S. F. (2005). "Evaluation of evapotranspirative covers for waste containment in arid and semiarid regions in the southwestern USA." *Vadose Zone Journal*, 4(1), 55-71.

Schnabel, W. E., Munk, J., Lee, W. J., and Barnes, D. L. (2012). "Four-year performance evaluation of a pilot-scale evapotranspiration landfill cover in Southcentral Alaska." *Cold Regions Science and Technology*, 82, 1-7.

Schroeder, P. R., C. M. Lloyd, P. A. Zappi, and N. M. Aziz (1994). "The Hydrologic Evaluation of Landfill Performance (HELP) Model, user's guide for version 3." *Rep. No. EPA/600/168a,* U.S. Environ. Prot. Agency Risk Reduction Eng. Lab., Cincinnati, Ohio.

Schuetz, C., Bogner, J., Chanton, J., Blake, D., Morcet, M., and Kjeldsen, P. (2003). "Comparative oxidation and net emissions of methane and selected non-methane organic compounds in landfill cover soils." *Environmental Science and Technology*, 37(22), 5150-5158.

Sharpley, A. N. (1985). "Depth of surface soil-runoff interaction as affected by rainfall, soil slope, and management." *Soil Science Society of America Journal*, 49(4), 1010-1015.

Shuttleworth, W. J., and Wallace, J. S. (1985). "Evaporation from sparse crops-an energy combination theory." *Quarterly Journal of the Royal Meteorological Society*, 111(469), 839-855.

Sissine, F. (2007). "Energy independence and security act of 2007: A summary of major provisions." *CRS order code RL34294*, Library of Congress, Congressional Research Service, Washington, DC.

Stothoff, S. A. (1997). "Sensitivity of long-term bare soil infiltration simulations to hydraulic properties in an arid environment." *Water Resources Research*, 33(4), 547-558.

Spence, C., and Woo, M. K. (2003). "Hydrology of subarctic Canadian shield: soil-filled valleys." *Journal of Hydrology*, 279(1), 151-166.

Tromp-van Meerveld, H. J., and McDonnell, J. J. (2006a). "Threshold relations in subsurface stormflow: 1. A 147-storm analysis of the Panola hill slope." *Water Resources Research*, 42(2).

Tromp-van Meerveld, H. J., and McDonnell, J. J. (2006b). "Threshold relations in subsurface stormflow: 2. The fill and spill hypothesis." *Water Resources Research*, 42(2).

UNESCO. (1979). "Map of the world distribution of arid regions. Accompanied by explanatory note." MAB Tech. Notes no. 7, UNESCO, Paris.

United States Environmental Protection Agency (USEPA). (1992). "USEPA Subtitle D Clarification. 40 CFR 257 and 258." *EPA/OSW-FR-92-4146-6*, Federal Register, 57(124), 28626-28632.

United States Environmental Protection Agency (USEPA) (2009). "Technical Guidance on Implementing the Stormwater Runoff Requirements for Federal Projects under Section 438

of the Energy Independence and Security Act." *EPA 841-B-09-001*, Office of Water, U. S. Environmental Protection Agency, Washington, D.C.

United States Environmental Protection Agency (USEPA) (2013). "Municipal Solid Waste in The United States: 2011 Facts and Figures." *EPA 530-R-13-001*, Office of Solid Waste, U. S. Environmental Protection Agency, Washington, D.C.

United States Government (2002). "Criteria for municipal solid waste landfills." Code of Federal Regulations, *40 CFR 258*, U.S. Gov. Printing Office, Washington, DC.

van de Giesen, N. C., Stomph, T. J., and de Ridder, N. (2000). "Scale effects of Hortonian overland flow and rainfall–runoff dynamics in a West African catena landscape." *Hydrological Processes*, 14(1), 165-175.

van de Giesen, N. C., Stomph, T. J., and de Ridder, N. (2005). "Surface runoff scale effects in West African watersheds: modeling and management options." *Agricultural Water Management*, 72(2), 109-130.

van Genuchten, M. T. (1980). "A closed-form equation for predicting the hydraulic conductivity of unsaturated soils." *Soil Science Society of America Journal*, 44(5), 892-898.

Vigiak, O., van Dijck, S. J., van Loon, E. E., and Stroosnijder, L. (2006). "Matching hydrologic response to measured effective hydraulic conductivity." *Hydrological Processes*, 20(3), 487-504.

Western, A. W., Grayson, R. B., Blöschl, G., Willgoose, G. R., and McMahon, T. A. (1999). "Observed spatial organization of soil moisture and its relation to terrain indices." *Water Resources Research*, 35(3), 797-810.

Weyman, D. R. (1973). "Measurements of the downslope flow of water in a soil." *Journal of Hydrology*, 20(3), 267-288.

Wilcox, B. P., Newman, B. D., Brandes, D., Davenport, D. W., and Reid, K. (1997). "Runoff from a semiarid ponderosa pine hill slope in New Mexico." *Water Resources Research*, 33(10), 2301-2314.

Wilcox, S. (2007). "National Solar Radiation Database 1991-2010 Update: User's Manual (No. NREL/TP-5500-54824)." National Renewable Energy Laboratory (NREL), Golden, CO.

Wood, E. F., Sivapalan, M., and Beven, K. (1986). "Scale effects in infiltration and runoff production." *Proc. of the Symposium on Conjunctive Water Use*, IAHS Publ., 156, 375-387.

Wood, E. F., Sivapalan, M., Beven, K., and Band, L. (1988). "Effects of spatial variability and scale with implications to hydrologic modeling." *Journal of Hydrology*, 102(1), 29-47.